AD-A061 798 FEDERAL AVIATION ADMINISTRATION WASHINGTON D C SYSTE--ETC F/G 1/2
SHORT RANGE TERMINAL RADAR (SRTR) DEFINITION STUDY.(U)
SEP 78

UNCLASSIFIED FAA/RD-78-64 NL

1 OF 2
AD A061798

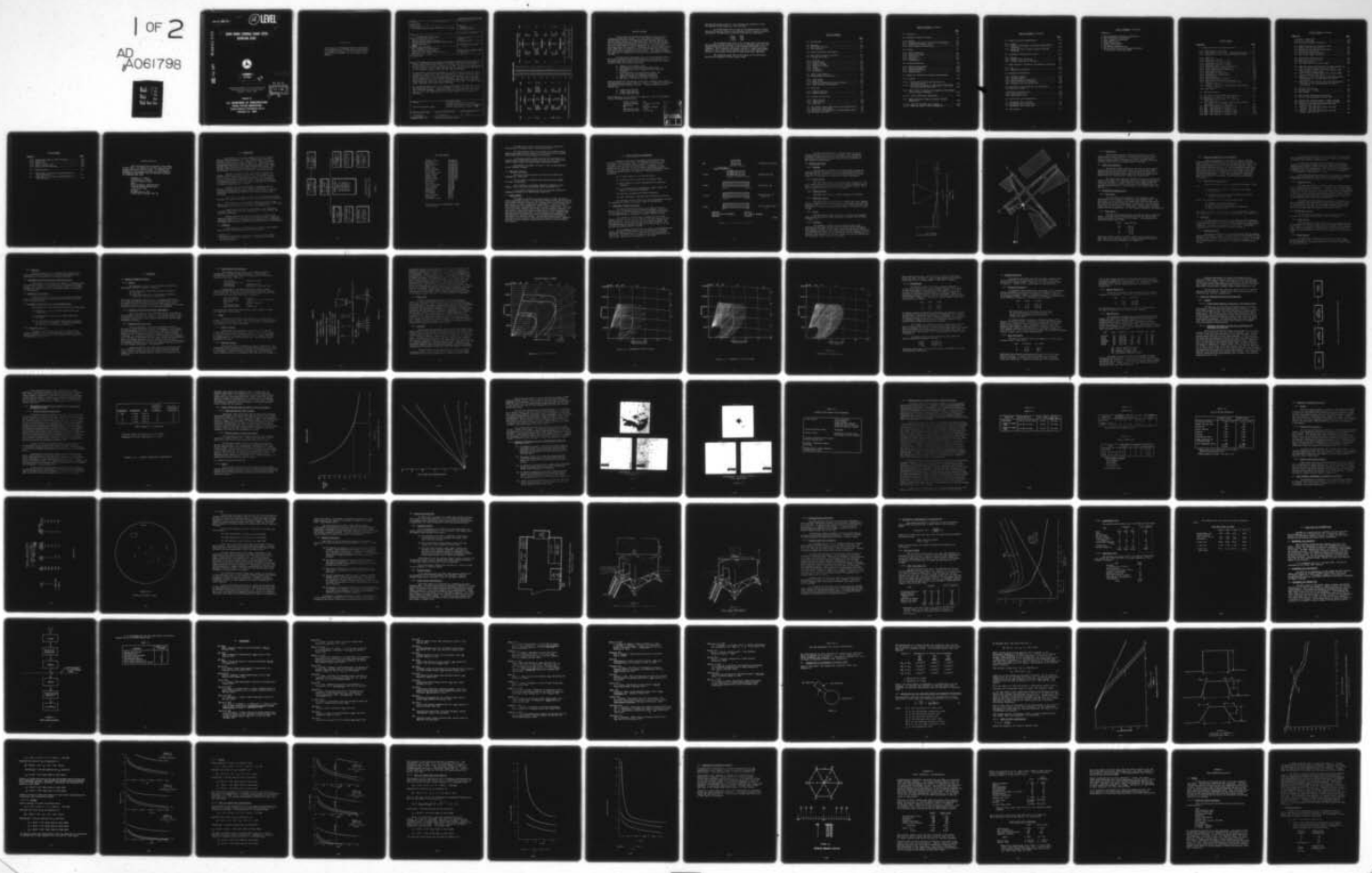

Report No. FAA-RD-78-64

(12) LEVEL II

SHORT RANGE TERMINAL RADAR (SRTR) DEFINITION STUDY

(11) September 1978

(9) Final Report.

Oct 74 - Oct 75.

(12) 144 p.

Prepared for

U.S. DEPARTMENT OF TRANSPORTATION
FEDERAL AVIATION ADMINISTRATION
Systems Research & Development Service
Washington, D.C. 20590

340 170

N O T I C E

This document is disseminated under the sponsorship of the Department of Transportation in the interest of information exchange. The United States Government assumes no liability for its contents or use thereof.

Technical Report Documentation Page

1. Report No.	2. Government Accession No.	3. Recipient's Catalog No.
FAA-RD-78-64		

4. Title and Subtitle	5. Report Date
Short Range Terminal Radar (SRTR) Definition Study	September 1978
	6. Performing Organization Code
	8. Performing Organization Report No.
7. Author(s) Primary Radar Study Group	
9. Performing Organization Name and Address Federal Aviation Administration & The John Hopkins University Applied Physics Lab. & Lincoln Laboratory & MITRE	10. Work Unit No. (TRAIS) 023 241 11. Contract or Grant No.
12. Sponsoring Agency Name and Address U.S. Department of Transportation Federal Aviation Administration Systems Research and Development Service Washington, D.C. 20591	13. Type of Report and Period Covered Final October 1974 - October 1975 14. Sponsoring Agency Code ARD-243

15. Supplementary Notes

16. Abstract: A Study group was convened in the Summer of 1974 by the FAA to define a Short Range Terminal Radar (SRTR) to be used at high traffic density VFR airports which do not presently qualify for an ASR. The study group was comprised of representatives from the Johns Hopkins University Applied Physics Laboratory, Lincoln Laboratory, MITRE, NAFEC, AAF, AAT, ASP, AEM and ARD.

The operational requirements developed for the SRTR include coverage on a small aircraft (one square meter radar cross section) out to 16 nautical miles; up to 10,000 feet altitude; and in an environment of precipitation clutter, ground clutter, angel clutter, and anomalous propagation. The MTBF goal is 500 hours and the MTTR goal is one hour. Using these operational requirements candidate radar systems were defined at three frequencies, L-band (1250 - 1350 MHz), S-band (2700 - 2900 MHz) and S'-band (3500 - 3700 MHz).

The recommended SRTR system is the S'-band system (3500 - 3700 MHz) and has the following characteristics: azimuth beamwidth of 3.4°, pulse width of 2 usecs, PRF of 2000 pps (average), instrumented range of 32 nautical miles, and a data rate of 4 sec. The establishment cost (in 1974 dollars) for this system is $324,000.

17. Key Words	18. Distribution Statement
Airport Surveillance Radar	Document is available to the public through the National Technical Information Service, Springfield, Virginia 22161

19. Security Classif. (of this report)	20. Security Classif. (of this page)	21. No. of Pages	22. Price
Unclassified	Unclassified	139	

Form DOT F 1700.7 (8-72) Reproduction of completed page authorized

METRIC CONVERSION FACTORS

Approximate Conversions to Metric Measures

Symbol	When You Know	Multiply by	To Find	Symbol
		LENGTH		
in	inches	*2.5	centimeters	cm
ft	feet	30	centimeters	cm
yd	yards	0.9	meters	m
mi	miles	1.6	kilometers	km
		AREA		
in^2	square inches	6.5	square centimeters	cm^2
ft^2	square feet	0.09	square meters	m^2
yd^2	square yards	0.8	square meters	m^2
mi^2	square miles	2.6	square kilometers	km^2
	acres	0.4	hectares	ha
		MASS (weight)		
oz	ounces	28	grams	g
lb	pounds	0.45	kilograms	kg
	short tons (2000 lb)	0.9	tonnes	t
		VOLUME		
tsp	teaspoons	5	milliliters	ml
Tbsp	tablespoons	15	milliliters	ml
fl oz	fluid ounces	30	milliliters	ml
c	cups	0.24	liters	l
pt	pints	0.47	liters	l
qt	quarts	0.95	liters	l
gal	gallons	3.8	liters	l
ft^3	cubic feet	0.03	cubic meters	m^3
yd^3	cubic yards	0.76	cubic meters	m^3
		TEMPERATURE (exact)		
°F	Fahrenheit temperature	5/9 (after subtracting 32)	Celsius temperature	°C

*1 in. = 2.54 (exactly). For other exact conversions and more detailed tables, see NBS Misc. Publ. 286, Units of Weights and Measures, Price $2.25, SD Catalog No. C13.10:286.

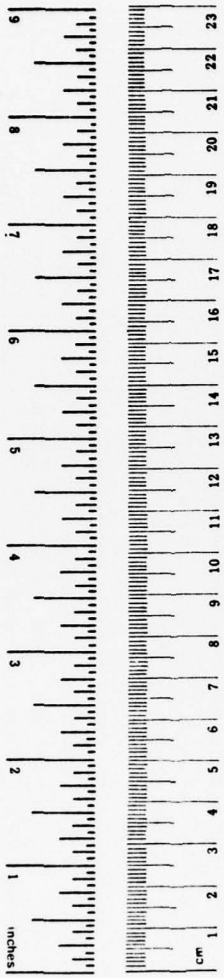

Approximate Conversions from Metric Measures

Symbol	When You Know	Multiply by	To Find	Symbol
		LENGTH		
mm	millimeters	0.04	inches	in
cm	centimeters	0.4	inches	in
m	meters	3.3	feet	ft
m	meters	1.1	yards	yd
km	kilometers	0.6	miles	mi
		AREA		
cm^2	square centimeters	0.16	square inches	in^2
m^2	square meters	1.2	square yards	yd^2
km^2	square kilometers	0.4	square miles	mi^2
ha	hectares (10,000 m^2)	2.5	acres	
		MASS (weight)		
g	grams	0.035	ounces	oz
kg	kilograms	2.2	pounds	lb
t	tonnes (1000 kg)	1.1	short tons	
		VOLUME		
ml	milliliters	0.03	fluid ounces	fl oz
l	liters	2.1	pints	pt
l	liters	1.06	quarts	qt
l	liters	0.26	gallons	gal
m^3	cubic meters	35	cubic feet	ft^3
m^3	cubic meters	1.3	cubic yards	yd^3
		TEMPERATURE (exact)		
°C	Celsius temperature	9/5 (then add 32)	Fahrenheit temperature	°F

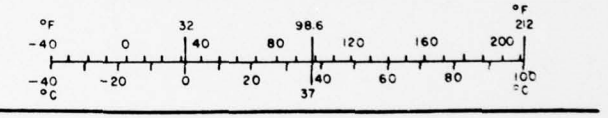

EXECUTIVE SUMMARY

A study group was convened in the summer of 1974 by the FAA to define two new radar systems. The study group was comprised of representatives from The Johns Hopkins University Applied Physics Laboratory, Lincoln Laboratory, MITRE, NAFEC, AAF, AAT, ASP, AEM, and ARD. One of these radars was designated as the ASR-( ) and it was envisioned that this system would be the next generation ASR. The other radar, which this report will describe, is designated as the Short Range Terminal Radar (SRTR) which is designed for use at high traffic density VFR airports which do not presently qualify for an ASR. This report documents the study group's deliberations, conclusions and recommendations concerning the SRTR.

The operational requirements to be met by the SRTR are that the system must be able to maintain surveillance on a small aircraft (i.e., one square meter radar cross section, Swerling Case I fluctuation characteristics) under the following conditions:

a. ranges up to 16 nautical miles
b. altitudes below 10,000 feet above ground level
c. with minimum resolution commensurate with separation standards
d. in an environment of precipitation, ground, and angel clutter and also anomalous propagation
e. compatible operation with TRACAB utilization
f. MTBF goal of 500 hours, MTTR goal of one hour.

Using the operational requirements listed above, candidate radar systems were developed using frequency bands of interest. Parameters were optimized considering system performance and cost. The three candidate systems defined were:

a. L-Band (1250-1350 MHz)
b. S-Band (2700-2900 MHz)
c. S'-Band (3500-3700 MHz)

These frequencies are all allotted for radar use. All of the candidates had the following characteristics:

azimuth beamwidth	3.4°
elevation coverage	6° basic, $\csc^2$ 6-20°
Pulse width	2 μsec
PRF	2000 PPS (average)
instrumented range	32 nmi
data rate/scan rate	4 sec/15 rpm

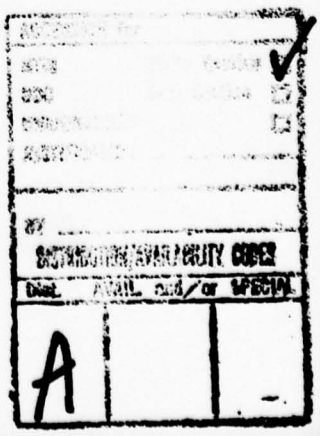

The peak and average powers for each candidate were calculated to give the required 16 nmi coverage on a small aircraft.

The establishment cost for each of the candidates which includes the radar system cost, spares, test equipment contractor turnkey, shipping, installation, documentation, and factory inspection is listed below:

L-Band	$310K
S-Band	316K
S'-Band	324K

The recommended SRTR system is the S'-Band system (3500-3700 MHz). This frequency has been allocated to the FAA for terminal radars and is not presently being used so that there will be minimum interference at this frequency. The S' frequency also permits the use of a small radar antenna (about 5.5' by 5') which can be mounted on the roof of the radar shelter. The cost of this system is basically the same as the other candidates.

The funding estimates used in this report are in 1974 dollars and should be adjusted to reflect current costs.

TABLE OF CONTENTS

TABLE OF CONTENTS (continued)

TABLE OF CONTENTS (continued)

TABLE OF CONTENTS (continued)

Appendices

LIST OF FIGURES

LIST OF FIGURES (continued)

LIST OF TABLES

ACKNOWLEDGEMENTS

Many individuals have contributed to the content of this report. All members of the Radar Study Group were generous with their time and efforts. In addition, the personnel at the following locations were most helpful in providing the team members with the information required to accomplish their task:

Allentown, Pa. Airport
Wilkes-Barre, Pa. Airport
New York Common IFR Room
NAFEC
Texas Instruments (ASR-8 Division)
Southwest Regional Headquarters;
Fort Worth, Texas
FAA Depot
Oklahoma City, Ok. FSS
Gichner Mobile Systems; York, Pa.

1.0 INTRODUCTION

The formation of an ad hoc committee to study the Federal Aviation Administration need for future terminal area radars was authorized by ARD 1974A.* Such a committee was formed in accordance with the organization chart shown in Figure 1.1. Essentially, two subcommittees were formed within the Radar Study group to investigate the DABS backup radar and a Short Range Terminal Radar (SRTR). This document serves as the SRTR subcommittee report to the study group and formalizes its deliberations, conclusions, and recommendations.

Interest in a class of radar systems which close the gap between a non-radar qualified airport and one which qualifies for a full ASR series terminal radar has been evident in the FAA for some years. The most recent investigation resulted in the circulation of a concept and plan in late 1972 (ARD 1972). This study was directed to establishing whether such a radar system is feasible in the context of technical, operation, and cost goals.

In order to derive the operational requirements given in Section 2 and place the study in the proper perspective as far as operational problems were concerned, elements of the SRTR subcommittee accompanied the Radar Study Committee on two familiarization trips. These were:

(a) A trip to Allentown and Wilkes-Barre, Pennsylvania airports followed by a visit to the common IFR room in New York and a visit to NAFEC.

(b) A trip to Texas Instruments Corporation at Dallas, Texas (briefing on the ASR-8 system), the Western Region headquarters at Ft. Worth, the FAA Depot and the Flight Service Station at Oklahoma City.

A special visit was made by some members of the subcommittee to Gichner Mobile Systems in York, Pennsylvania to obtain technical and cost data on shelters.

Special attention was directed to problems encountered and operational experience of personnel at the various locations. These were considered paramount in the subcommittee's formulation of the operational requirements and were always considered during deliberations on alternatives.

1.1 RATIONALE

The rationale for the SRTR study is to define a radar system which will meet the following operational requirements:

---

* References to bibliographic material are given with an identifier and year of publication. The material is alphabetically ordered in the Bibliography.

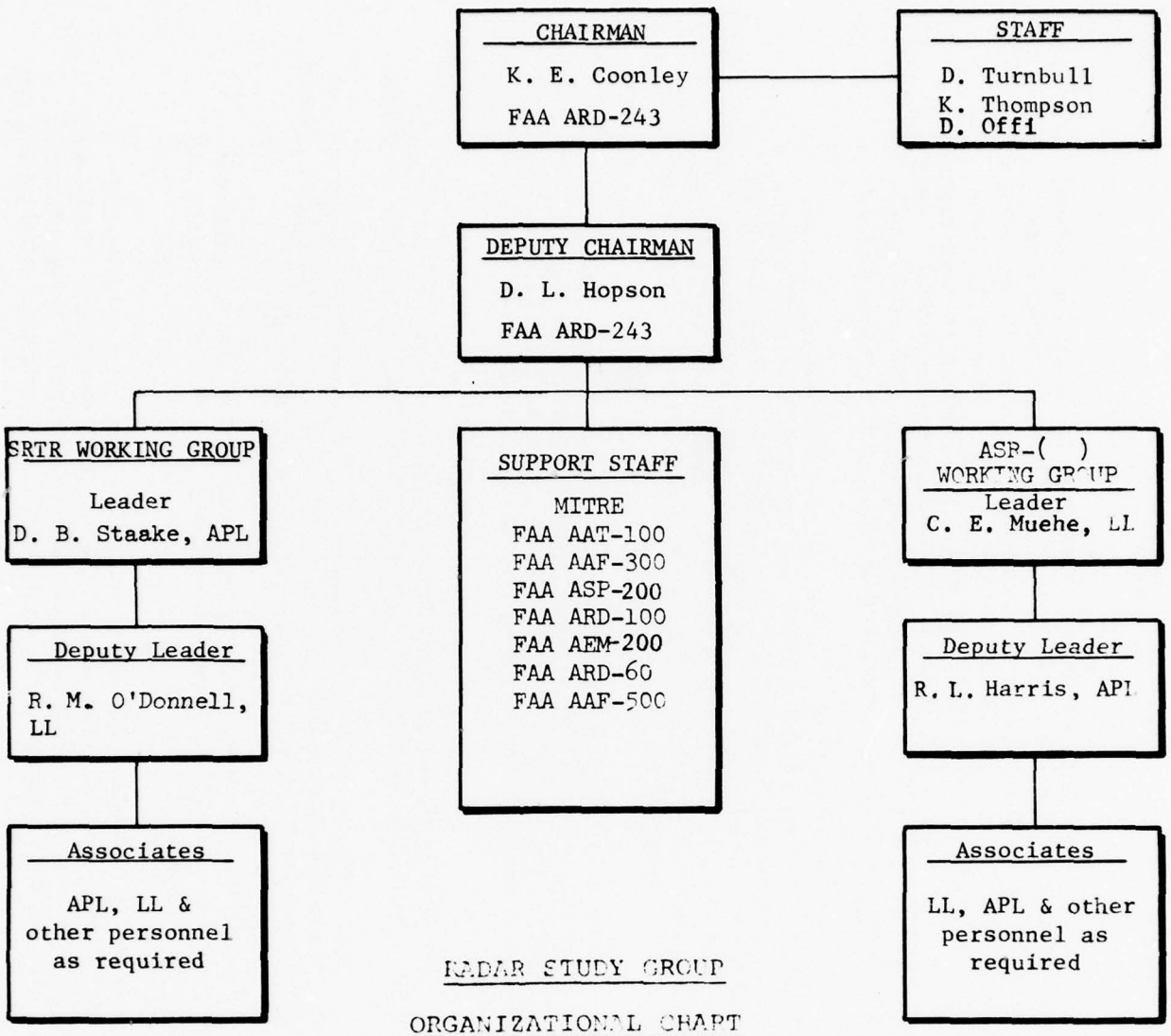

RADAR STUDY GROUP

ORGANIZATIONAL CHART

FIGURE 1.1

SRTR TEAM MEMBERS

Kenneth Coonley	FAA/ARD-243
Dan Hopson	FAA/ARD-243
Donald Turnbull	FAA/ARD-243
Wayne Karl	FAA/AAF-560
Gerald Carp*	FAA/AEM-200
Kenneth Thompson	FAA/ARD-243
R. A. Ramos	FAA/ARD-120
Charles Kohlhousen	FAA/AAF-320
Wesley Rowland	FAA/AAT-120
Dominick Offi	FAA/ANA-120
Steven Zaidman	FAA/ASP-100
William Reytar	FAA/ARD-60
Ray Harris*	APL/JHU
Don Staake	APL/JHU
Arthur Williamson	APL/JHU
J. F. Bradshaw	APL/JHU
Frank Castella	APL/JHU
John Berry	APL/JHU
Steven Epsom	MITRE
C. E. Muehe	MIT/LL
Robert O'Donnell	MIT/LL
John Beusch	MIT/LL
Jean-Claude Sureau	MIT/LL

*Not with the noted organization at date of publishing

(a) High traffic density airports which do not qualify for installation of a terminal control radar/beacon system.

(b) Other airports that do not qualify for a terminal control radar/beacon system, but may require a cost effective sensor to improve safety procedures and increase operational efficiency.

(c) Airports which are newly qualified for installation of a terminal control radar/beacon system but may not have the control area size or traffic density to warrant highly sophisticated systems.

(d) Possible replacement for ASR-4, -5 and -6 being relocated in the "LEAPFROG" program.

1.2 SRTR STUDY OBJECTIVE

There were several objectives to be met by the SRTR Study Subcommittee. These were:

(a) To present to the Radar Study Group functional designs for their consideration,

(b) To perform a set of basic parametric tradeoffs on such designs to meet operational requirements while minimizing costs.

(c) To provide technical data and cost estimates required as background information for specification production.

1.3 STUDY APPROACH

The number of parameter variations required to meet the operational requirements are many. The approach devised to handle these variations was to define candidate systems in the frequency bands of interest and analyze their ability to meet the operational requirements. Candidate systems were also examined from the standpoint of initial and life cycle costs. The sources from which candidate systems were initially conceived were FAA reports (e.g., FAA 1973C), existing radar systems, and the available literature. As the candidate systems were analyzed modifications to their parameters were made and the system reevaluated. As these candidates were formulated they were presented to the Radar Study group and modified and reevaluated in conformance with comments received. The candidate systems contained in this report are the product of the described interactive process. Appendix C includes the radar parameter calculations from which the final candidates were selected.

2.0 SYSTEM OPERATIONAL REQUIREMENTS

A number of operational requirements were established for the SRTR by the Radar Study group. As mentioned in Section 1, these requirements were formulated based on interaction with operational personnel as well as committee deliberations. In summary, it was decided that the SRTR must be able to maintain surveillance on small aircraft (i.e., one square meter radar cross section with Swerling Type I fluctuation characteristics; see Appendix E) under the following conditions:

(a) At ground ranges up to 16 nautical miles,

(b) At altitudes below 10,000 feet above ground level,

(c) With a minimum resolution commensurate with separation standards,

(d) In an environment of precipitation, clutter (ground and angel), and anomalous propagation,

(e) Compatible operation with TRACAB utilization,

(f) With a MTBF goal of 500 hours and a MTTR goal of one hour.

The following sections discuss the various requirements in detail and establish the explicit and implicit items for consideration.

2.1 OPERATIONAL FREQUENCY ALLOCATION

The frequency bands considered for the SRTR are given in Figure 2.1.1. The UHF band shown is included (although no allocation has been requested for it due primarily to the excessive size and cost of the antenna system) to accommodate a possible candidate system.

The 1250 MHz to 1350 MHz band is divided into two 50 MHz segments of which the lower one is allocated for joint usage by the FAA and the military. It is understood that this portion is probably not available for the SRTR leaving just the upper 50 MHz available. The 2700-2900 MHz band is presently assigned to the FAA for use by the ASR and has been assumed usable by the SRTR.

In an agreement between FAA and the Office of Telecommunications Policy, the band from 3500-3700 MHz has been reallocated to include Aeronautical Radionavigation as a coequal service with Radiolocation (FAA 1973B). The reallocation was made with the understanding that the FAA low cost radars would be accommodated in this band.

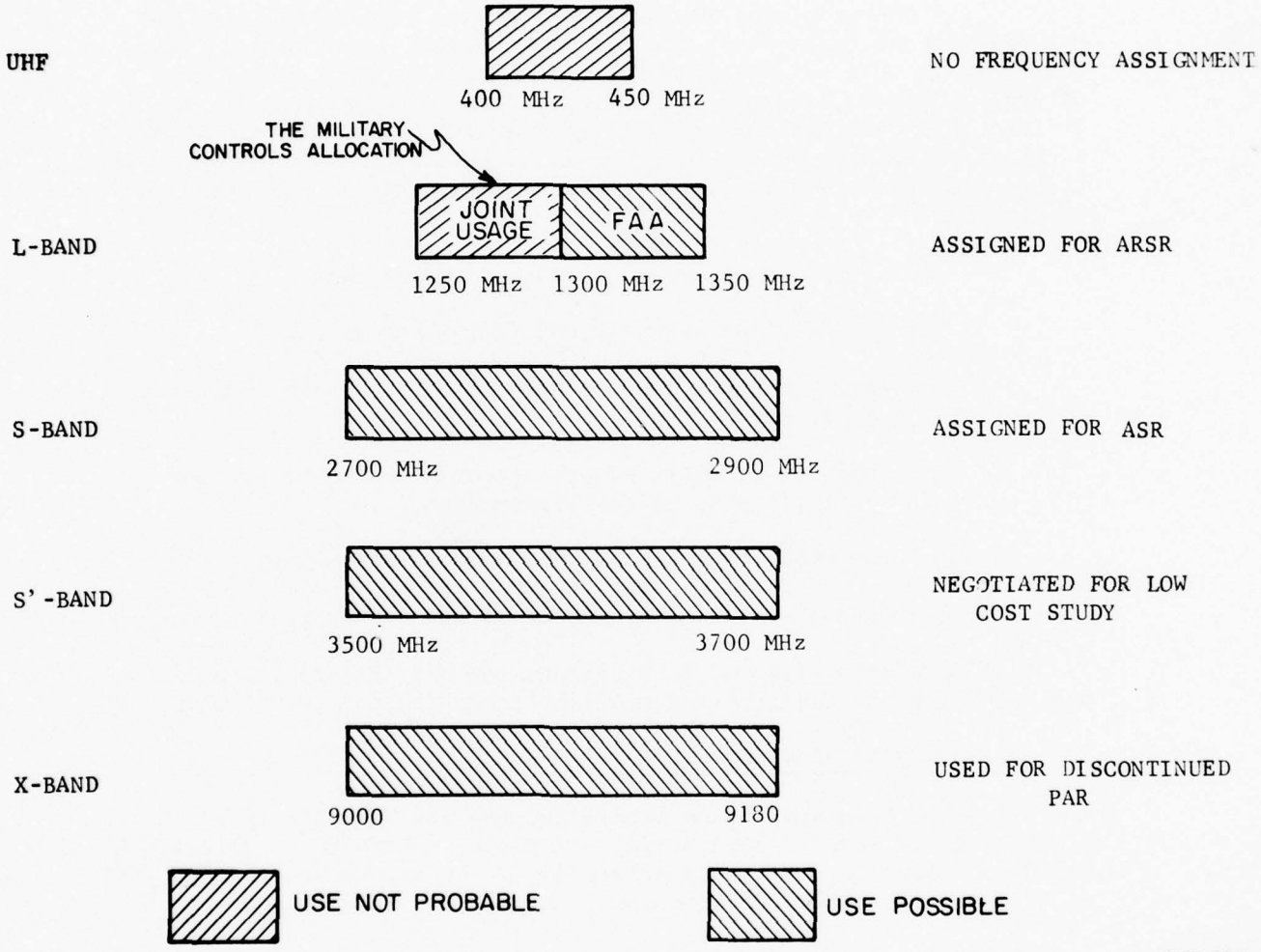

FIGURE 2.1.1 SRTF FREQUENCY ALLOCATION

The 9000 to 9180 MHz band is available since its use for Precision Approach Radar has been discontinued. For completeness, a candidate system operating in this band has been considered, but rejected due primarily to excessive transmitter power necessary to meet operational requirements.

2.2 COVERAGE AND SITING

2.2.1 Coverage

The SRTR should be capable of providing radar coverage and controlled aircraft separations in Control Zones extending out to 15 to 20 nmi from the terminals and up to ten thousand feet in altitude. Figure 2.2.1 illustrates the range/height coverage requirements.

2.2.2 Range Coverage

The radar should provide instrumented range coverage to 32 nmi. It is assumed that aircraft whose radar cross section is greater than or equal to 1 square meter would be detectable at a surface range of 16 nmi with a probability of detection of 0.75 or greater.

2.2.3 Azimuth Coverage

The radar will provide an azimuth coverage of 360 degrees.

2.2.4 Elevation Coverage

The SRTR should provide elevation coverage from 1 to 20 degrees (0.5 to 20 degrees desirable) resulting in 1 square meter target detection capability from 1700 feet to ten thousand feet at a range of 16 nmi. Ten thousand foot coverage would be maintained inbound to a range of at least 4.5 nmi.

2.2.5 Siting

The SRTR shelter should be located in an area at the terminal which provides unobstructed radar visibility of critical areas as shown in Figure 2.2.2.

2.2.6 Visibility

As a minimum, the SRTR should be sited to provide radar visibility of the Airport Traffic Area from traffic pattern altitude to three thousand feet AGL, and the pattern final approach for all runways. For instrument operations, radar siting should provide coverage of a control zone extending to a radius of up to 20 nmi and up to ten thousand feet in altitude. Good visibility of the final approach fix and final approach for each instrument runway should also be assured.

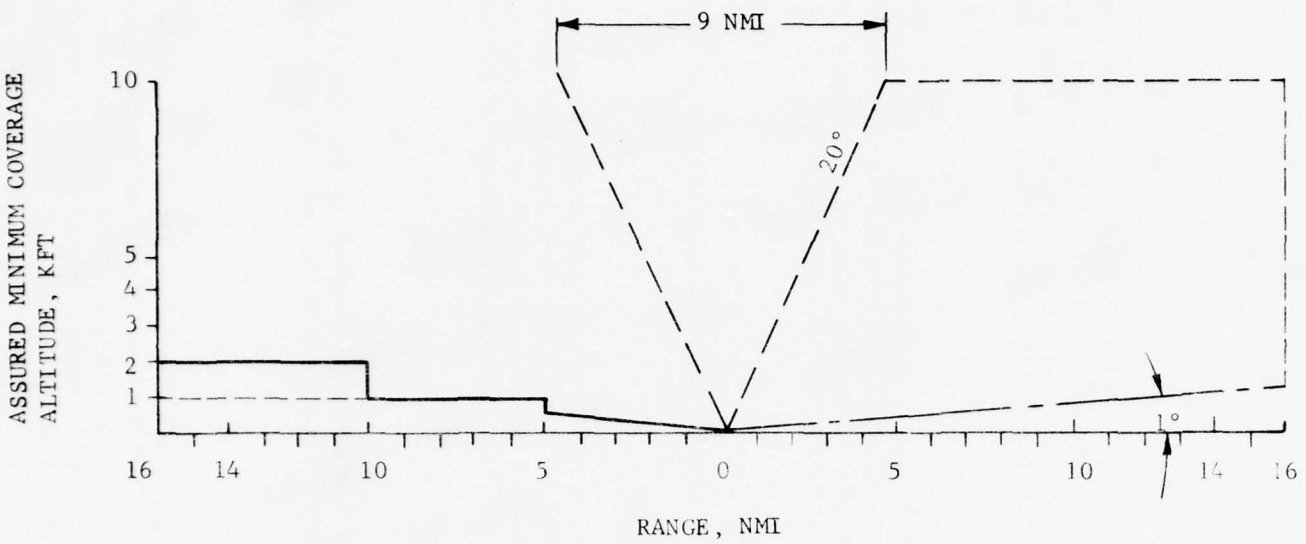

SHORT RANGE TERMINAL RADAR - RANGE/HEIGHT COVERAGE

$1M^2$ TARGET

FIGURE 2.2.1

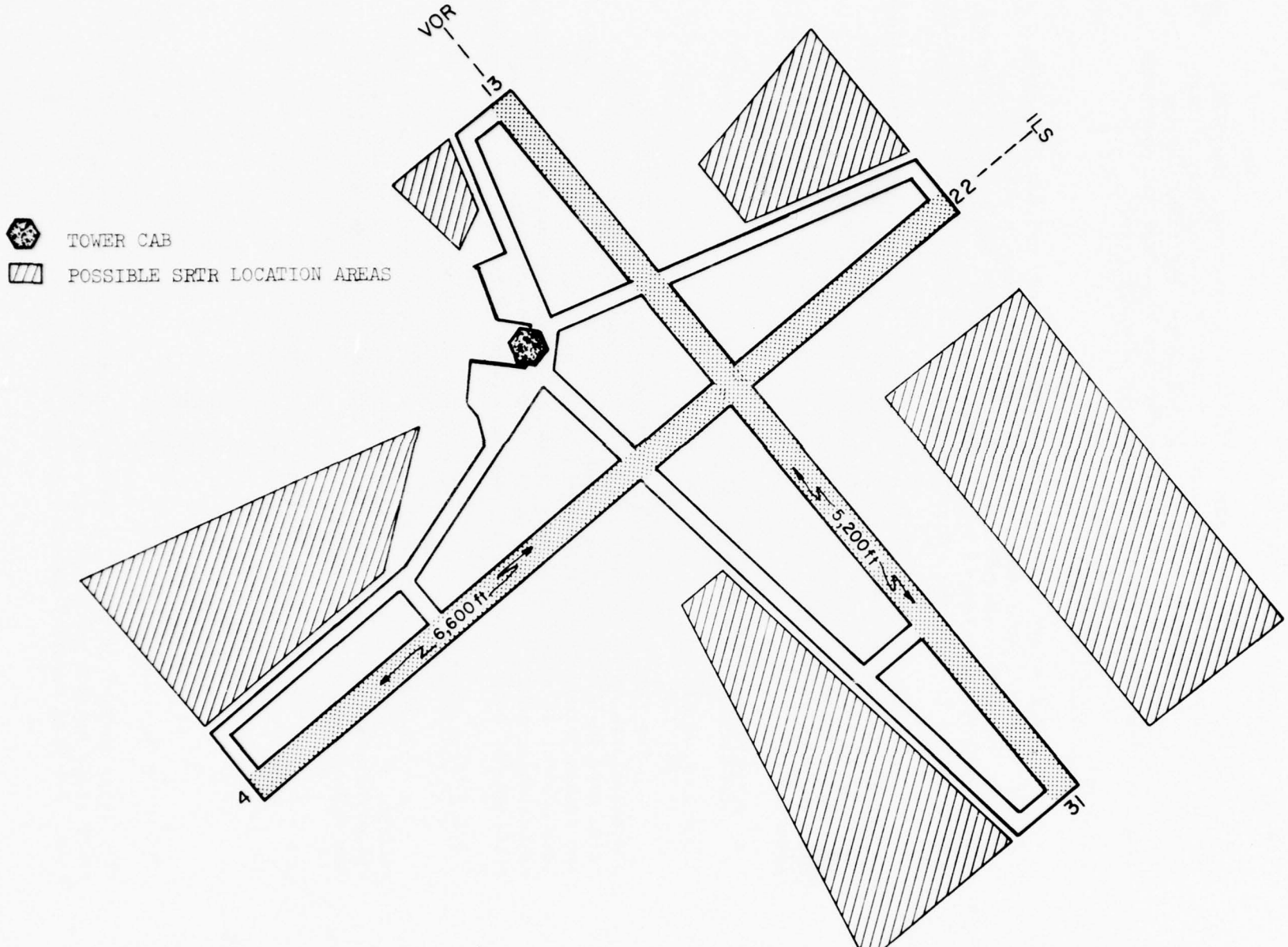

FIGURE 2.2.2 TYPICAL AIRPORT LAYOUT (TEXARKANA MUNICIPAL-WEBB)

F3E-617

2.2.7 Installation

After considering radar visibility requirements, the SRTR configuration should be adaptive to installation in a variety of locations to minimize effort and cost. In all cases, the radar shelter should be located within a reasonable distance of commercial power and telephone grade lines for the transmission of radar data.

2.3 TARGET CHARACTERISTICS

The aircraft targets assumed for the study are small, general aviation aircraft whose mean cross section is one square meter with a Rayleigh fluctuation distribution. The fluctuations are assumed to be slowly varying (correlated pulse-to-pulse but not scan-to-scan) and are characterized by a Swerling Case 1 target (see Skolnik 1970).

The target range rates will generally be from 0 to 250 knots but larger targets beyond the calculated coverage of the SRTR may show range rates up to 600 knots. In some locations, targets (again outside the calculated coverage) may exhibit range rates up to 2000 knots but it is expected that this would be a rare occurrence. For further details, see Appendix E.

2.4 ENVIRONMENTAL CHARACTERISTICS

2.4.1 Land Clutter

The land clutter model assumed for this study has a value characteristic of 95 percent of observations (see Nathanson 1969). The value used is -18 dB relative to one square meter of radar cross section per square meter of area illuminated by the radar beam. The velocity of land clutter is essentially zero though a few feet per second of apparent radial velocity may be caused by leaf flutter. Ground traffic may cause problems but can be masked out. For more detailed information, see Appendix D.

2.4.2 Rain Clutter

The rain clutter model used was one which provided a pessimistic number. A rainfall rate of 16 millimeters per hour was used and this characterizes some 99.5 percent of all rainfall. (See Nathanson 1969). The values used are given below:

BAND	CROSS SECTION*
UHF	-107 dB
L	- 88 dB
S	- 74 dB
S'	- 70 dB
X	- 53 dB

*The cross section is given in decibels relative to one square meter of radar cross section per cubic meter of volume illuminated by the radar beam. For more detailed information, see Appendix D.

2.4.3 Anomalous Propagation and Angel Returns

Anomalous propagation in this report is used to describe essentially any radar returns which are not attributable to weather, land, or targets. It may cover ducting phenomena and angel returns, the latter being composed of bird and insect returns primarily. Since these returns may have associated with them considerable Doppler shifts due to their range rate (10-60 knots) some characteristics other than velocity must be used to differentiate them from targets of interest. Such characteristics may be combinations of radar cross section and fluctuation distributions. In any case, elimination or reduction of angel clutter should be considered. For more detailed information, see Appendix D.

2.4.4 Radio Frequency Interference

There are two major sources of potential RFI problems. These are:

(a) Interference from SRTR to SRTR when in the vicinity of one another.

(b) Interference from other radars operating in the same frequency band as the SRTR.

Some of the techniques for mitigating interference are:

(a) Frequency separation between radars
(b) Range separation between radars
(c) Use of trapezoidal pulses (spectrum compression)
(d) Minimum antenna sidelobes.

The ability of SRTRs to operate without excessive interference requires that the design reflect judicious use of these factors. (See Section 3.7.)

2.5 RESOLUTION

The radar parameters related to the angle and range resolution of the SRTR were derived from the operational requirements as specified and agreed upon by the SRTR Study Group. The logic applied in defining these parameters is discussed in paragraphs 2.5.1 and 2.5.2. Computations substantiating these selections are included in Section 3.

2.5.1 Angular Resolution

The angular resolution of the SRTR was derived from the presently proposed IFR separation standard (proposed revision to FAA Handbook 7110.8D, paragraph 1300; Proposal Change No. AAT-322-74-8) of 1.5 nmi at 15 nmi range. For two aircraft of equal cross-sectional returns, the required -3 dB (one way) azimuth beamwidth of the antenna was computed to be approximately 5.7 deg.

It is known that the cross-sectional returns of aircraft will vary significantly both as a function of aspect (head-on vs. broadside) and physical size (single vs. multi-engine).

To arrive at an azimuth beamwidth which will provide the capability of resolving in angle, targets of significantly different cross-sectional returns, the -20 dB beamwidth of the main lobe of the antenna was used in the computations. This resulted in the selection of an azimuth -3 dB (one way) beamwidth of 3.4 deg. which corresponds to a -20 dB beamwidth of approximately 5.7 deg.

This selection results in the ability to resolve two targets in angle, whose cross-sectional returns differ by approximately 40 dB (two-way beamwidth) and which are separated 1.5 nmi at 15 nmi range.

2.5.2 Range Resolution

The range resolution of the SRTR evolved from several factors. First, the minimum range requirement of 0.5 nmi dictates a maximum pulse-width of approximately 6 microseconds. A somewhat narrower pulse would be necessary due to such factors as T/R recovery time, the use of trapezoidal pulses, etc. Second, the instrumented range dictates the upper limit of the PRF, which in turn dictates the minimum pulsewidth required to obtain the average power necessary to meet the range requirement. Third, for clutter considerations a narrow pulse is desirable.

Considering the above factors, to arrive at a pulsewidth which will be compatible with a relatively low power transmitter tube within the current state of the art, a 2 microsecond pulsewidth was selected. This selection will more than meet the minimum range requirement and provide a practical range resolution of less than 2000 feet.

2.6 ACCURACY AND DATA RATE

The following are considered to be the minimum achievable accuracies by utilizing current state of the art techniques.

2.6.1 Angle Accuracy

The utilization of modern signal processing in conjunction with the application of well known beam splitting techniques should yield an angle accuracy of at least 0.1 beamwidth for the expected signal to noise ratio. For the recommended 3.4 degree azimuth beamwidth for the SRTR antenna the resulting angle accuracy will be less than 520 feet at 15 nmi range.

2.6.2 Range Accuracy

The application of leading edge tracking and modern signal processing is expected to yield at least 0.1 pulsewidth range accuracy. For the recommended 2 microsecond pulsewidth the resulting range accuracy is less than 100 feet.

2.6.3 Data Rate

Previous experience in the terminal areas indicate that a four-second data rate is adequate. This value was selected by the study group to be incorporated in the design of the SRTR.

2.7 AIR TRAFFIC CONTROL RADAR BEACON SYSTEM COMPATIBILITY

When required, the SRTR should be capable of providing a radar pre-trigger and antenna position information to a beacon interrogator system. It is anticipated that the SRTR antenna drive will be capable of physically supporting a beacon interrogator antenna, in addition to the SRTR antenna.

2.8 WEATHER DATA REQUIREMENTS

Weather data should be presented on a display in the form of a one or two level contour giving an indication of returns existing above a settable threshold.

2.9 RELIABILITY, MAINTAINABILITY, AND AVAILABILITY GOALS

The following goals were established by the SRTR working group:

(a) Reliability or mean time between failure (MTBF) goal of 500 hours.

(b) Maintainability or mean time to repair (MTTR) goal of 1 hour.

(c) The availability was computed based on the above goals and resulted in 99.8 percent. The method of obtaining the availability is presented in Section 3.9.

2.10 LIFE CYCLE COST GOALS

The goal of the SRTR Study Group was to ensure that the parametric design of the system precluded high risk items. In this fashion, significant cost savings (on the order of 40-50 percent) may be realized over a full ASR.

3.0 DISCUSSION

3.1 CANDIDATE PARAMETER SELECTION

3.1.1 General

The selection of a set of radar parameters to satisfy the requirements outlined in Section 2 involves:

(a) the operational requirements outlined in Section 2,
(b) cost, and
(c) other constraints such as FAA frequency allocation, maintenance and logistics systems, etc.

These lead to the general conclusion that the selected radar for the short range terminal application should be a conventional 2D (azimuth and range) system with a simple pulse (non modulated) and coherent processing to handle the clutter environment. The rationale for selecting specific parameters is presented in the following paragraphs.

3.1.2 Parameters Dictated by Operational Requirements

Most of the important radar parameters can be chosen based on the operational requirements of Section 2. They include certain antenna characteristics, such as azimuth beamwidth and elevation coverage, some transmitter characteristics, such as pulse width and PRF, and the signal processing and display.

3.1.3 Parameters Dictated by Cost

Once the operational requirements have been satisfied by selection of proper parameters, cost must be considered. All or nearly all the requirements can be met by radars on a variety of RF frequencies. The band of frequencies to be considered can be narrowed by taking a general look at the calculations shown in Appendix C from which Figure C.1 is derived. If a transmitter peak power of 150 kilowatts and an antenna size of 30 feet are considered practical limits to meet cost and reliability goals, the range of frequencies to be considered can be limited to approximately 1000-4000 MHz. At UHF the size and cost of an antenna system is considered prohibitive and at X-band the required transmitter power and cost is considered prohibitive. (See Appendix C.)

Another possibility which might appear to be attractive would be to use many portions of the ASR-8 in order to minimize development costs. However, the analysis presented in Appendix B shows that this approach is not cost effective when all factors of life cycle cost are considered.

3.1.4 Other Parameter Considerations

The frequency selection range can be further narrowed by consideration of frequency allocation problems. In the range of 1000-4000 MHz there are three bands which are possible for use on any reasonable time scale. These are:

1250-1350 MHz (Lower half-joint use)	Assigned for ARSR
2700-2900 MHz	Assigned for ASR
3500-3700 MHz	Negotiated for Low Cost Study

The remainder of the discussion will be limited to three candidate systems; one in each of the listed bands. All other characteristics except peak and average power will be held constant at the values deduced from the operational requirements as follows:

Azimuth Beamwidth	3.4 deg.
Elevation Coverage	6 deg. basic - $\csc^2$ 6 to 20 deg.
Pulse Width	2 μsec.
PRF	2000 PPS (average)
Instrumented Range	32 nmi
Data Rate/Scan Rate	4 sec/15 rpm

All calculations assume these values although minor tradeoffs may need to be made later in the program.

3.2 ANTENNA

The general requirements, both operational and cost, seem to dictate a straightforward reflector-feed antenna system rotating in azimuth and driven by a single drive motor system. Other antenna considerations are discussed in the following paragraphs.

3.2.1 Azimuth Beamwidth

The maximum azimuth beamwidth is dictated by the separation standard employed. The calculations are shown in Figure 3.2.1. As can be seen, the required azimuth beamwidth relates to a 1.5 nmi separation at a range of 15 nmi. The other standards relate to longer ranges than the approximately 20 nmi required for the SRTR. The resulting azimuth beamwidth is 3.4 deg.

3.2.2 Elevation Coverage

The required elevation coverage was stated in Section 2.2. The requirements are to see small aircraft targets flying within about 16 miles of the airport (the radar site) and at altitudes from 10K feet down to as low as possible. The lower limit in many cases will be determined by terrain characteristics but in relatively flat clear areas the coverage can

RESOLUTION

CURRENT SEPARATION STANDARD

3 MILES/TO 40 MILES

5 MILES/FROM 40 TO 60 MILES

PROPOSED IFR SEPARATION STANDARD

1.5 MILES/FROM 1.5 TO 15 MILES

3 MILES/FROM 15 TO 40 MILES

5 MILES/FROM 40 TO 60 MILES

APPROXIMATE ANGLE REQUIREMENT

D	R	$\theta/1.7$
1.5	15	3.4°
3	40	2.5°
5	60	2.8°

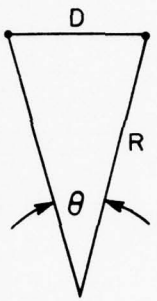

$D = R \frac{\theta}{1.7}$

NOTE: THE FACTOR OF 1.7 RELATES THE -20 db WIDTH TO THE 3db WIDTH OF THE MAIN BEAM.

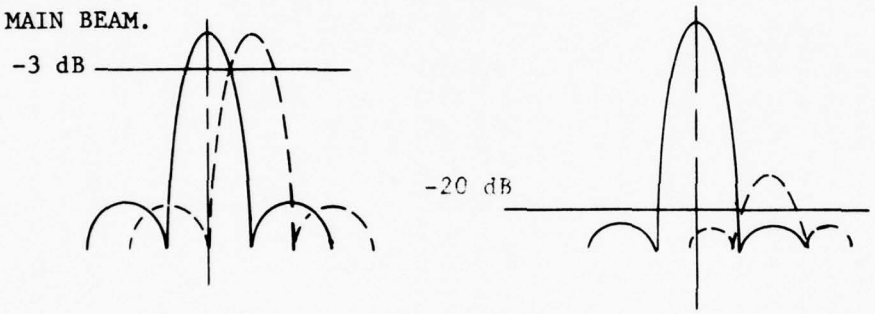

FIGURE 3.2.1

practically be about 0.5 deg. elevation angle. This will result in the theoretical coverage shown in Figure 3.2.2. In areas of especially intensive ground clutter it may be necessary to tilt the antenna upwards by an additional 1 deg. or more in order to reduce the illumination of surface objects. Of course larger targets will be seen at longer ranges and higher altitudes. [The coverage obtained with tilts of 3 deg. (3 dB point at the horizon) and 4 deg. is for targets of 1 square meter cross section (Swerling Type I fluctuation)]. The antenna assumed in these calculations has a conventional 6 deg. beamwidth elevation pattern spoiled in such a way as to produce a $\csc^2$ pattern up to 20 deg. The 20 deg. is considered practical and adequate for the purpose. If a fourth power STC is required (see Section 3.4 on signal processing) out to the order of 4 or 5 miles, targets higher than 20 deg. will not be seen. This antenna will then have a "cone of silence" such that targets above 20 deg. elevation angle will have a very low probability of detection.

3.2.3 Polarization

As will be seen later in Section 3.4 and as detailed in Appendix C, linear polarization can be used at all three frequency bands being considered. This is in part due to the fact that the signal processing chosen is dictated by ground clutter and will handle the weather case easily without resorting to circular polarization to reduce the backscatter from the rain (see Figure C.2). Furthermore, the short range required by the SRTR permits it to realize an advantage in the inverse square range relation of rain clutter over a longer range radar which has to cope with much lower signal strengths. Linear polarization is, therefore, a good selection because of two factors. First a circularly polarized system requires more transmitted power with resultant higher cost. Second, the circularly polarized antenna is slightly more expensive than a linearly polarized antenna. All succeeding considerations in this section will assume linearly polarized antennas.

3.2.4 Multipath

Any discussion of multipath, especially over land, must be very general because of the variety of reflectivity factors encountered. Highly idealized plots of the vertical coverage have been produced for the three frequency bands considered. These are shown in Figures 3.2.3, 3.2.4, and 3.2.5. These plots assume a reflectivity of 0.5 invariant with elevation angle. In practice the reflectivity will vary from near zero to near 1 and will have various phase angles. The figures show a near worst case for overland propagation. They show that as a target flies toward the radar at constant altitude it may suffer multipath fades. The number of the fades will depend on target altitude and frequency as well as the ground reflectivity at the point of reflection between the target and the radar.

The effect exists at all frequencies and will result in discontinuous tracks. It can be seen from the figures that at the higher frequencies the duration of the fades for a straight incoming constant

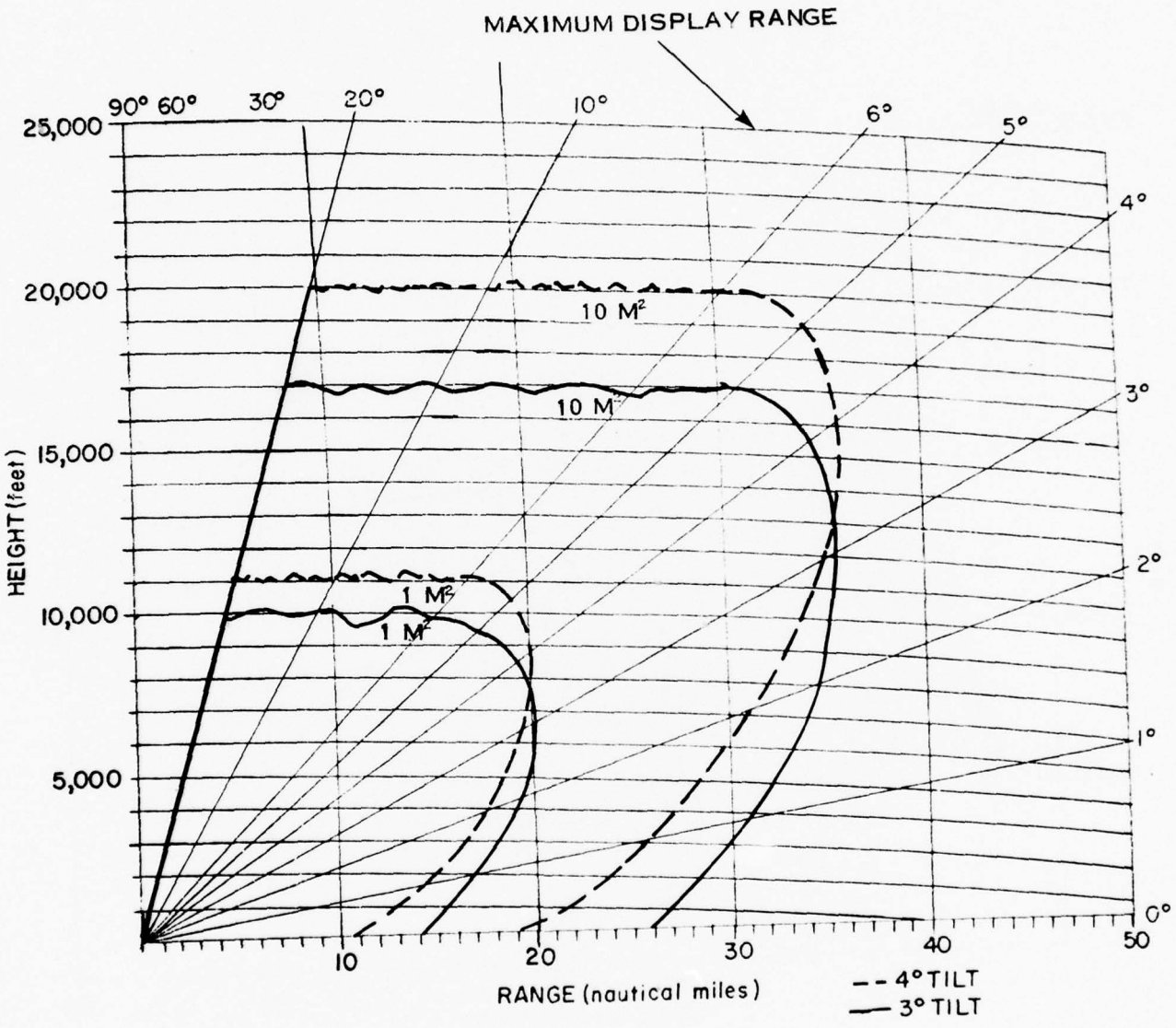

FIGURE 3.2.2 THEORETICAL COVERAGE

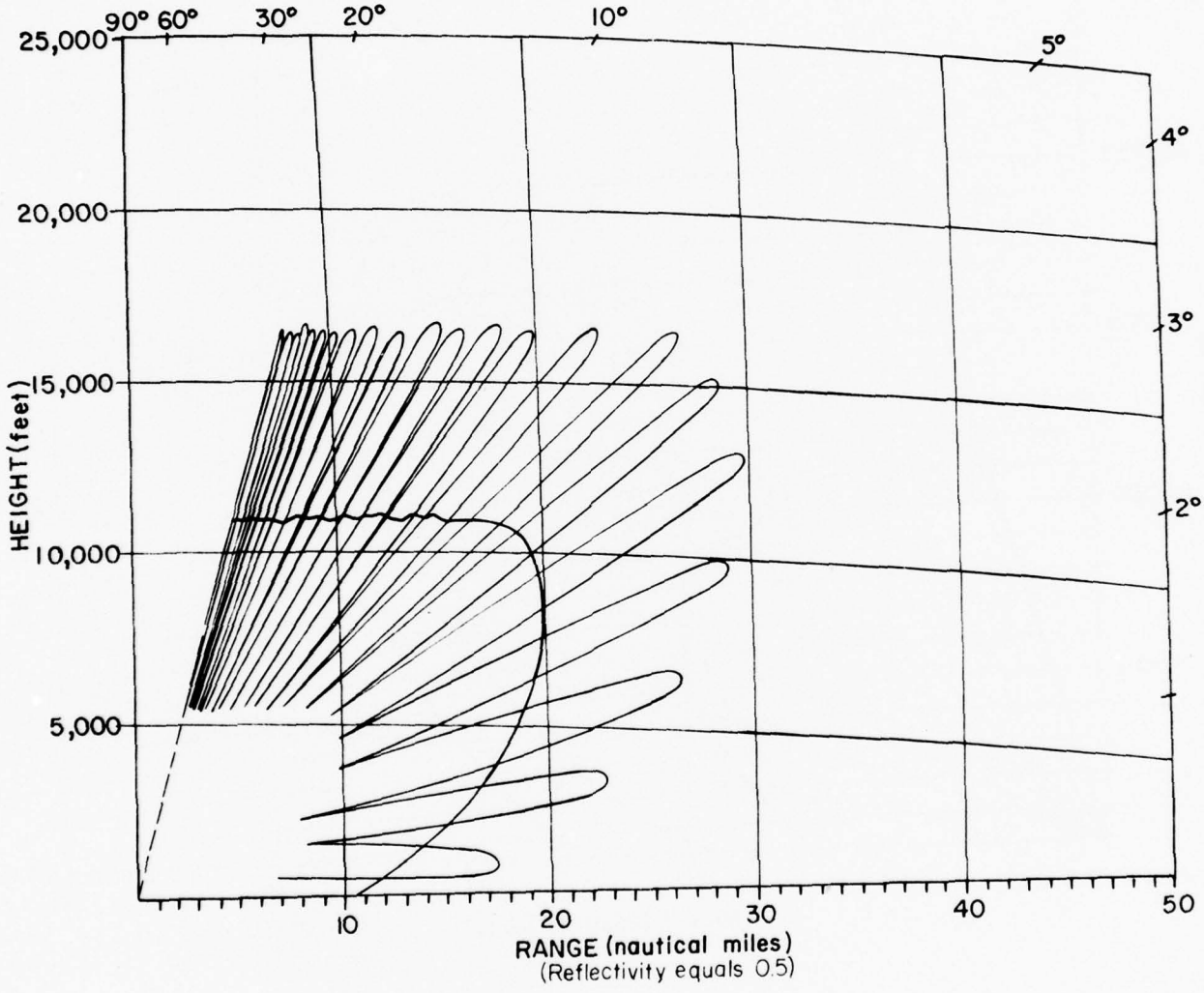

FIGURE 3.2.3 INTERFERENCE PATTERNS (L-BAND)

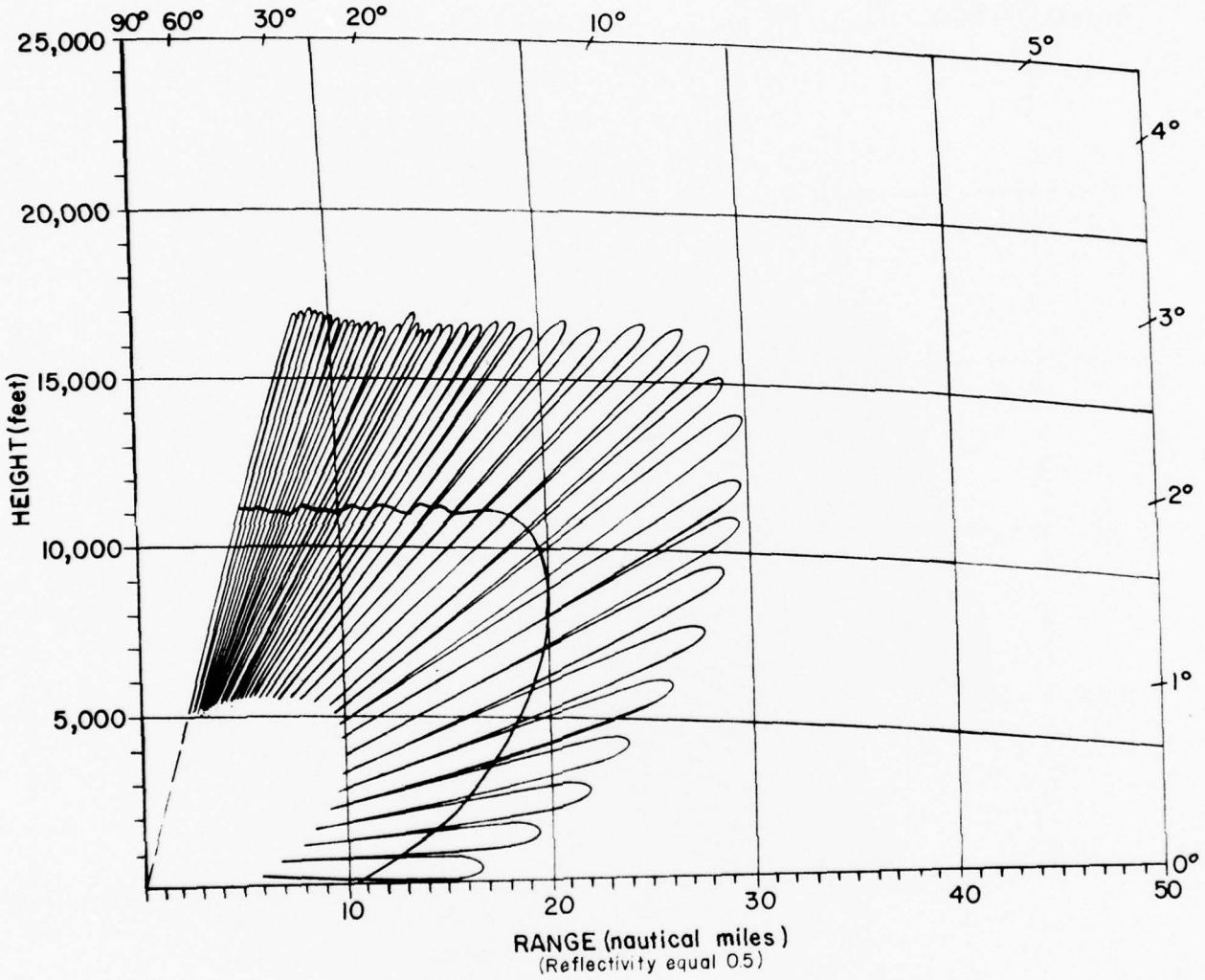

FIGURE 3.2.4 INTERFERENCE PATTERNS (S-BAND)

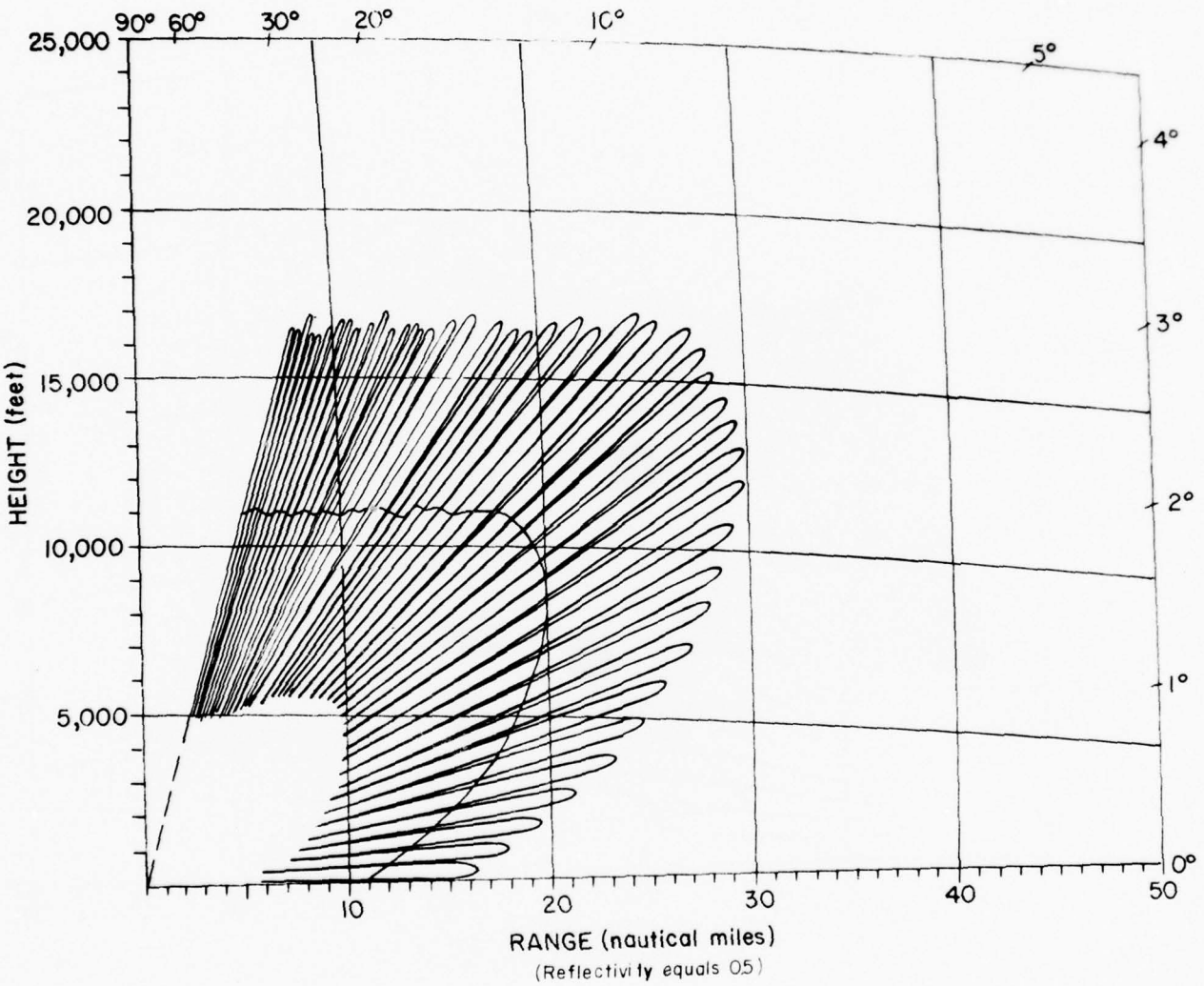

FIGURE 3.2.5

INTERFERENCE PATTERNS (S'-BAND)

speed target will be less. From this point of view the S'band would be best for SRTR. The effect is small enough, however, that multipath alone should not be a strong argument in selection of frequency.

3.2.5 Implementation

The antenna required should have an azimuth beamwidth of 3.4 deg. and should have an elevation beamwidth of 6 deg. (0 to 6 deg.) and should approximate a csc^2 pattern at higher angles (6 to 20 deg.). In order to determine succeeding parameters, it will be necessary to calculate the approximate gain and size of the antennas. These can be approximated by methods outlined in Skolnik (see Skolnik 1962) and shown in more detail in Appendix C. The gain of such an antenna is about 29 dB and its size is as follows:

BAND	WIDTH	HEIGHT
L	15'	9'-15'
S	7'	4'-6.5'
S'	5.5'	3'-5'

The height variation is dependent on whether the csc^2 pattern is obtained by distorting and extending the reflector (from parabolic) or by use of multiple feeds. The multiple feed approach is preferred since it requires the smaller reflector at the cost of additional feed horns and couplers. (A preliminary analysis indicates that a satisfactory pattern can be obtained with one additional horn and one coupler).

If a multiple horn approach is chosen, consideration should be given to using a thumb pattern to increase gain at higher angles and improve performance when small targets at high elevation angles are competing with low altitude clutter (especially birds) at the same slant range. A simplified first cut analysis of such an antenna and feed system is shown in Appendix F.

By comparison with existing systems the total antenna and pedestal weights are estimated as follows:

L-Band	1200-1500 lbs.
S-Band	400-600 lbs.
S'-Band	300-500 lbs.

Additional studies need to be conducted in order to minimize cost of the antenna/pedestal combination.

3.3 TRANSMITTER/RECEIVER

The required transmitter power for the various frequency bands can be calculated from the parameters listed in Section 3.1 and from receiver noise figures assumed. Details of these calculations are shown in Appendix C. Results of these calculations are discussed below.

3.3.1 Coherency Requirements

In Appendix C the required clutter improvement (CI) is calculated. Clutter improvement is defined as the ratio of the signal to clutter at the input of the signal processor to the signal to clutter at the output of the signal processor. These calculations are based on a standard clutter model described in Section 2.4. The results are as follows:

BAND	CI-RAIN	CI-LAND*
L	7 dB	38-44 dB
S	21 dB	38-44 dB
S'	25 dB	38-44 dB

*The lower number is for an antenna tilt of 4 deg. and the higher number is for a tilt of 3 deg. See Section 3.2.2 for elevation coverage with the various tilt angles.

The numbers indicate the need for coherent processing (MTI or doppler) on a per sweep basis. Elimination of second time around ground clutter due to either high ground or anomalous propagation (AP) dictate sweep to sweep coherency. These requirements, which are treated more completely under Signal Processing, Section 3.4, indicate the need for a fully coherent transmitter whose stability is sufficient to support a CI of at least 50 dB. The receiver should be designed with the signal processing in mind. Dynamic range is a prime consideration.

3.3.2 Power Requirements

The required transmitter power (see Appendix C) for the various frequency bands is shown below:

BAND	PEAK POWER	AVG. POWER
L	8 kW	32 W
S	60 kW	236 W
S'	100 kW	391 W

These powers are considered reasonable and the use of any of the bands should be possible. It should be noted that these calculations are critically dependent on assumptions concerning RF losses, processing losses, and antenna gain. Conservative estimates of these values were

used but final design selection of transmitter power should be based on a specific design study which should also take into account possible operational degradation of system elements. Implementation is covered in Section 3.3.4. The cost considerations will be covered in Section 3.10.

3.3.3 Receiver Sensitivity

The receiver sensitivity numbers are based on noise figures attainable "off-the-shelf". The numbers used are summarized below:

BAND	N.F.	SENSITIVITY
L	4 dB	-112 dBm
S	5 dB	-111 dBm
S'	5 dB	-111 dBm

Any improvement that can be achieved will pay off in reduced power and could be considered to be a cost effective tradeoff.

3.3.4 Implementation

The transmitter implementation is probably straightforward. However, the details will be highly dependent on the availability of transmitter tubes. The coherency dictates the use of a master oscillator/power amplifier system (MOPA). Tubes used in typical systems are 3 and 4 cavity klystrons and TWTs. Tubes with near the correct characteristics are shown below. (These are primarily military and are not considered complete. This information is provided to illustrate the general state of the art):

TUBE	MANF.	FREQUENCY	PK PWR	AVG PWR	GAIN	TYPE
SAL41501	SPF	1215-1365	8K	--	28	KLY3
STL161	SPG	1215-1365	6K	36	37	TWT
STL162	SPG	1250-1350	7K	60	38	TWT
VTS5650A1	VAE	2850-3350	100K	500	27	TWT
JAN8128	RAW	2850-3350	60K	1260	20	TWT
PT1006	VAR	2700-3050	200K	270	44	KLY4

SPG - Sperry, Gainesville, Fla.
VAR - Varian, Palo Alto, Calif.
RAW - Raytheon, Waltham, Mass.
VAE - EMI-Varian, Middlesex, England

The general status at L-band is good although some minor modification may be required. The situation at S-band and S'-band is slightly less optimistic in that fewer tubes are available and more modification may be required. In particular, frequency scaling probably will be necessary. Extreme stability and long life should be readily achievable at the power levels indicated.

Modulator requirements are modest with voltage/current of 16-20 kV/4-5 amps being required at L-band and 30-40 kV/14-18 amps being required at S or S'-bands. Solid state modulators of the type developed for the ASR-8 promise high-stability and long life in the SRTR application. Drive signals for the tubes indicated range from 600 W down to 1 W. The drivers may be solid state or possibly require another klystron or TWT.

The receivers are well within the state of the art. Parametric amplifiers may be required. Dynamic range, noise figure, stability and reliability are the major considerations.

3.4 SIGNAL AND INFORMATION PROCESSING CONSIDERATIONS

3.4.1 General

3.4.1.1 General Block Diagram and Description of Processing System

The radar and its processing and display system may be simply represented by the functional block diagram shown in Figure 3.4.1. The radar system consists of the radar which sends data to a signal processor, usually an MTI type processor, whose filter shape discriminates against fixed targets. This is followed by a detector and then by some type of noncoherent post-detection integration system to help enhance the signal in the presence of noise and extraneous clutter, such as rain and strong ground clutter backscatter. The resulting signals are then presented on a PPI (Plan Position Indicator) display which presents those signals which have exceeded a fixed threshold.

3.4.1.2 Historical Techniques for Processing, Thresholding and Displaying ASR Radar Data

When aircraft surveillance radars were developed for air defense purposes in the late 1940's and early 1950's, inexpensive, fast, reliable, low cost, solid state logic modules had not yet been developed. General purpose digital computers were just being developed. In that time frame, all signal and post-detection processing were done using analog techniques and the results were displayed on an analog display, the PPI. With these PPI's, the amplitude of the thresholded and processed signals (targets) could only be displayed with limited dynamic range. In order to optimize the operators' detection of aircraft on PPI's, it was found that limiting the clutter at the IF stage of the radar receiver would make the RMS noise due to clutter equal to that due to the receiver, and under these conditions and assumptions the detection of aircraft was optimized. Also, these systems employed a fixed threshold for the entire radar coverage. This threshold could be controlled by the radar operator, but it could not be varied from geographical area to area.

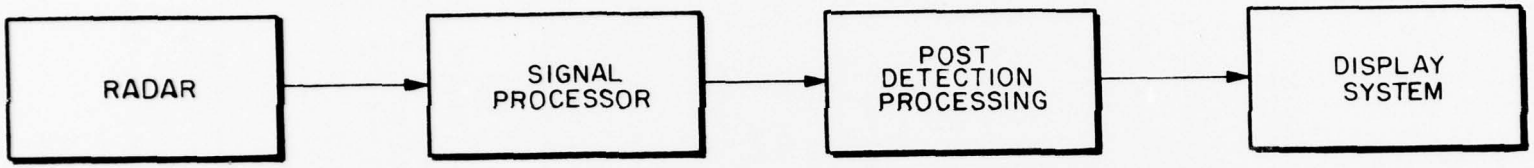

FIGURE 3.4.1 SIMPLIFIED RADAR SYSTEM BLOCK DIAGRAM

Since these early days of radar, technology has changed drastically. Of greatest importance, the advent of low cost, reliable, fast, solid-state integrated circuit logic has made possible revolutionary changes in the ability of the radar to process large quantities of data fast and reliably. With the use of these new techniques, significant advances (see Booker 1947, Freehafer 1951, and Randall 1966) have been made to optimally process, threshold and display air traffic control radar data.

3.4.2 Implications of Coherency and Inexpensive Fast Digital Logic on Signal Processing

3.4.2.1 Clutter Improvement Requirements

The ground clutter backscatter coefficient varies appreciably from spot to spot in the area of coverage. The main contribution to the spectral spread of the ground clutter comes from the amplitude modulation of the ground clutter by the antenna's beam shape as the radar scans by the clutter from pulse to pulse. The present ASR radars suppress ground clutter by three mechanisms: MTI (Moving Target Indicator) techniques, antenna tilt and by mounting the antenna close to the ground to take advantage of the shielding effect of nearby objects. The MTI processors in these radars employ limiting in the IF, followed by a phase detector. The purpose of the limiting is to normalize the video output so that clutter residue from the MTI filter is reduced to the average noise level. This limiting action spreads the clutter spectrum so that it is more difficult to see moving targets in the presence of ground clutter than if the normalization had been done by some other mechanism not involving nonlinearities. The performance of S-band, three-pulse cancellers with and without limiting are presented in Freehafer 1951.

In order to obtain a reasonable signal-to-clutter ratio, it is commonplace for the present ASR's to tilt the antenna upward by 2 to 5 degrees depending on the local clutter situation. This advantage is offset by the degraded detectability of aircraft flying at low elevation angles.

By keeping the receiver and signal processing systems linear, greatly improved subclutter visibility can be achieved. The necessary clutter improvement for both rain and ground clutter have been calculated and are presented for L-band, S-band and UHF in Figure 3.4.2. These assume a 2 microsecond pulse, a 3.4 degree azimuthal beamwidth, a 2000 Hz PRF and a ground clutter cross section of -18 dB (95 percentile value obtained from Levingston). (see Levingston 1970)

In the so-called "second-time-around" clutter effect, returns are being received due to illumination of clutter beyond the nonambiguous range by the next-to-last pulse transmitted. These returns are prevalent where conditions for anomalous propagation exist or in regions where

FREQUENCY	PULSEWIDTH	PRF	*CLUTTER IMPROVEMENT (RAIN) 16 mm/hr.	**CLUTTER IMPROVEMENT Level dB
UHF	2 μsec	2000 Hz	0	44
L	2 μsec	2000 Hz	7	44
S	2 μsec	2000 Hz	21	44
S'	2 μsec	2000 Hz	25	44

Table assumes 3.4° Beamwidth

*Assumes Linear Polarization on all Bands

**Assumes 6 dB Tilt Improvement (3° Tilt)

FIGURE 3.4.2 CLUTTER IMPROVEMENT REQUIREMENTS

mountains exist beyond the nonambiguous range. Present ASR's use magnetron transmitters that transmit pulses with random phase from pulse to pulse. Thus, it is impossible to maintain the phase relation between the first- and second-time-around clutter returns and the two cannot be filtered out simultaneously. As shown later, if a coherent, klystron or TWT-type transmitter is employed and then groups of pulses are coherently processed in the MTI processor, the second-time-around clutter problem may be eliminated.

3.4.3 Range Coverage and Range and Doppler Velocity Ambiguities

3.4.3.1 Range and Elevation Angle Coverage

Operational requirements state that the radar should have good detectability against a one square meter target at 16 nmi on the horizon. Because the antenna will be tilted up slightly (3 degrees) this implies a detection range of 20 nmi on a one square meter target. This coverage will extend to 6 degree csc^2 beam shape. It should be noted that with these performance characteristics the radar will have the ability to detect targets of 10 square meter size out to a range of about 32 nmi and an altitude of about 17,000 feet. These coverage patterns for 3 and 4 degree elevation angle tilt are shown in Figure 3.2.2. Because of this added capability, the radar will be instrumented to 32 nmi.

3.4.3.2 Range and Doppler Velocity Ambiguities

The relationship between ambiguous range and pulse repetition rate (PRF) is shown in Figure 3.4.3. This figure shows that any PRF below 2700 Hz will have no range ambiguities from zero to 32 nmi.

The ambiguous doppler velocity is related to both the PRF and the radar frequency. This relationship is plotted in Figure 3.4.4 for the frequency bands under consideration; high S-Band (S'), S-band, L-band and UHF. Since aircraft in the terminal control area are required to have a speed less than 250 knots, note that for high S-band and S-band even at a PRF of 2700 Hz, the velocity will be ambiguous at times. This ambiguity can be resolved by transmitting coherent pulse trains at alternating PRF's differing by 20 percent or so. At L-band, there is no problem with velocity ambiguities even at 2000 Hz.

3.5 SIGNAL PROCESSING IMPLEMENTATION

3.5.1 General

Over the past four years MIT Lincoln Laboratory has developed for use with the present and future ASR's, a signal processing system which significantly enhances the ability of the ASR's to automatically detect all aircraft in its coverage while still rejecting ground clutter, weather clutter and angels.

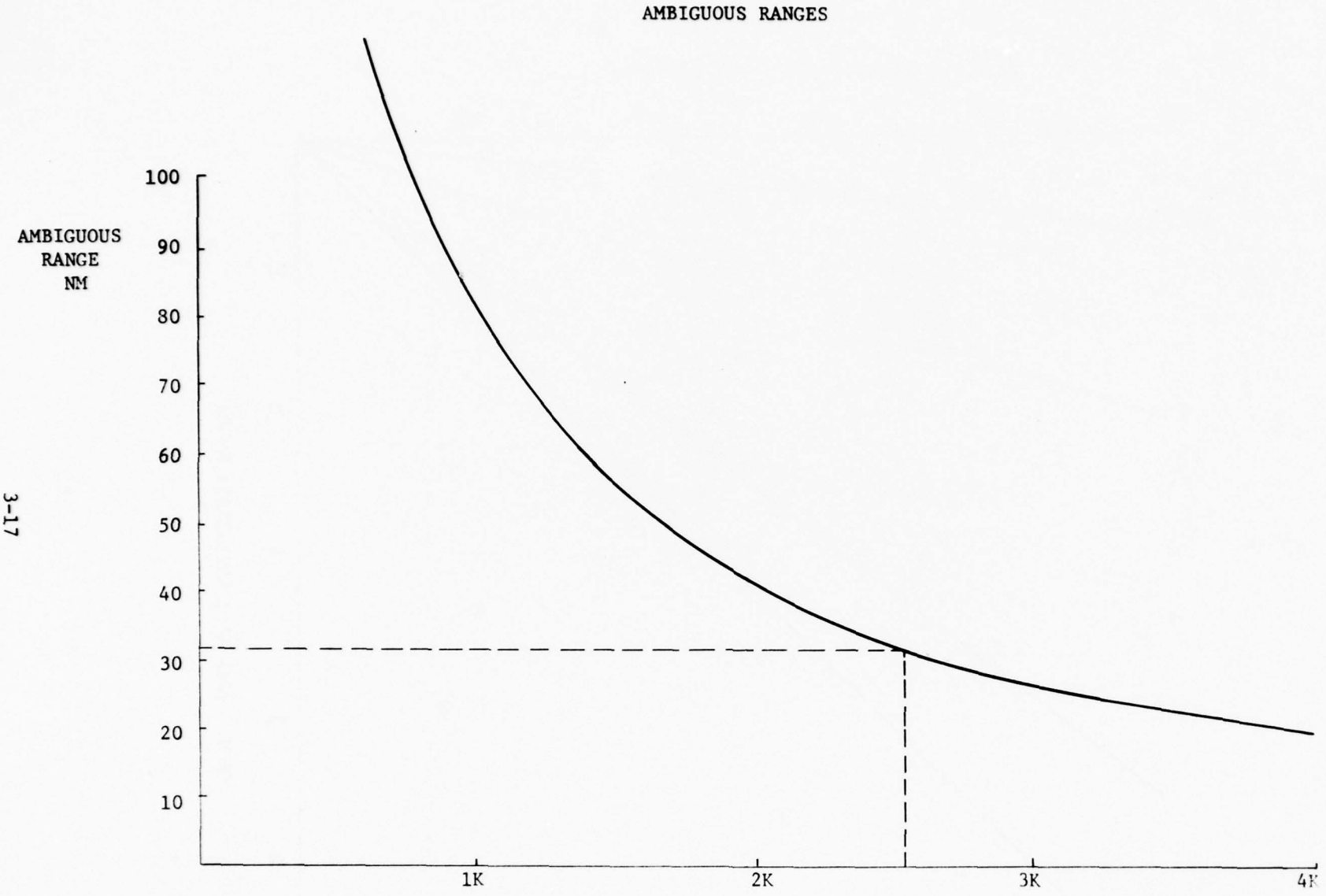
AMBIGUOUS RANGES
AMBIGUOUS RANGE NM
100
90
80
70
60
50
40
30
20
10
1K
2K
3K
4K
PULSE REPETITION RATE (PRF) IN Hz

FIGURE 3.4.3

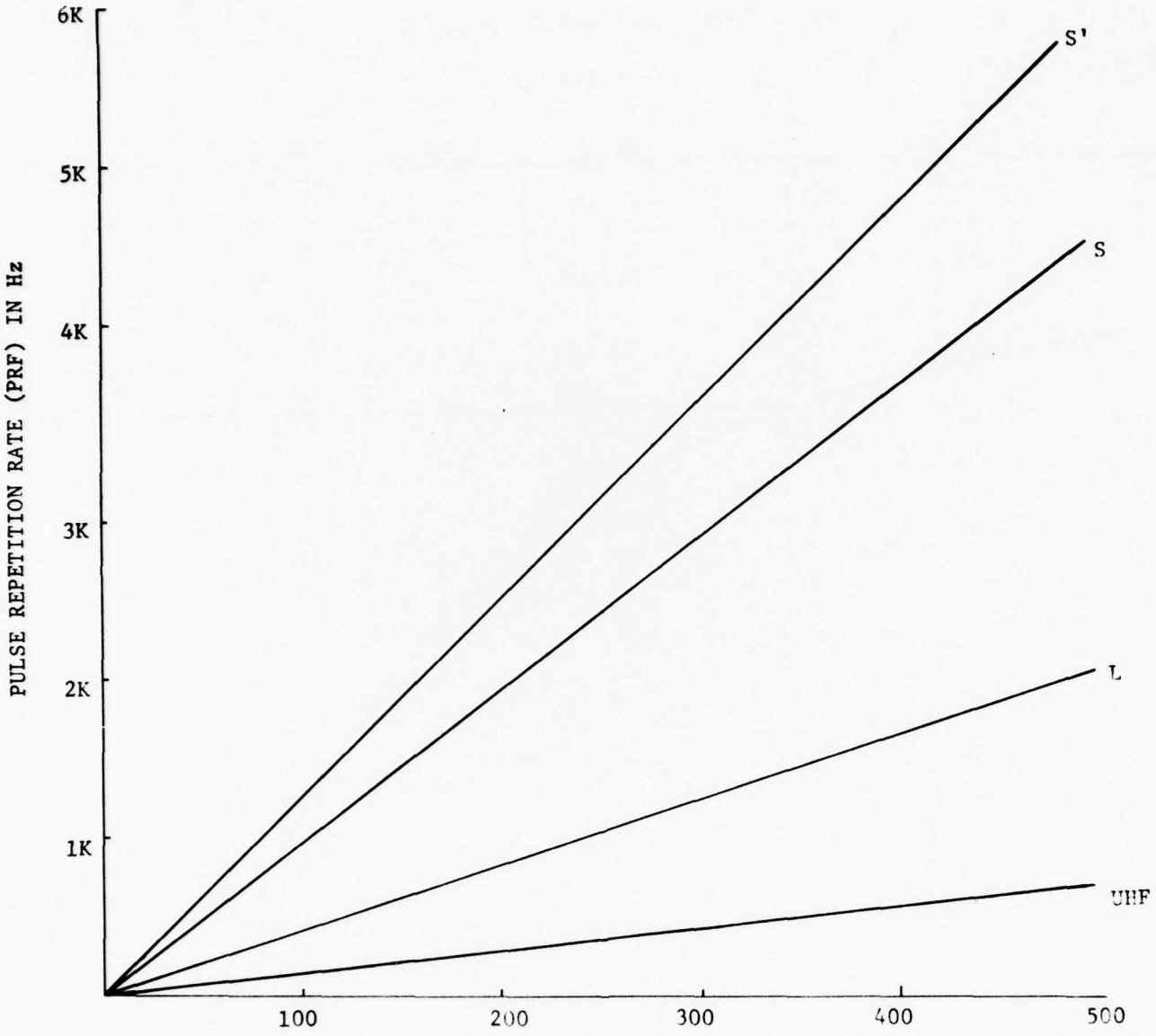

FIGURE 3.4.4 BLIND SPEED IN KNOTS

This system, developed for the FAA (ARD-240) was tested at NAFEC during the summer of 1975. Results indicate that these newly developed techniques can be exploited in the design of the Short Range Terminal Radar (SRTR) and the cost of the signal processor employing these new techniques for SRTR will be less than for ASR implementation, but will have the same optimal performance.

The first MTD (Moving Target Detector) processor (see Appendix G) was a special purpose, hard-wired, digital signal processor. The processor which coherently integrates ten pulses has both a fine grained clutter map for optimal thresholding in high ground clutter environments and a mean-level thresholding scheme for filtering those doppler cells which contain heavy precipitation. Because of the processor's ability to detect targets in a high ground clutter environment, air traffic control radars will be able to operate their antennas at lower elevation angles and, thus, have better coverage of low flying aircraft near the terminal.

The processor has been initially tested on a highly modified, coherent, S-band, FPS-18 radar. The stability of the klystron transmitter was improved so that it would not limit system performance and a new, wide bandwidth, linear receiver was provided. Also tested alongside the MTD was the RVD-4, a non-coherent digitizer developed recently by the FAA. Results of simultaneous radar only output from the ARTS-III tracker are displayed in Figures 3.4.5 and 3.4.6 for the tests in heavy rain and ground clutter.

3.5.2 Summary of Advantages of Processor Employing MTD Technology (see Table 3.5.1)

(a) By keeping the receiver linear over the entire range of anticipated ground clutter amplitude, the MTI subclutter visibility has been increased by about 20-25 dB, thus achieving good detectability even at long range and low elevation angles.

(b) The ground clutter map thresholding scheme gives good visibility against targets with zero radial velocity whose cross section is larger than that of the ground clutter.

(c) By coherently processing groups of pulses whose interpulse period is constant from pulse to pulse, second-time-around clutter problems are eliminated.

(d) By doppler processing and mean-level thresholding each doppler cell independently and by employing multiple PRF's, aircraft are clearly detected in the presence of rain while the rain does not produce false detections.

(e) Optimal adaptive thresholding results in such clean data that it may be remoted to display system over low cost, narrow bandwidth transmission lines.

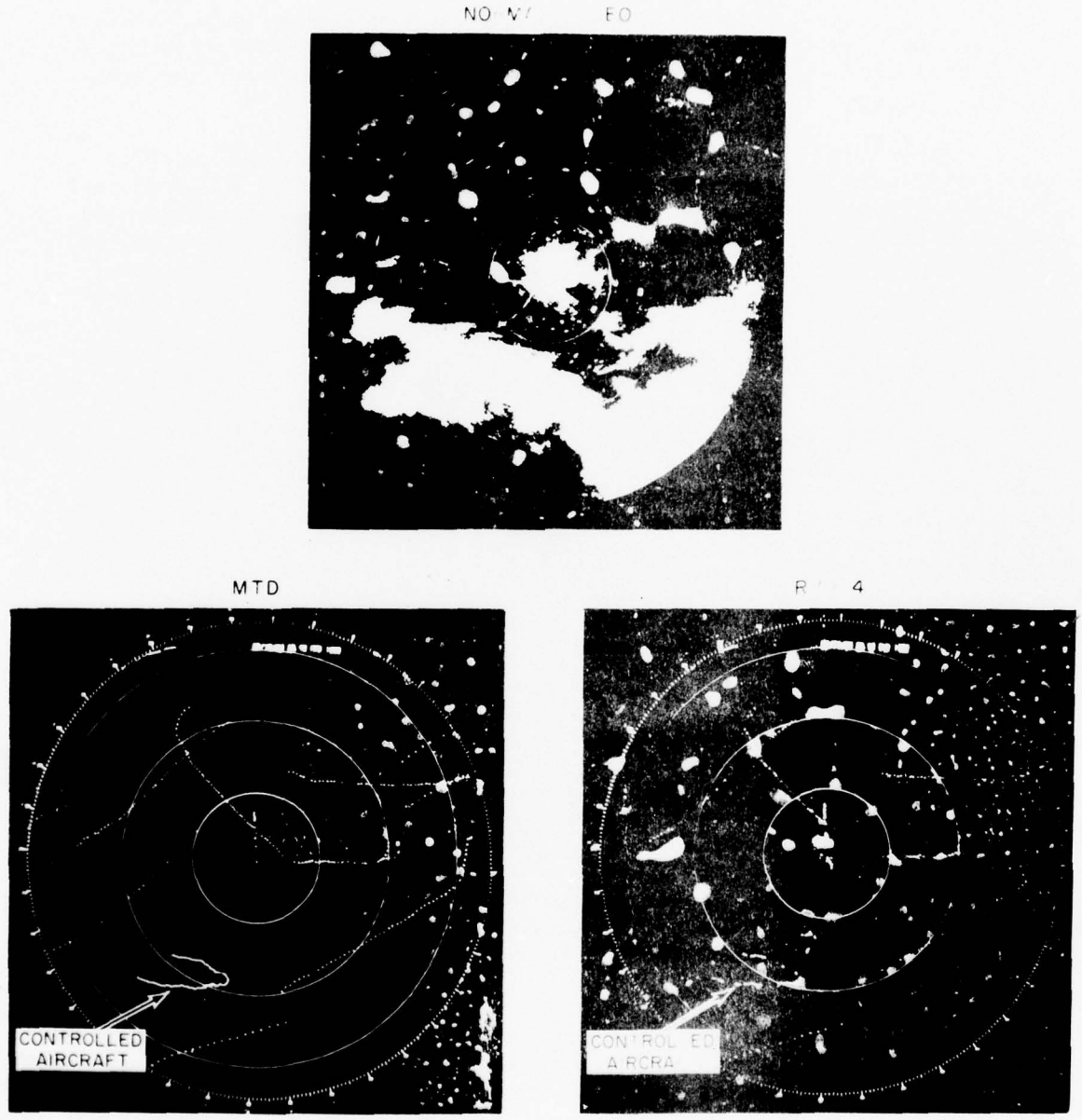

PERFORMANCE IN PRECIPITATION
(5 nmi. Range Rings)

FIGURE 3.4.5

NORMAL VIDEO

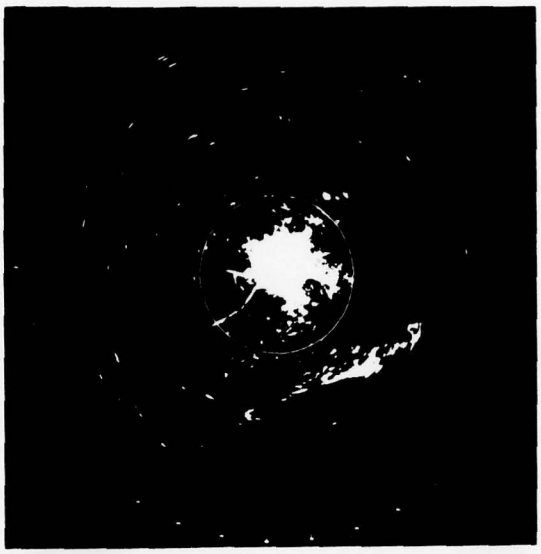

MTD

RVD-4

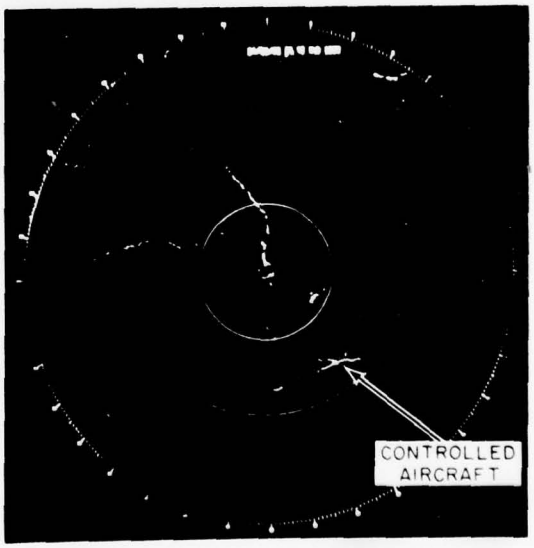

PERFORMANCE IN GROUND CLUTTER
(5 nmi Ronge Rings)

FIGURE 3.4.6

TABLE 3.5.1

MOVING TARGET DETECTOR (MTD) ADVANTAGES

Ground Clutter	20 dB Improvement Siting Freedom Better Velocity Response Tangential Target Visibility Better Low Altitude Coverage
Second-Time-Around Clutter	Eliminated
Weather Clutter	Elimination of False Alarms Most Target Velocities Visible
Detection Optimized for Each Range, Azimuth, Velocity Cell	
No Knobs - Completely Adaptive With Time	
Digital Output - Narrow Bandwidth Transmission of Data	

3.5.3 Design and Cost of Signal Processor Using MTD Technology

In October 1976, the FAA initiated funding of a second generation Moving Target Detector (MTD-II). This MTD-II will be microprogrammable and will have parallel structure (see Appendix G). The signal processing and thresholding algorithms will be similar to those used in MTD-I but will have better MTI performance and better performance in rain. In addition, the structure of the processor has been designed for increased reliability and maintainability. The MTD-II was developed to use the signal processing algorithms tested successfully in MTD-I at NAFEC by implementing them in a system that can be readily commissioned for field use by the Airways Facilities Branch in operational ASR's and ARSR's.

With these developments in mind, the general design and performance of the SRTR signal processor would be the same as that of the MTD-II processor. It should be noted that almost all of the SRTR/MTD-II research and development will have been done in the ASR-7/MTD-II development now underway. A major part of the cost of the MTD's parts is the core memory storage used to store the complex voltage samples of the 10 pulses for each of the 760 range cells and also the disc used to store the ground clutter level for thresholding each of the ASR's 350,000 range azimuth cells. Since the SRTR would have both a larger range and azimuth cell size and shorter instrumented range (32 nmi as opposed to 48 nmi), the capacity of these storage devices and, thus, their cost will decrease drastically, but the processor performance of the MTD design will not be compromised. In Table 3.5.2 the number of range cells is shown for the FPS-18/MTD configuration and for the SRTR instrumented to 32 and 20 nmi. In Table 3.5.3 a similar comparison is made for the number of azimuth cells. In the MTD prototype there is an azimuth cell stored on the clutter map for each CPI (Coherent Processing Interval) while with the SRTR the map will use the average clutter level for a beamwidth to conserve storage space. In Table 3.5.4 the number of range azimuth cells is compared. With the MTD's 370,000 range azimuth cells in the clutter map a disc is the most economical means of storage, but in a 32-nmi SRTR digital CCD memory will be the most economical means of implementation.

With the reduced storage requirements the cost of MTD-type processing is quite reasonable. Table 3.5.5 breaks down the component costs of the processor. These costs are for parts but the $5/IC cost estimate includes an estimate for interconnecting. The cost for a production version of an MTD-type processor for the SRTR would likely be less than $30K, the value used in our radar system cost estimates. It is also felt that the extra cost of instrumenting the radar out to 32 nmi instead of 20 nmi is small compared to the total cost of the processor. A lot of coverage on large targets is gained at little processing cost. Also, it should be noted that the cost per function of integrated circuits has dropped a factor of two per year for the last ten years and is projected to continue at this rate for at least the next eight to ten years. Thus, these signal processing costs which are in 1976 dollars should be judged conservative when it is realized that the SRTR would be procured several years hence, and that the integrated circuit costs are dropping much faster than inflation is rising.

Finally, it is concluded that all of the performance features of the MTD-type processor can be incorporated into the SRTR at reasonable cost.

TABLE 3.5.2

RANGE CELLS

RADAR TYPE	RANGE RESOLUTION	MAX. RANGE	NO. OF RANGE CELLS
FPS-18/MTD	1/16 nmi (0.833 μsec)	48 nmi	760 cells
L-band or S-band SRTR	0.15 nmi (2 μsec)	20 nmi	133 cells
L-band or S-band SRTR	0.15 nmi (2 μsec)	32 nmi	213 cells

TABLE 3.5.3

AZIMUTH CELLS

RADAR TYPE	AZIMUTH BEAMWIDTH	NO. CPI/ REVOLUTION	PRF	NO. AZIMUTH CELLS
FPS-18/MTD	1 1/2°	480	1200 Hz	480
L-band or S-band (SRTR) (2 μ sec)	3.4°	900*	2000 Hz	100

*4 sec/revolution of antenna assumed

TABLE 3.5.4

RANGE - AZIMUTH CELLS

RADAR	NO. RANGE CELLS	NO. AZIMUTH CELLS	NO. RANGE-AZIMUTH CELLS
FPS-18/MTD	768	480	370,000
SRTR* (20 nmi range)	**123	100	12,300
SRTR* (32 nmi range)	**198	100	19,800

*SRTR Parameters Assumed

3.4° beamwidth
2000 Hz PRF
2 μsec pulse
4 sec data rate

**Instrumented Range

TABLE 3.5.5

COST OF THE MTD PROCESSING*

	SRTR**(32 nmi)	SRTR**(20 nmi)
Processing Elements	$ 3,600 (3 PE's)	$ 2,400 (2 PE's)
Memory and Map Cards	920	740
Controller	1,200	1,200
Power Supplies	900	900
Cabinet	1,500	1,500
Cabling	1,100	1,100
Distribution Cards	1,800	1,800
Radar Controller and Interrupt Vector	1,200	1,200
Slice Assignment Module	800	800
	$13,020	$11,640

*These costs are for parts only, but IC costs include interconnection costs

**SRTR parameters assumed - see Table 3.5.4

3.6 INFORMATION PROCESSING AND DISPLAY

3.6.1 General

After the signal processor, two types of processing are required to filter the radar output before presenting it to the controller. First is intra-scan correlation which consolidates the many threshold crossings from one target into a single report and from the many reports, estimates the target centroid in amplitude, range, doppler and azimuth. Second, there is the function of inter-scan correlation; this process would correlate reports over a few scans, deleting reports from low velocity tracks such as cars and bird flocks. These two functions can easily be performed in a minicomputer.

3.6.2 Weather Output Processing

In order to determine the capability of a proposed system to detect weather, it is necessary to calculate the amplitude of the signal received from rainfall. This has been done using the equation at the top of Figure 3.6.1. It is assumed that if the rain return exceeds the receiver noise by 10 dB that it will be detectable. The range at which the rain-to-noise ratio equals 10 dB has been calculated for two rain rates, 1 mm/hr and 16 mm/hr. The ranges are tabulated in Figure 3.6.1. The results show that a 16 mm/hr rain can be detected by any of the radars listed out to a range of at least 20 nmi. A 1 mm/hr rain can be marginally detected at S-band and S'-band but cannot be satisfactorily detected at L-band.

At present the MTD processor has a weather level output. It is formed by summing the amplitudes of the returns for doppler cells 1 through 7 for each range azimuth cell. This data can then be routed to a minicomputer and single level weather contours (Figure 3.6.2) can be generated for display to the air controllers.

3.6.3 Displays (Scan History Display)

Radar target data from the information processor (mini-) computer will be displayed on a digital display in a standard scan history format. One or more levels of weather contours will also be displayed. The target reports from the most recent scan will be displayed with a symbol different from that used to display the previous scan's target reports. This will indicate the direction of the aircraft to the air controllers. A typical scan history display format is shown in Figure 3.6.2.

3.7 RADIO FREQUENCY INTERFERENCE AND BANDWIDTH UTILIZATION

The determination of parameters for minimizing Radio Frequency Interference (RFI) tend to establish how an available bandwidth may best be utilized. RFI is, therefore, considered first and its implications on bandwidth utilization taken up next.

RAIN AMPLITUDE

$$R^2 = \frac{P_T G_T G_R \sigma_0 \theta \phi \frac{C\tau}{2} \lambda^2}{(4\pi)^3 (KTBF) L_T L_R \frac{RAIN}{NOISE}}$$

BAND	PRF (PPS)	(μSEC) (PW)	AZIMUTH BEAMWIDTH	RANGE (NMI) 1 MM/HR	RANGE (NMI) 16 MM/HR
L	2000	2	3.4	2	20
S	2000	2	3.4	14	100
S'	2000	2	3.4	16	110
S (ASR-8 MOD)	1000	0.8	1.5	16	100
S (ASR-8)	1000	0.8	1.5	80	500

FIGURE 3.6.1

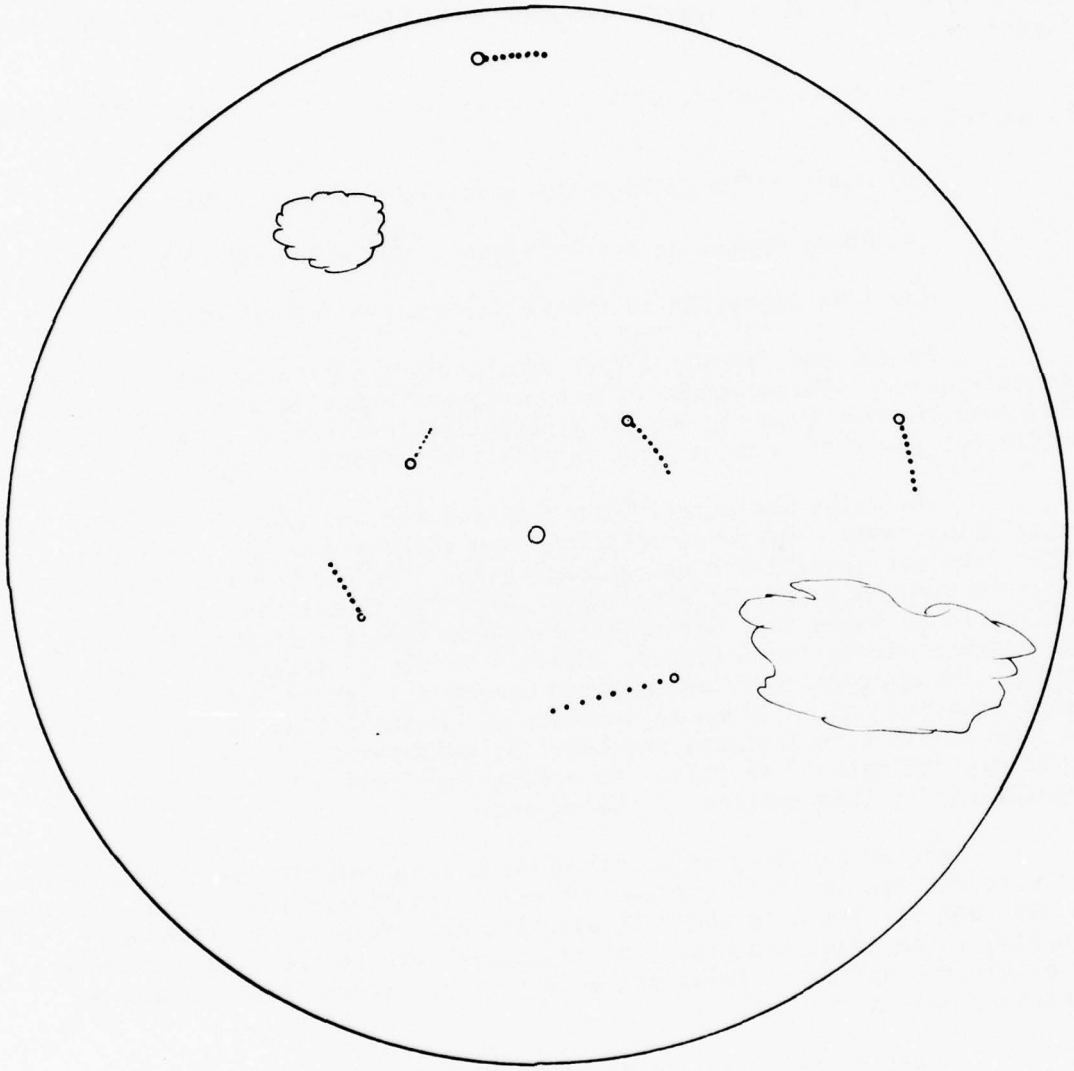

FIGURE 3.6.2

TYPICAL SCAN HISTORY DISPLAY

3.7.1 RFI

The SRTR may be exposed to many sources of RFI, such as electrical machinery noise and spurious emitter signals. However, the latter tend to be random in nature and, though important, do not have the impact of radars operating at the same band and within reasonable distances. The radar RFI problem is further aggravated because pulse widths, PRFs, and scan rates become comparable in equipment designed to perform similar if not identical functions.

The three most important sources of radar RFI to the SRTRs would be as follows:

(a) Other SRTRs within a vicinity of the victim SRTR,

(b) ARSRs operating in the vicinity of an L-Band SRTR,

(c) ASRs operating in the vicinity of an S-Band SRTR.

In (b) and (c) the effect of the SRTRs on the ARSRs or ASRs is not calculated. Calculations of frequency and range separation to prevent SRTR interference from these radars establish that the SRTR cannot muster sufficient power or antenna gain to affect the ARSRs or ASRs.

The radar characteristics that enhance interference are the interfering radar's RF power spectrum, and antenna gain and the victim radar receiver sensitivity and antenna gain. The factors that tend to lower interference are the propagation loss and the victim receiver ability to be tuned to a different frequency than the interfering radar. The measure of how these factors interact is the interference to noise ratio. The expression relating these parameters is derived from the radar range equation and is given in Appendix A. A significant reduction of RFI is also possible in a signal processor by establishing logic that rejects obviously "illogical" targets. No attempt has been made to explore this possibility in this section of the report.

The probability of mutual antenna gain coupling is calculated in A.1 with the result that, for two uniformly scanning antennas, the sidelobe to sidelobe situation is the most significant. Mainlobe to sidelobe coupling is at least two orders of magnitude less probable and mainlobe to mainlobe coupling is least probable by four orders of magnitude, as clearly expected.

A set of calculations detailed in A.2 permit the quantification of range separation as a function of frequency separation for three values of interfering pulse spectral power density. The calculations were made for the three interfering sources discussed above. It must be pointed out that in all cases where value judgements were made during the calculation the results were slanted to provide conservative estimates, thus predicting

"worst case" bounds. For example, the required interference to noise ratio was set at unity though it is possible to operate with a value of 10. (See Skolnik, 1970).

The plots indicate that SRTR to SRTR range separations of 10 nautical miles are highly plausible, given 50 MHz center frequency separations, and accepting the low probability main beam to main beam interference. The ARSR to L-Band SRTR range separation should be 22.5 miles for the same frequency separation. The ASR to S-Band range separation should be about 17.5 miles for the chosen 50 MHz separation.

3.7.2 Bandwidth Utilization

The results of the calculations discussed in the previous section lead to some conclusions concerning bandwidth utilization. These are:

(a) The frequency allocation at L-Band is rather small (100 MHz possible, 50 MHz probable) thus leading to some difficulty of siting SRTRs close together. Furthermore, interference from a neighboring ARSR could be a problem. A 20 MHz frequency separation at range separations of 15 nautical miles is possible.

(b) The frequency allocation at S-Band is 200 MHz alleviating the choice of frequencies. However, the population of ASRs makes potential interference from this source a greater problem than in (a) above.

(c) The frequency allocation at S'-Band is 200 MHz and there seems to be no potential source of interference from other than SRTRs.

(d) Serious consideration should be given to shaping the SRTR transmit pulse to reduce spectrum spreading. One technique is to form rise and fall times of at least 10 percent of the pulsewidth. Ideally a Gaussian pulse shape would produce the least sideband power but other considerations may preclude such a waveform.

(e) The design of the antenna should have as a goal the reduction of sidelobes to a minimum. Even though -20 dB sidelobe values were used in the calculation it is felt that the maximum sidelobe levels of -25 dB are achievable.

An example of a possible coexistence of seven SRTRs operating in a rather small area is presented in A.3. Its purpose is to place into perspective the results of the range and frequency separation curves in A.2.

3.8 PACKAGING CONSIDERATIONS

The SRTR should be packaged in a manner which provides efficient utilization of space with emphasis on ease of servicing and maintenance. All equipment except display and remote controls should be contained within a semiportable, low cost environmentally controlled enclosure/shelter.

3.8.1 Equipment Cabinets

It is anticipated that the SRTR will be contained within three primary cabinets (approximately 72 x 19 x 22 inches). (See Figure 3.8.1.) For example, these cabinets could contain:

(a) The transmitter, modulator, synchronizer, power supply, transmitter built-in test equipment and cabinet level fault isolation circuitry,

(b) the receiver/moving target detector, power supply and cabinet level fault isolation circuitry, and

(c) the radar video processor, power supply, cabinet level and master fault isolation circuitry. Space could be allocated in the processor cabinet for including a solid state, low power beacon interrogator and defruiter; however, an additional cabinet could be easily accommodated.

Sub-assemblies within the cabinets should, insofar as possible, be arranged functionally with sub assembly level fault isolation circuitry, to facilitate trouble shooting and corrective maintenance.

Power distribution, antenna drive control, etc. could be located in the transmitter or receiver cabinet.

3.8.2 Antenna Assembly

It is anticipated that the entire radar antenna assembly could be accommodated on the enclosure/shelter roof; however, a separate adjacent tower might be necessary if the "L" band SRTR is selected.

3.8.3 Beacon Antenna Considerations

Two options appear to be available for configuring the beacon antenna system. The option selected will be generally influenced by the SRTR operating frequency band and the resulting radar antenna reflector size and shape. In each case, the sidelobe suppression (P2) omnidirectional dipole could be mounted on a short mast attached to the enclosure/shelter. Option one (Figure 3.8.2) could apply if an "L" band SRTR is selected. This would allow a beacon interrogator dipole feed utilizing the SRTR reflector as the beacon directional (P1/P3) antenna. In option two a beacon antenna would be utilized and mounted either below or atop the SRTR reflector as with ASR systems. (Figure 3.8.3.)

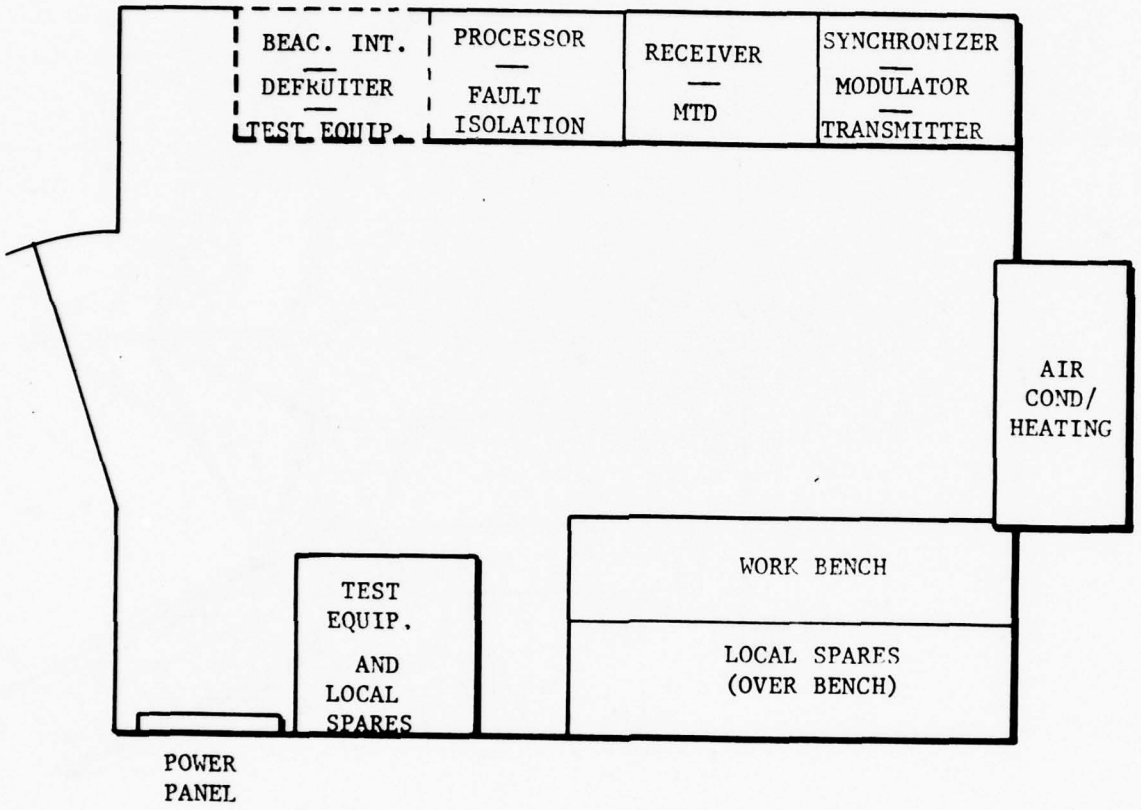

FIGURE 3.8.1 SHORT RANGE TERMINAL RADAR ENCLOSURE
DIMENSIONS - 12'x8'x8'

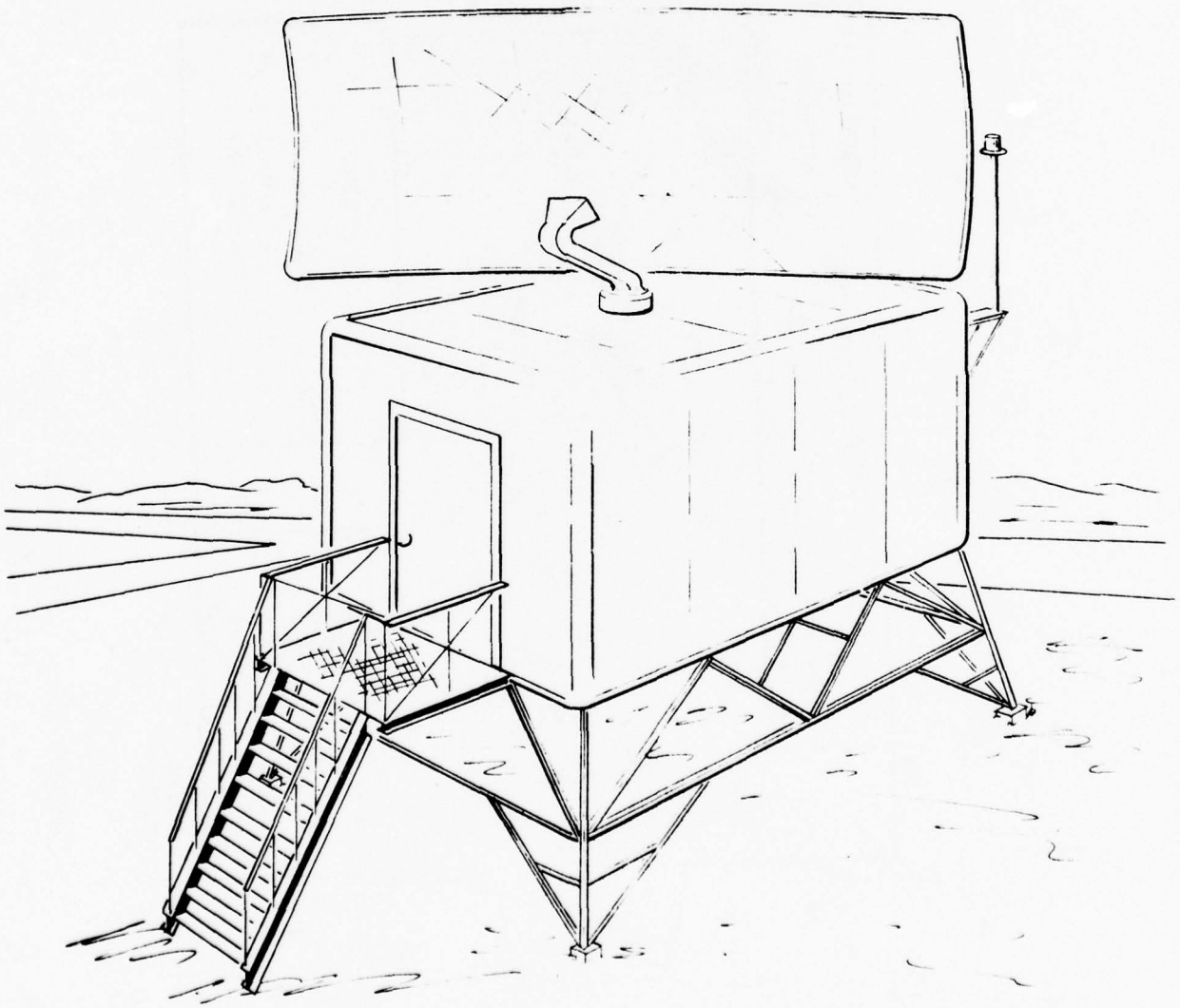

FIGURE 3.8.2

OPTION 1: ADD P2 OMNI ANTENNA/DIPOLE FED COMMON FEEDER

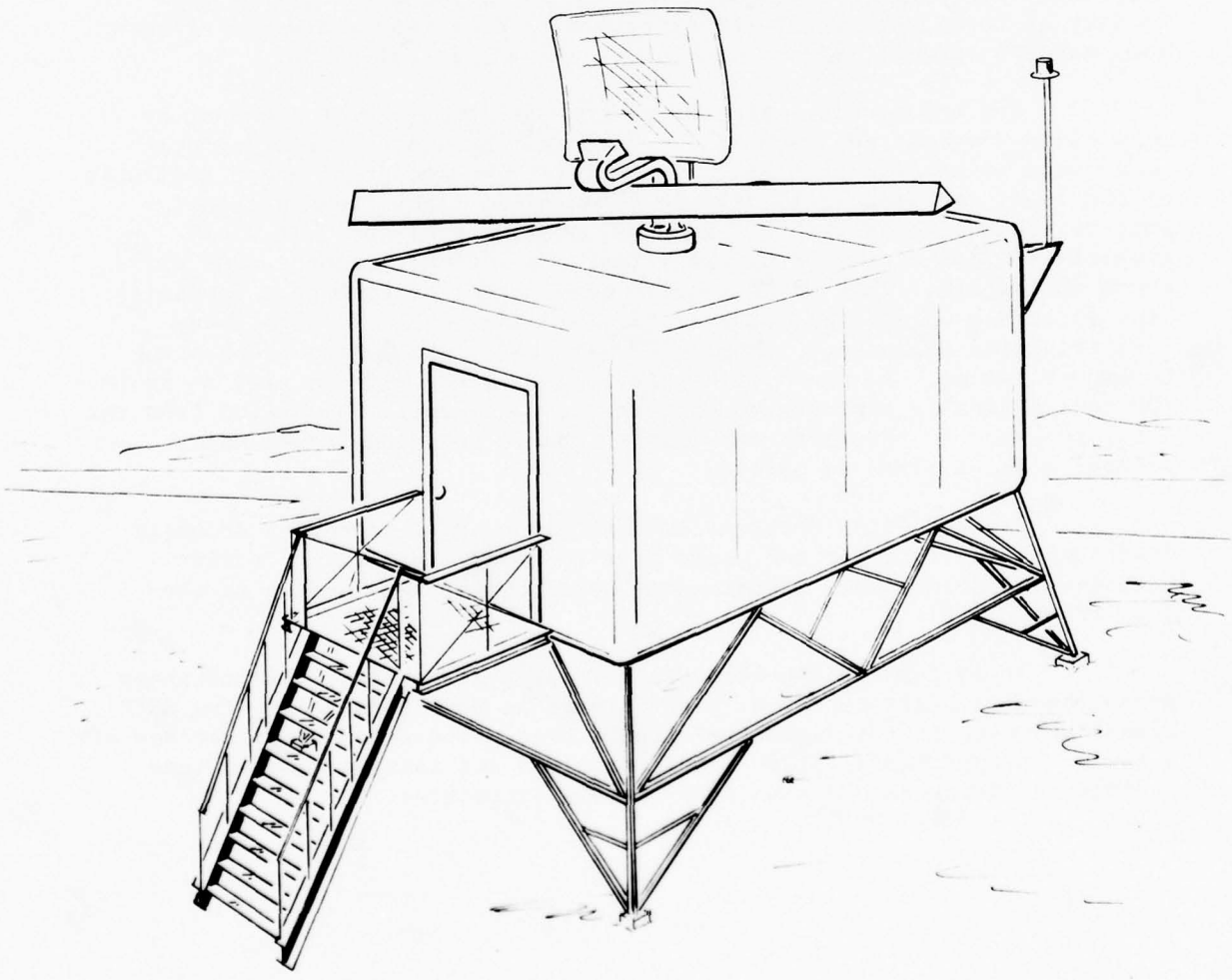

FIGURE 3.8.3

OPTION 2: ADD P2 OMNI ANTENNA/MOUNT
BEACON ANTENNA ON RADAR PEDESTAL

3.8.4 Enclosure/Shelter Description

The SRTR enclosure should be a prefabricated, lightweight, fully insulated, semiportable structure with dimensions of approximately 12 x 8 x 8 feet. It should include limited options for controlling the environment; i.e., temperature and humidity. An electrical power entrance panel with adequate circuit breakers, utility outlets and interior lighting should also be provided.

The enclosure should be shippable by various common modes of transport without unusual handling requirements. It should be suitable for rapidly mounting on prepared base structures of various heights.

3.8.5 Potential Tower Cab Installation

It is possible that the S or S' candidates would have antennas small enough that installation on a tower cab might be feasible. The SRTR Study Group did not consider this to any great extent since the variety of tower cab structures dictate a case by case analysis. However, some general comments may be made about such an installation.

The structural integrity of the particular tower cab must be examined for weight and wind loading. If not adequate, the structure would need to be strengthened. Furthermore, the amount of space available on the tower cab roof would have to be examined since these presently support items such as lights, antennas, anemometers, etc. It would probably be most efficient to place just the antenna, support, and drive motor on the cab. This would require some method of routing a transmission line (probable waveguide), power cable, and data cable to some space containing the equipment. This would have to be done without obscuring tower cab vision. As shown in Figure 3.8.1 a space with an area of 75 to 100 square feet is adequate to contain the equipment. Connection from the data processor to the tower cab display should be accomplished using telephone grade lines as before.

Antenna drive motor noise that might add an annoying acoustic environment in the tower cab would have to be eliminated. Effective acoustic isolation would require some development, thus adding to the cost of the SRTR.

It is felt by the SRTR Study Group that remoting via telephone grade lines is sufficiently straightforward to permit emplacing the SRTR almost anywhere in the immediate airport area. The added complications of a tower cab roof installation should preclude its consideration unless individual circumstances make it extremely attractive.

3.9 RELIABILITY, MAINTAINABILITY, AND AVAILABILITY

The system availability is related to the Mean Time Between Failure (MTBF) and the Mean Time to Repair (MTTR) in the following manner:

$$\text{Availability (\%)} = 1 - \left[\frac{\text{MTTR}}{\text{MTBF}}\right] 100$$

Members of the SRTR Study Group agreed that the following were reasonable and feasible goals:

MTBF = 500 hours minimum
MTTR = 1 hour

Using the above factors, the system availability was computed to be 99.8 percent.

3.10 LIFE CYCLE COSTING

The life cycle costs for each of the three SRTR candidates is presented in Section 3.10.4. These life cycle costs were computed based on a 15 year life cycle with 10 percent compound interest imputed as outlined in "OMB Document Dated March 27, 1972, Circular A-94 (Revised)." In addition to the 15 year cost, the annual and the hourly cost is included.

3.10.1 Radar Procurement Cost

The major portion of the cost of the SRTR would be the cost of the transmitter and the antenna system. Figure 3.10.1 is a plot of cost versus frequency of these items. The conclusion to be drawn is that the total cost (sum plot) of these two items is essentially the same between 1 GHz and 4 GHz. The three candidate system costs for the transmitter and antenna were obtained from this plot. It was assumed that the cost of the signal processor, shelter, built-in test equipment, assembly and test would be the same for each of the candidates. Listed below is a summary of the procurement costs.

ITEM	CANDIDATE L	CANDIDATE S	CANDIDATE S'	*10 MI. VERSION S'
Transmitter/Receiver	$ 30K	$ 55K	$ 64K	$ 35K
Antenna/Pedestal	60	40	38	38
Signal Processor	30	30	30	20
Shelter	5	5	5	5
Remoting and Display	30	30	30	30
Built-In Test Equip.	10	10	10	10
Assembly and Test	20	20	20	20
	$185K	$190K	$197K	$158K

*Subsequent to the basic study it was asked if the SRTR costs could be lowered if the range requirement was reduced to 10 miles. The results of this brief study is presented in the dotted box.

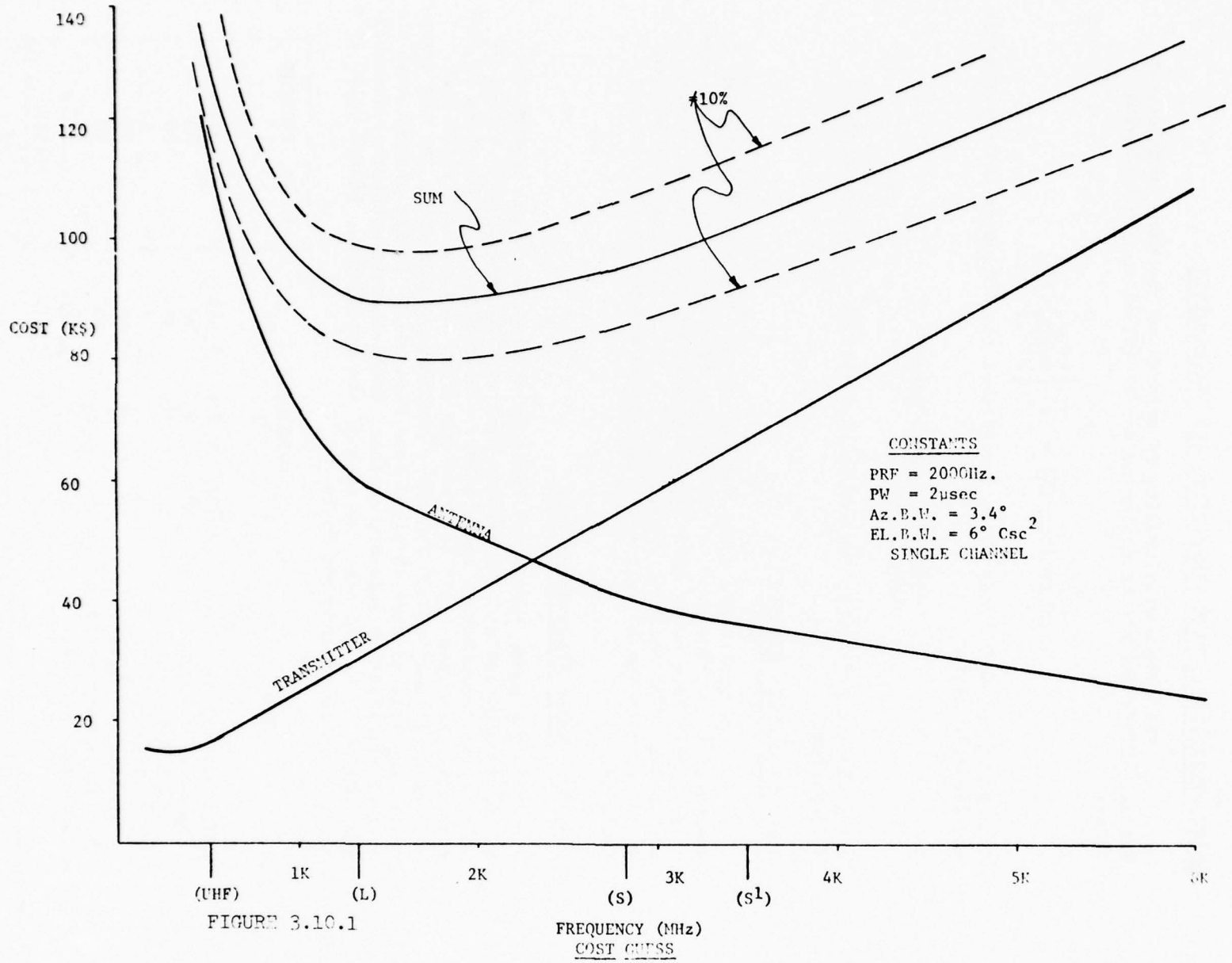
140
120
100
COST (K$)
80
60
40
20
SUM
10%
ANTENNA
TRANSMITTER
CONSTANTS
PRF = 2000Hz.
PW = 2μsec
Az.B.W. = 3.4°
EL.B.W. = 6° Csc^2
SINGLE CHANNEL
1K
2K
3K
4K
5K
6K
(UHF)
(L)
(S)
(S^1)
FREQUENCY (MHz)
COST GUESS

FIGURE 3.10.1

3.10.2 Establishment Costs

The estimated establishment costs of the SRTR are listed below:

ITEM	CANDIDATE L	CANDIDATE S	CANDIDATE S'	10 MI. VERSION S'
Radar	$185K	$190K	$197K	$158K
Spares	23	24	25	20
Test Equipment	6	6	6	6
MTI Ref. Target	1	1	1	1
Contractor Turnkey and Shipping	30	30	30	30
Installation (Regional Cost)	50	50	50	50
Documentation	10	10	10	10
Factory Inspection	5	5	5	4
	$310K	$316K	$324K	$279K

3.10.3 Maintenance Costs

The estimated maintenance costs for the SRTR are listed below. It is assumed that these costs will be the same regardless of which candidate is selected.

ITEM	COST
Personnel (0.43 man/yr/yr at $19.6K)	$126K
Spares attrition at $100/failure (MTBF = 500 hr)	26
Equipment refurbishment	15
Maintenance Training	45
Utilities (8 kW at .05/kWh)	53
Test equipment replacement and refurbishment	10
TOTAL	$275K

The estimated life cycle cost for 15 years is presented below:

LIFE CYCLE COSTS (15 YEARS)

	L-Band	S-BAND	S'-BAND	S' (10 MI.)
Establishment Cost	$310K	$316K	$324K	$279K
Imputed Interest (at 0.13147 per yr)	302	308	315	271
Maintenance	275K	275K	275K	275K
15 Year Cost	$887K	$899K	$914K	$825K
1 Year Cost	$ 59K	$ 59K	$ 61K	$ 55K
1 Hour Cost (24 hr. day)	$6.74	$ 6.74	$6.96	$6.28

4.0 CONCLUSIONS AND RECOMMENDATIONS

The SRTR is a state-of-the art, generally low risk system that may be implemented for a relatively low cost. It should be a highly reliable, low maintenance system by virtue of its modest RF power, small antenna size and proposed solid state modular construction.

4.1 RECOMMENDED SRTR CANDIDATES

Three candidate systems have been addressed thus far in the report. This section summarizes the study group recommendations for a specific system. The S' candidate system has a preponderance of advantages in its favor. The small antenna size leads to cost savings, weight savings, and lowered drive power. The frequency allocation bandwidth of 200 MHz with concomitant exclusive use lowers interference and permits more widespread use of the system. Its cost is not significantly different from the other candidates. The only disadvantage appears to be the higher RF power than the other candidate systems. However, the power level required appears to be achievable.

It is recommended that the S' candidate (3500 - 3700 MHz) be established as the primary SRTR candidate.

4.2 RECOMMENDED SRTR CONFIGURATION

The SRTR will be comprised of the radar signal and data processor, signal conditioning and interface (MODEM), scan history circuitry, and x-y display (Figure 4.1.) The necessary triggers, rotary joint path, antenna mounting capability, and shelter space will be provided to accommodate an ATCRBS if required.

4.3 RECOMMENDED SRTR PROGRAM PLAN

The SRTR concept is sufficiently unique to warrant some development work in the areas of the transmitter, signal processor, and detector/tracker/display. The 42 month program plan milestones proposed in Table 4.1 below includes the fabrication and evaluation of an Advanced Development Model (ADM) to serve as a tool in the development. It is estimated that such a step would cost about a million dollars but would be well worth it over a production "buy" of 25 units. As seen in Section 3.10 and Appendix B this amount would raise the 15 year life cycle cost of such a number by 3.5 percent to 4.0 percent. The percentage would, of course, be reduced in proportion to the number of units in excess of 25 that may be acquired.

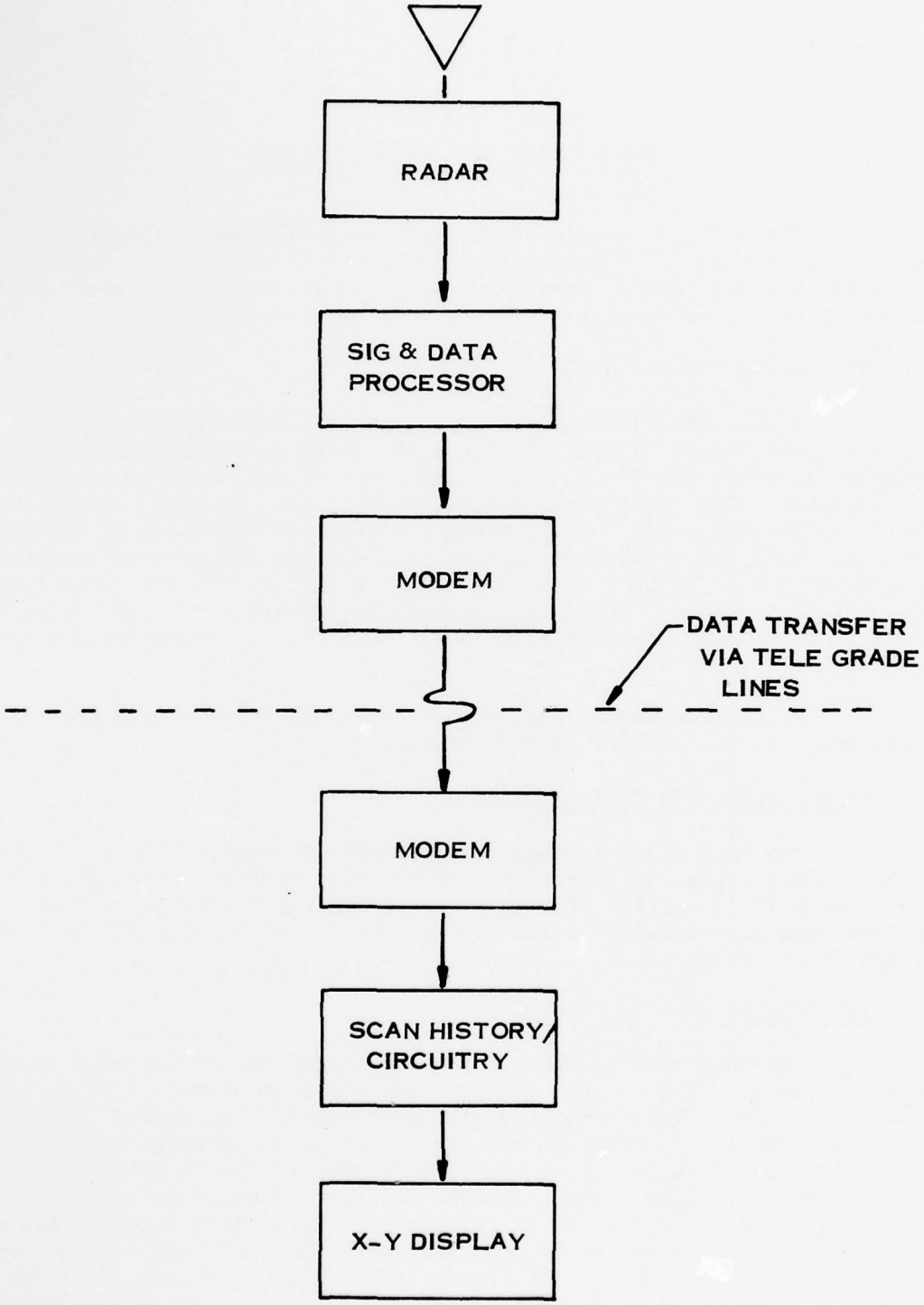

FIGURE 4.1

SRTR BLOCK DIAGRAM

It is recommended that the time scale shown in the table be adopted for use in the SRTR Program Plan:

TABLE 4.1

MILESTONE	RUNNING TOTAL IN MONTHS
Program Authorization	0
ADM Contract Let	3
ADM Construction Complete	15
ADM Tests Complete	24
Specification Complete	27
First Article Contract Let	30
First Article Delivered and Tested	42

5.0 BIBLIOGRAPHY

ARD 1974A
DRAFT, "Analysis of Radar R and D Requirements", ARD-243 (15 April 1974)

ARD 1974B
"Radar Program (O-2) Reorientation", ARD-1 letter to AED-2 (July 26, 1974)

ARD 1972
DRAFT, "Concept and Plan for a Low Cost ASR Program", ARD-200 (17 January 1973)

Barton 1964
D. K. Barton, "Radar System Analysis", Prentice Hall, Inc., Englewood Cliff, New Jersey (1964)

Bassford 1974
Ronald S. Bassford, "X-Band Terminal Radar T and E", FAA, FAA-RD-73-109 (January 1974)

Batten 1959
L. J. Batten, "Radar Meteorology", University of Chicago Press, Chicago (1959)

Bean et al 1970
B. R. Bean, E. J. Dutton and B. D. Warner, "Weather Effects on Radar", Radar Handbook, ed. by M. Skolnik, McGraw-Hill Book Co., New York (1970)

Bean et al 1968
B. R. Bean and E. J. Dutton, "Radio Meteorology", Dover Pub., New York (1968)

Bean et al 1966
B. R. Bean, B. A. Cahoon, C. A. Samson and G. D. Thayer, "A World Atlas of Radio Refractivity", Environmental Sciences Services Administration, Monograph #1, Washington (1966)

Bean et al 1957
B. R. Bean and B. A. Cahoon, "The Use of Surface Weather Observations to Predict the Total Atmospheric Bending of Radio Waves at Small Elevation Angles", IRE 45 No. 11, pp. 1545-1546, (November 1957)

Blake 1969
L. V. Blake, "A Guide to Basic Pulse Radar Maximum-Range Calculation", NRL Report 693[illegible] (1969)

Booker et al 1950
H. G. Booker and W. E. Gordon, "A Theory of Radio Scattering in the Troposphere", Proceedings of the IRE, pp. 401-412 (April 1950)

Booker et al 1947
H. C. Booker and W. Walkinshaw, "The Mode Theory of Tropospheric Refraction and Its Relation to Wave Guides and Diffraction", Meteorological Factors in Radiowave Propagation, pp. 80-127, The Physical Society, London (1947)

Booker 1946
H. G. Booker, "Elements of Radio Meteorology: How Weather and Climate Cause Unorthodox Radar Vision Beyond the Geometrical Horizon", JIEE, Vol. 93, pt. IIIa, pp. 69-78 (1946)

Chang 1971
H. T. Chang, "The Fffect of Tropospheric Layer Structures on Long-Range VHF Radio Propagation", IEEE Trans. Ant. and Prop. AO-19, No. 6, pp. 751-756 (November 1971)

Dresp 1972
M. R. Dresp, "Radiowave Propagation in the Presence of a Tropospheric Duct", The MITRE Corp., MTR-2455 (30 June 1972)

Dresp 1971
M. Dresp, "Introduction to Analysis of Tropospheric Duct Propagation at UHF Frequencies on Air to Air and Air to Ground Communication Links", The MITRE Corp., WP-4095 (11 November 1971)

Du Castel 1966
F. Du Castel, "Tropospheric Radio Wave Propagation Beyond the Horizon", Pergamon Press, Oxford (1966)

FAA 1974A
"Current Aviation Statistics", FAA (July 1974)

FAA 1974B
"Analysis of Radar R and D Requirements", FAA, Staff Study FAA/ARD-243 (April 15, 1974)

FAA 1973A
"Air Traffic Activity FY 1973" (extracts) FAA (August 1973)

FAA 1973B
"Low Cost Radar Program", FAA. Reading File (June 15, 1972-July 11, 1973)

FAA 1973C
"A High Performance Low Cost, Air Traffic Control Radar", FAA, ESD-TR-73-62, Tech. Note 1973-12 (15 February 1973)

FAA 1973D
"Concept and Plan for a Low Cost ASR Program", Draft FAA ARD-240 (January 17, 1973)

FAA 1973E
"Static Cross Section of Light Aircraft", FAA, FAA-RD-74-99 (Vols. I, II, III, IV) (December 1973)

FAA 1972A
"Concepts, Design and Description for the Upgraded Third Generation Air Traffic Control System", FAA FAA-ED-01A (August 1972)

FAA 1972B
"Air Traffic Control Radar System Definition Report", FAA, FAA-EM-72-1 (March 1972)

FAA 1971A
"Operational Test of Plessey ACR-430", FAA, Draft report (November 26, 1971)

FAA 1971B
"Specification FAA-E2506, including Amendment 3 (8-15-72), Airport Surveillance Radar (ASR) Transmitter Receiver (T/R) Subsystem", FAA (November 12, 1971)

FAA 1971C
"Technical Development Plan for a Discrete Address Beacon System", FAA, FAA-RD-71-79 (October 1971)

FAA 1971D
"F and E Cost Estimate Summaries May 1971", FAA (extracts for Radar and Beacon) (May 1971)

FAA
"Specification, FAA-G-2100C 'Electronic Equipment, general requirements'" (draft) (no date given)

FAA
"National Airspace System Automated Radar Terminal System III (ARTS III) (no date given)

Fehlner 1962
L. F. Fehlner, "Marcum's and Swerling's Data on Target Detection by a Pulsed Radar", The Johns Hopkins Applied Physics Laboratory Report No. TG 451 (2 July 1962)

Freehafer 1951
John E. Freehafer, "Propagation of Short Radio Waves", Tropospheric Refraction, in D. E. Kerr (ed.), MIT Radiation Laboratory Series vol. 13, pp. 9-22, McGraw-Hill Book Company, New York (1951)

Holoman AFB 1973
"Static Radar Cross-Section of Light Aircraft", Vol. I, "CESSNA 150L at L-, S-, and C-Bands" (Dec 1973), Vol. II, "Cherokee 140 at L-, S-, and C-Bands" (December 1973), Vol. III, "Piper PA-18 Super Cub at L-, S-, and C-Bands" (January 1974), Holoman AFB FAA-RD-74-99 (December 1973 - January 1974)

Hunn 1972
Spencer S. Hunn, "F and E Cost Estimates, FAA, FAA-RD-2510.29B (February 28, 1972)

Israel 1972
David R. Israel, "A Handfull of Rules-of-Thumb" Think Paper, FAA (November 1972)

Jeske et al 1966
H. Jeske and K. Brocks, "Comparison of Experiments on Duct Propagation Above the Sea with the Mode Theory of Booker and Walkinshaw", Radio Science, Vol. 1, No. 8 (August 1966)

JHU/APL 1973
"Angel Clutter and the ASR Air Traffic Control Radar", Vol. I "Study Results", Vol. II "Appendices", JHU/APL MSO-F-199 (February 28, 1973)

Levingston 1970
D. C. Levingston, "The Physics of Microwave Propagation", Prentice-Hall, Inc., Englewood Cliffs, New Jersey (1970)

Lincoln Lab 1974
"ATC Surveillance/Communication Analysis and Planning (Task B)", Lincoln Labs Quarterly Technical Summary, FAA-RD-74-60 and FAA-RD-74-105 (March 1, 1974)

Muehe et al 1973
C. E. Muehe, M. Lobitt, B. Gold, D. Pruslin, J. Cremin, V. Iferrino, E. Hofstetter, "Concepts for Improvement of Airport Surveillance Radars", Lincoln Labs, FAA-PD-72-148 (February 26, 1973)

Nathanson 1969
Fred E. Nathanson, "Radar Design Principles", McGraw-Hill Book Co. (1969)

NTSB 1974
"Recommendation to FAA re Hazardous Weather", NTSB Safety Recommendations A-74-12 through 14 (April 18, 1974)

O'Donnell 1972
R. M. O'Donnell, "The Effect of Tropospheric Ducting on Frequency Selection for Siting of an SLBM Radar", MTR-2516, MITRE (December 22, 1972)

Offi 1974
Dominick L. Offi, "Test and Evaluation of Passive Horn Antenna for the Airport Surveillance Radar ASR-5", FAA, FAA-RD-74-113 (July 1974)

Pallin 1972
G. E. Pallin, "Distribution of Radar Angels", IEEE-AES Volume AES-8 Number 6 (November 1972)

Ragan 1974
Lawrence H. Ragan, "Pulse Compression Radar Study", Texas Instrument, Inc. FAA-RD-192 (March 1974)

Randall 1966
D. L. Randall, "Tropospheric Radio Duct Meteorology at VHF and UHF in Theory and as Observed on a Trip Around the World", Naval Research Laboratory, NRL Report 6404 (May 31, 1966)

Rawlinson 1974
Paul E. Rawlinson, "ASR-5 Radar Dual Feedhorn Antenna Modification", Vol. I, "Description of Hardware and Summary of Feasibility Effort", Vol. II, "Description of Feasibility Effort", FAA, FAA-RD-74-88 (April 1974)

Rawlinson 1973
Paul E. Rawlinson, "ARSR-2 Radar Dual Feedhorn Modification", FAA, FAA-RD-73-28 (December 1973)

Schelling, et al 1933
J. C. Schelling, C. R. Burrows, and E. B. Ferrell, "Ultra-Short-Wave Propagation", Proc. IRE, Vol. 21, pp. 427-463 (March 1933)

Skolnik 1970
Merril I. Skolnik, Editor-in-Chief, "Radar Handbook", McGraw-Hill Book Co. (1970)

Skolnik 1962
Merrill I. Skolnik, "Introduction to Radar Systems", McGraw-Hill (1962)

Smith et al 1953
E. K. Smith and S. Weintraub, "The Constants in the Equation for Atmospheric Refractive Index at Radio Frequencies, Proc. IRE 41, 1035-1037 (1953)

Swerling 1954
"Probability of Detection for Fluctuating Targets", Rand Corp. Report No. RM-1217 (March 17, 1954)

Wells et al 1973
W. I. Wells, R. Kramer, "Surveillance Communication Issues in the Transition to a Discrete Address Beacon System", Lincoln Labs, FAA-RD-73-125; ATC-31 (26 December 1973)

APPENDIX A

RFI AND BANDWIDTH UTILIZATION CALCULATIONS

The calculations in this appendix are based on the techniques given in Section 29 of Skolnik 1970. In all cases where a value judgement was required, a conservative estimate was taken in order to establish "worst case' conditions.

A.1 PROBABILITY OF OCCURRENCE OF MUTUAL GAINS

Using a two level, two dimensional radiation model (see Figure A.1)

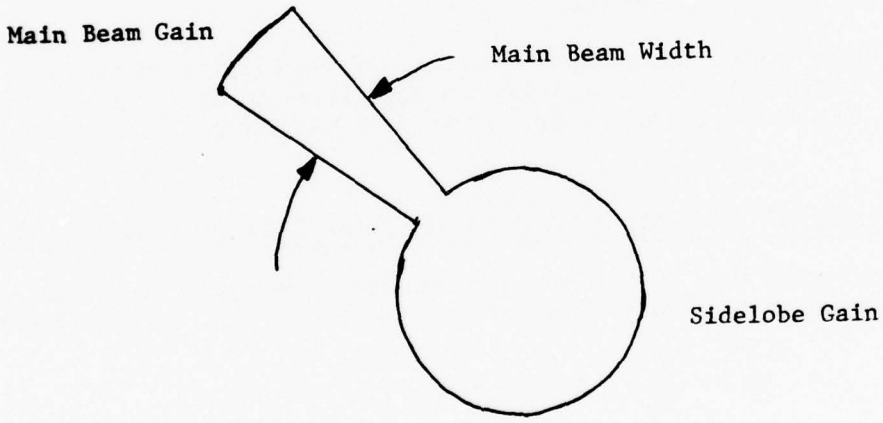

FIGURE A.1

The probability of a given mutual gain occurring over one scan is the product of the fraction of scan intervals over which each gain level of interest occurs. The following table gives the results:

TABLE A.1 PROBABILITY OF MUTUAL GAIN OCCURRENCE

	SRTR TO SRTR	ASR TO SRTR*	ARSR TO SRTR**
MB_1 to MB_2	8.92×10^{-5}	3.94×10^{-5}	3.15×10^{-5}
MB_1 to SL_2	9.36×10^{-3}	9.41×10^{-3}	9.41×10^{-3}
MB_2 to SL_1	9.36×10^{-3}	4.13×10^{-3}	3.3×10^{-3}
SL_1 to SL_2	9.81×10^{-1}	9.86×10^{-1}	9.87×10^{-1}

* Operating at S-Band

** Operating at L-Band

Though the above model is simplistic, it establishes that the mainbeam to sidelobe and sidelobe to sidelobe mutual gain coupling are far more significant than the mainbeam to mainbeam case.

A.2 CALCULATION OF I/N FOR GIVEN RANGE AND FREQUENCY SEPARATIONS

The expression used for calculating the interference to noise ratio for a given range and frequency separation is as follows:

$$\frac{I}{N} = \frac{P_T G_T}{L_P} \times \frac{G_R}{R_S \phi(\beta) \phi(\Delta f)} \qquad (1)$$

where $\frac{I}{N}$ is the interference to noise ratio

P_T is the interfering transmitter power

G_T is the interfering antenna gain

G_R is the receiving antenna gain

R_S is the receiver noise power level

$\phi(\beta)$ is the bandwidth correction factor

$\phi(\Delta f)$ is the off tune correction factor

L_P is the propagation loss

In decibel form, the above equation is:

$$\frac{I}{N} = P_T + G_T - L_P + G_R - R_S - \phi(\beta) - \phi(\Delta f) \qquad (2)$$

$\phi(\Delta f)$ is the ratio of the spectral power density at the separation frequency of interest to the spectral power density at the tuned frequency of the transmitter. A curve of the sideband envelopes for 2μsec. rectangular and trapezoidal pulses is furnished as Figure A.2. The definition of pulsewidth and rise and fall times (δ's) is given in Figure A.3. Only symmetrical δ's were considered for this report, thus tending to give pessimistic results.

The receiver noise level (R_s) is computed as

$$R_s = kTB \times N.F. \times L_R \qquad (3)$$

where kT is the product of Boltzman's constant and the absolute temperature and is -174 dBm per cycle, N.F. is the assigned noise figure, and L_R are the antenna to receiver input losses. The bandwidth for the SRTR is defined as $1.2/\tau$ = 600 kHz for this report.

$\frac{I}{N}$ is set equal to 0 dB thus giving a pessimistic answer since it requires the interfering signal to equal the receiver noise.

L_P is read from a curve taken from Skolnik 1970 giving the propagation loss between two antennas at a height of 25 feet over sea water with vertical polarization (Figure A.4). These curves will tend to produce a conservative estimate for the land case since masking and attenuation due to terrain features are not involved. The curves assume a smooth 4/3 radius earth and a uniformly refracting atmosphere.

$\phi(\beta)$ is the ratio of bandwidth of the transmitter to the receiver and is 0 dB if they are not far different. If the transmitter bandwidth is wider than the receiver bandwidth the impact of the interference is reduced.

The values used for transmitter power, antenna characteristics are either taken from Appendix C or FAA 1972B.

A.2.1 SRTR to SRTR Interference

A.2.1.1 S'BAND

Using the equation (3) above in decibel form,

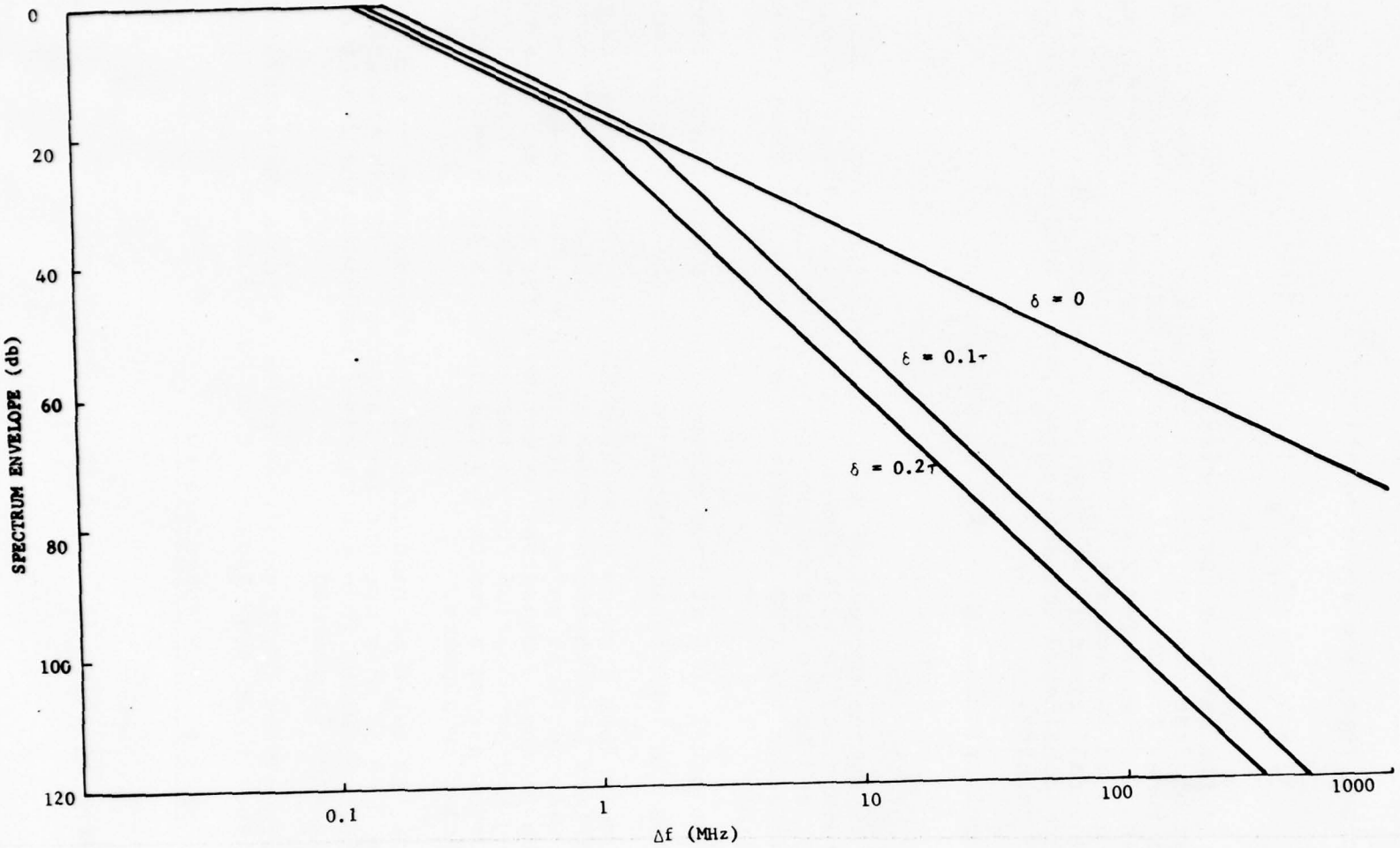

PULSEWIDTH = 2 μSEC

FIGURE A.2

SPECTRUM AS A FUNCTION OF PULSE SHAPES

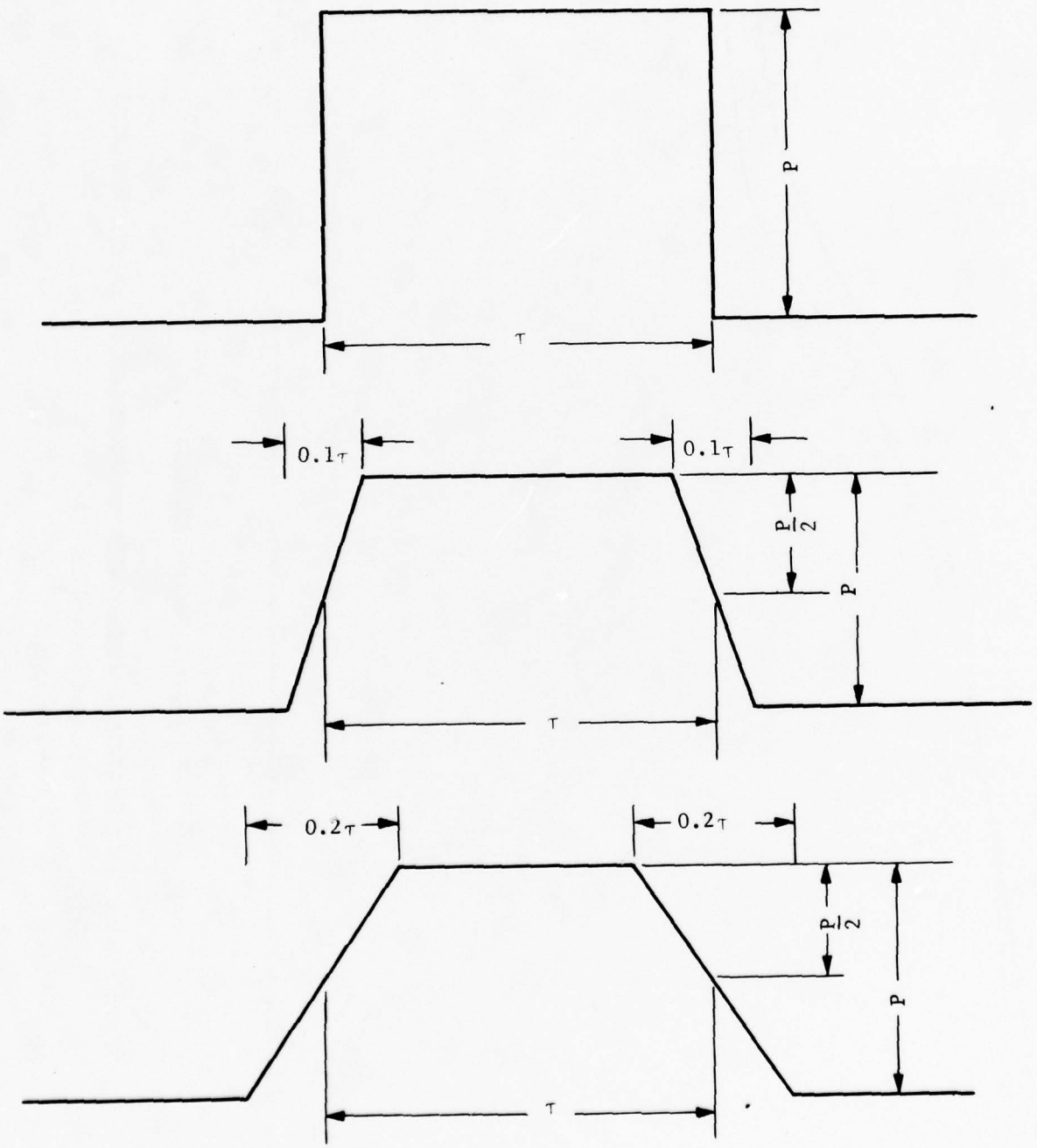

FIGURE A.3

RELATIONSHIP OF PULSEWIDTH (τ)
TO RISE AND FALL TIMES (δ's)

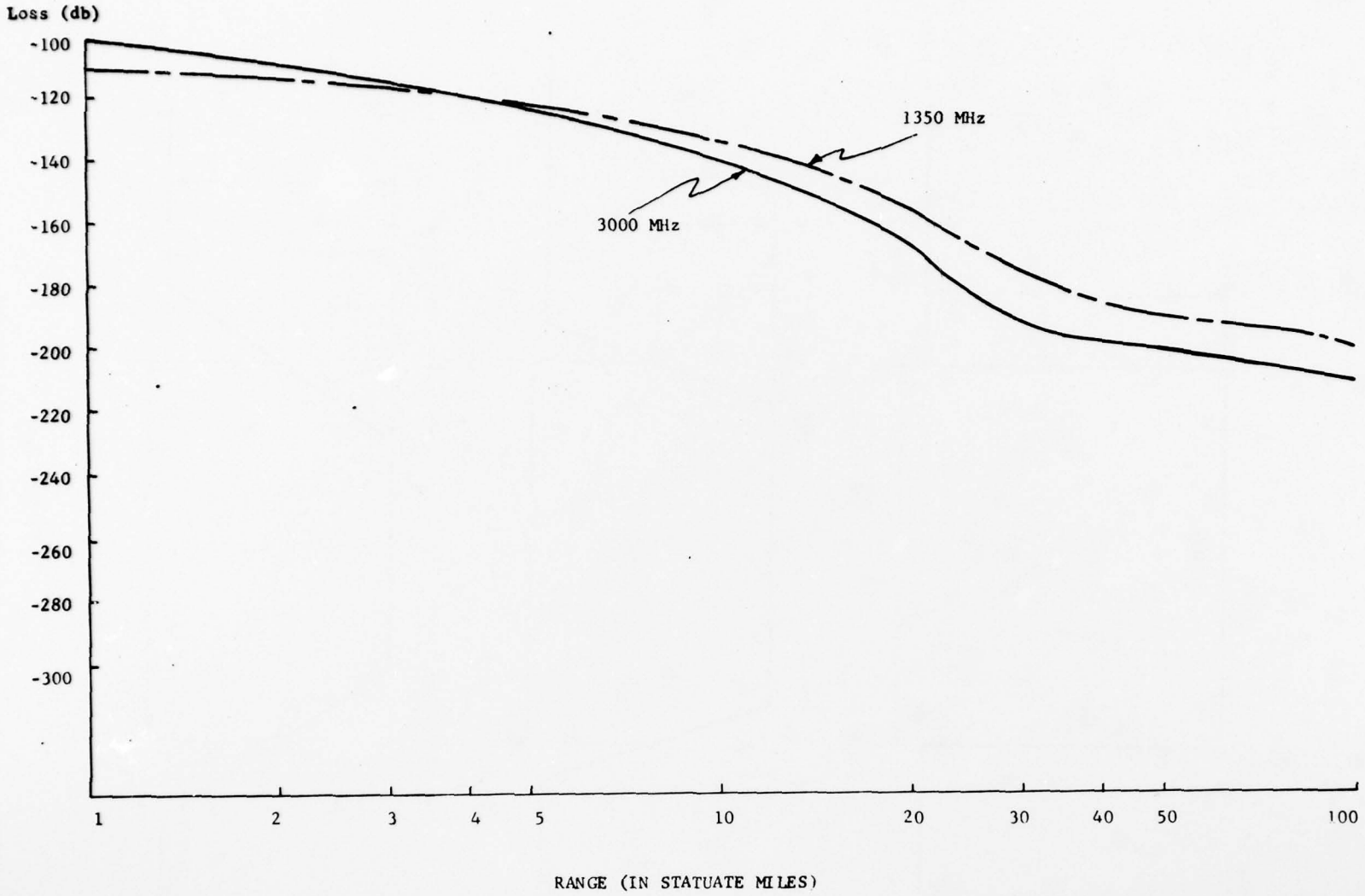

FIGURE A.4 THE PROPAGATION LOSS BETWEEN TWO VERTICALLY POLARIZED ANTENNAS AT 25 FT. OVER SEA WATER

$$R_s = -174 + 57.8 + 5 + 2 = -109.2 \simeq -109 \text{ dBm}$$

Entering the value of R_s in equation (2)

$$\frac{I}{N} = (80-2) + 29 - L_p + 29 + 109 - \phi(\Delta f)$$

Setting $\frac{I}{N} = 0$ dB and solving for L_p and $\phi(\Delta f)$

$$L_p + \phi(\Delta f) = 245 \text{ (Main Beam to Main Beam)}$$

Figure A.5 gives the results for the calculation using rectangular and trapezoidal pulses. The assumption is made that the sidelobe level is 20 dB below the mainbeam. Therefore, the following two equations also apply:

$$L_p + \phi(\Delta f) = 225 \text{ (Main Beam to Side Lobe)}$$

$$L_p + \phi(\Delta f) = 205 \text{ (Side Lobe to Side Lobe)}$$

Figure A.6 and A.7 show the results of the latter calculations for rectangular and trapezoidal pulses.

A.2.1.2 S-Band

Using equation (3) above in decibel form,

$$R_s = -174 + 57.8 + 5 + 2 = -109.2 \simeq -109 \text{ dBm}$$

Entering the value of R_s in equation (2)

$$\frac{I}{N} = (78-2) + 29 - L_p + 29 + 109 - \phi(\Delta f)$$

Setting $\frac{I}{N} = 0$ dB and solving for L_p and $\phi(\Delta f)$

$$L_p + \phi(\Delta f) = 243 \text{ (Main Beam to Main Beam)}$$

$$L_p + \phi(\Delta f) = 223 \text{ (Main Beam to Side Lobe)}$$

$$L_p + \phi(\Delta f) = 203 \text{ (Side Lobe to Side Lobe)}$$

The above results are sufficiently close to those for S' calculated in Section A.2.1 that Figures A.5, A.6, and A.7 also apply.

FIGURE A.5

SRTR - SRTR
Mainbeam to Mainbeam
S & S'

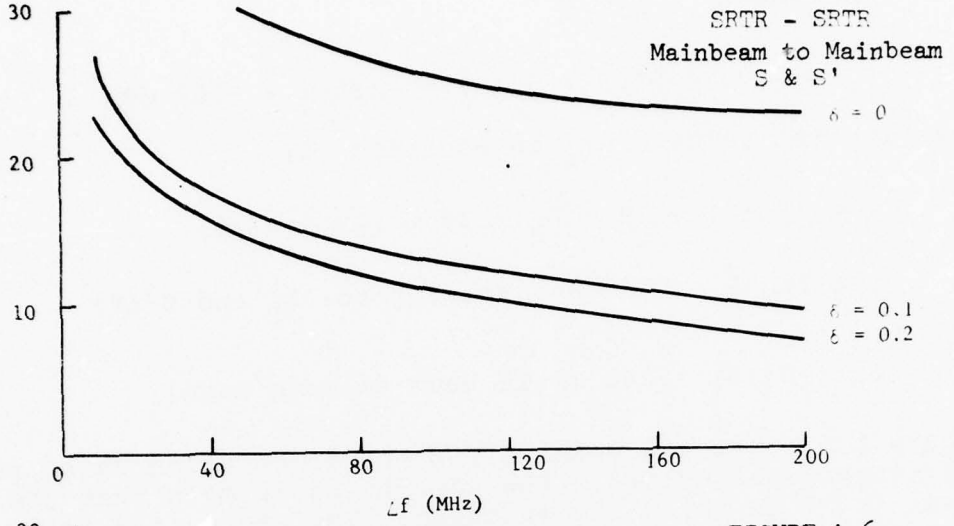

FIGURE A.6

SRTR - SRTR
Mainbeam to Sidelobe
S & S'

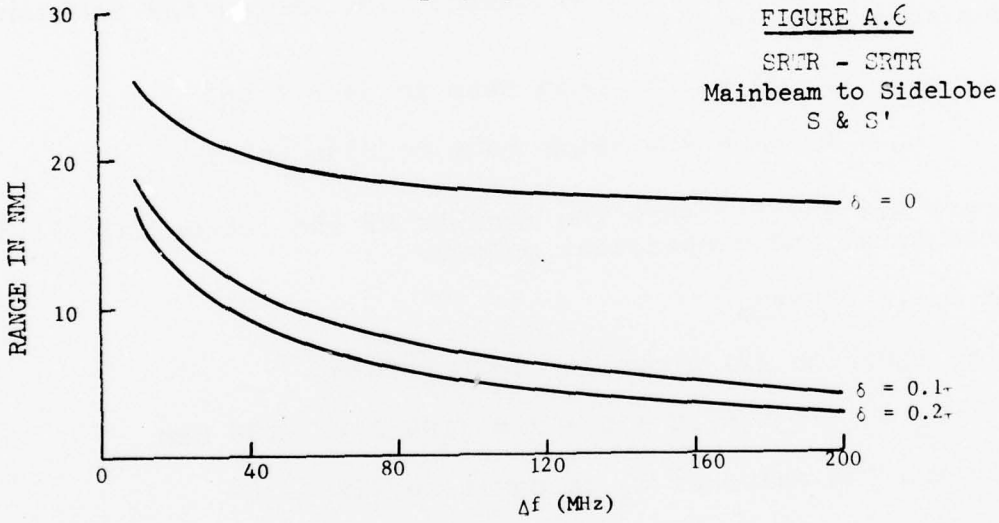

FIGURE A.7

SRTR - SRTR
Sidelobe to Sidelobe
S & S'

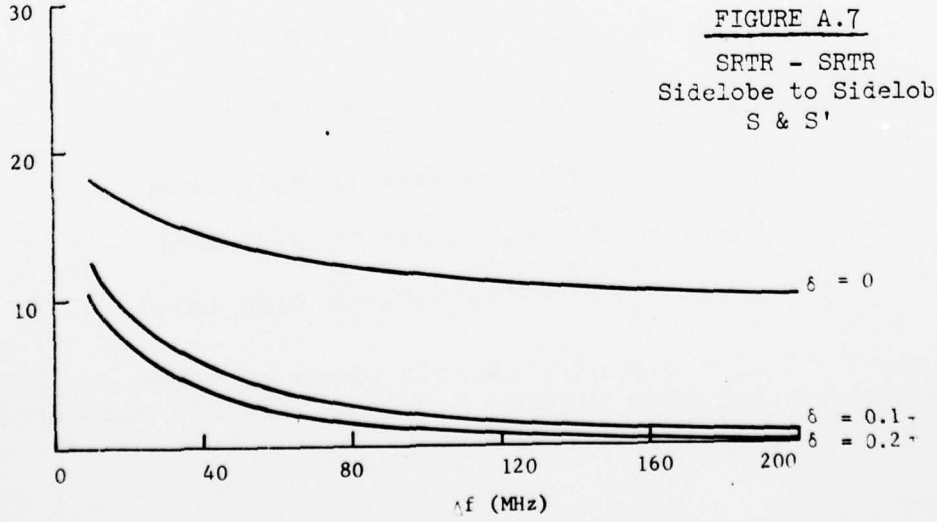

A.2.3 L-Band

Using equation (3) above in decibel form,

$$R_s = -174 + 57.8 + 4 + 1.5 = -110.7 \approx -111 \text{ dBm}$$

Entering the value of R_s in equation (2)

$$\frac{I}{N} = (69-1.5) + 29 - L_p + 29 + 111 - \emptyset(\Delta f)$$

Setting $\frac{I}{N} = 0$ dB and solving for L_p and $\emptyset(\Delta f)$

$$L_p + \emptyset(\Delta f) = 236 \text{ (Main Beam to Main Beam)}$$

$$L_p + \emptyset(\Delta f) = 216 \text{ (Main Beam to Side Lobe)}$$

$$L_p + \emptyset(\Delta f) = 196 \text{ (Side Lobe to Side Lobe)}$$

The results of the above calculations are given in Figures A.8, A.9, and A.10 respectively. A dashed line is shown at a separation frequency of 100 MHz since the spectrum allocation at this band is only that wide. The curves were produced beyond this point only for convenience.

A.2.4 ARSR to L-Band SRTR Interference

The purpose of this calculation is to determine interference for range and frequency separation on L-Band SRTR operating in the vicinity of an ARSR. Using equation (3) in decibel form,

$$R_s = -174 + 57.8 + 4 + 1.5 = -110.7 \approx 111 \text{ dBm}$$

Entering the value of R_s in equation (2)

$$\frac{I}{N} = (96 - 1.5) + 34 - L_p + 29 + 111 - \emptyset\Delta f$$

Setting $\frac{I}{N} = 0$ dB and solving for L_p and $\emptyset(\Delta f)$,

$$L_p + \emptyset(\Delta f) = 268.5 \approx 268 \text{ (Main Beam to Main Beam)}$$

The ARSR sidelobe level is without doubt lower than -20 dB, however, its exact value is not known. Therefore, a level of -20 dB is assumed as with the SRTR. It follows that,

$$L_p + \emptyset(\Delta f) = 248 \text{ (Main Beam to Side Lobe)}$$

$$L_p + \emptyset(\Delta f) = 228 \text{ (Side Lobe to Side Lobe)}$$

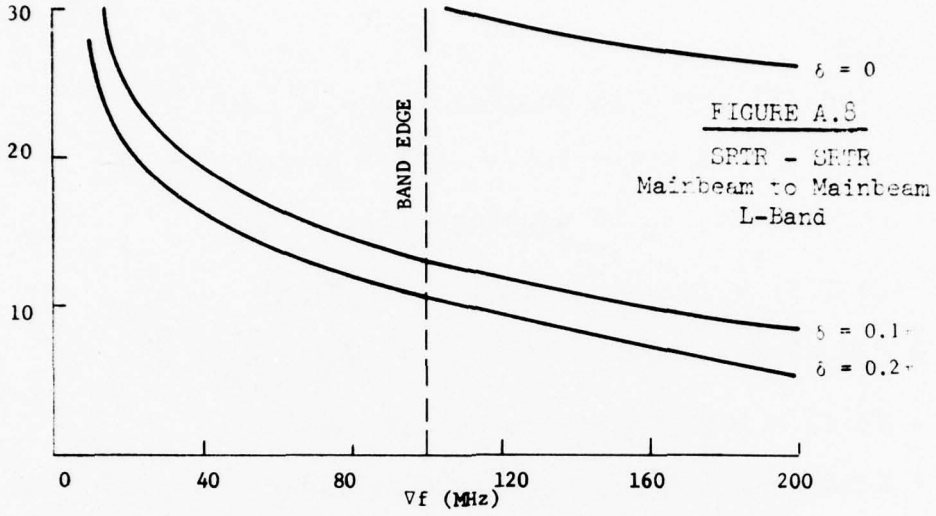

FIGURE A.8

SRTR - SRTR
Mainbeam to Mainbeam
L-Band

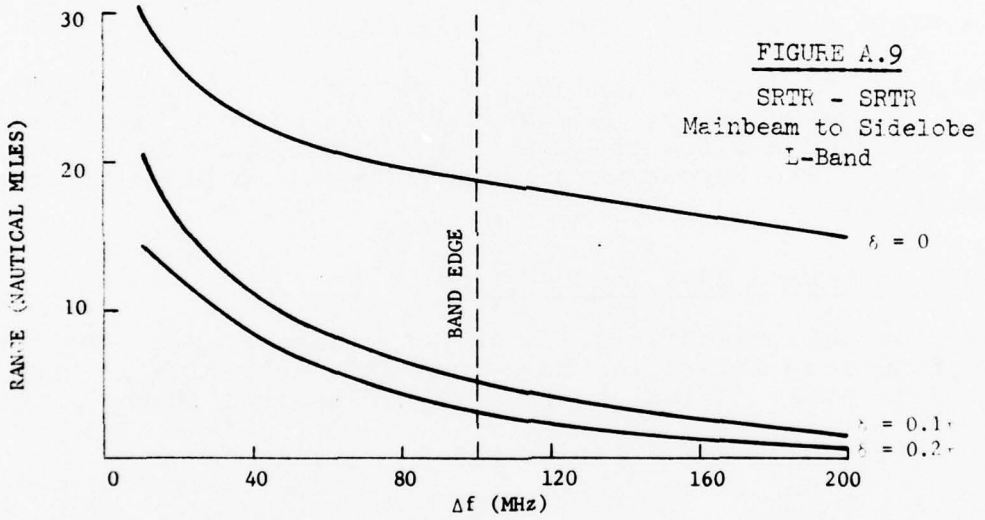

FIGURE A.9

SRTR - SRTR
Mainbeam to Sidelobe
L-Band

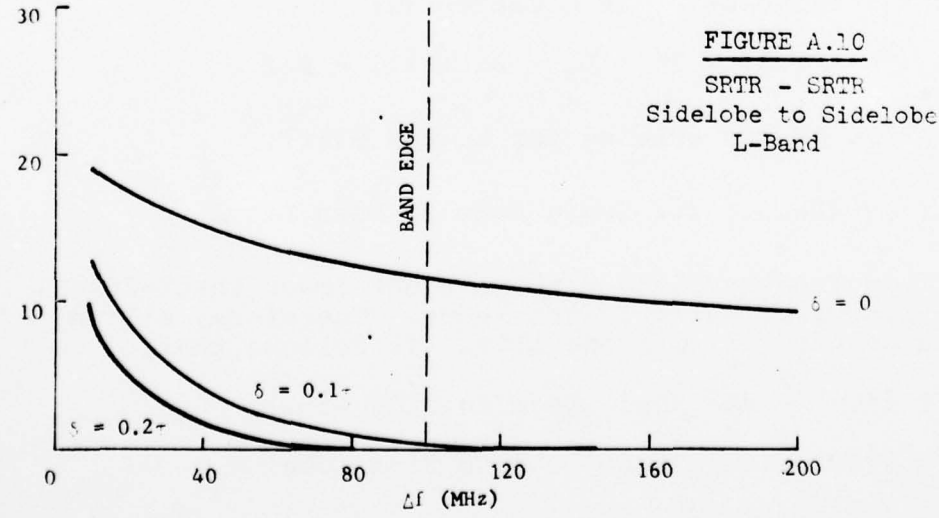

FIGURE A.10

SRTR - SRTR
Sidelobe to Sidelobe
L-Band

The results of the above are plotted in Figure A.11. The rectangular pulse case $\delta=0$ or the trapezoid $\delta=0.2\tau$ is not considered for the ARSR since its pulse shape is closer to a trapezoid with a $\delta=0.1\tau$. The curve for 25 foot to 25 foot antenna height was used to determine range from L_p. However, if the ARSR were as high as 100 feet the results would not differ very much.

A.2.5 ASR to S-Band SRTR Interference

The purpose of this calculation is to determine interference for range and frequency separation with an S-band SRTR operating in the vicinity of an ASR. Using equation (3) in decibel form,

$$R_s = -174 + 57.8 + 5 + 2 = -109.2 \simeq -109 \text{ dBm}$$

Entering the value of R_s in equation (2)

$$\frac{I}{N} = (86-2) + 34 - L_p + 29 + 109 - \emptyset(\Delta f) - \emptyset(\beta)$$

$\emptyset(\beta)$ is not zero due to the difference in bandwidth between the ASR and the SRTR. It is given by,

$$\emptyset(\beta) = \left(\frac{1}{0.833 \times 10^{-6}}\right)\left(6 \times 10^5\right)^{-1} = 2 \text{ or } 3 \text{ dB}$$

Setting $\frac{I}{N} = 0$ dB and solving for L_p and $\emptyset(\Delta f)$,

$$L_p + \emptyset(\Delta f) = 253 \text{ (Main Beam to Main Beam)}$$

$\emptyset(\Delta f)$ is taken from a spectrum envelope similar to Figure A.2 but not included. The $\delta=0.1\tau$ is the only one considered since it approaches the ASR pulse shape. The ASR sidelobe level is without doubt lower than -20 dB, however, its exact value is not known. Therefore, a level of -20 dB is assumed as with the SRTR. It follows that,

$$L_p + \emptyset(\Delta f) = 233 \text{ (Main Beam to Side Lobe)}$$

$$L_p + \emptyset(\Delta f) = 213 \text{ (Side Lobe to Side Lobe)}$$

The results of the above are plotted in Figure A.12.

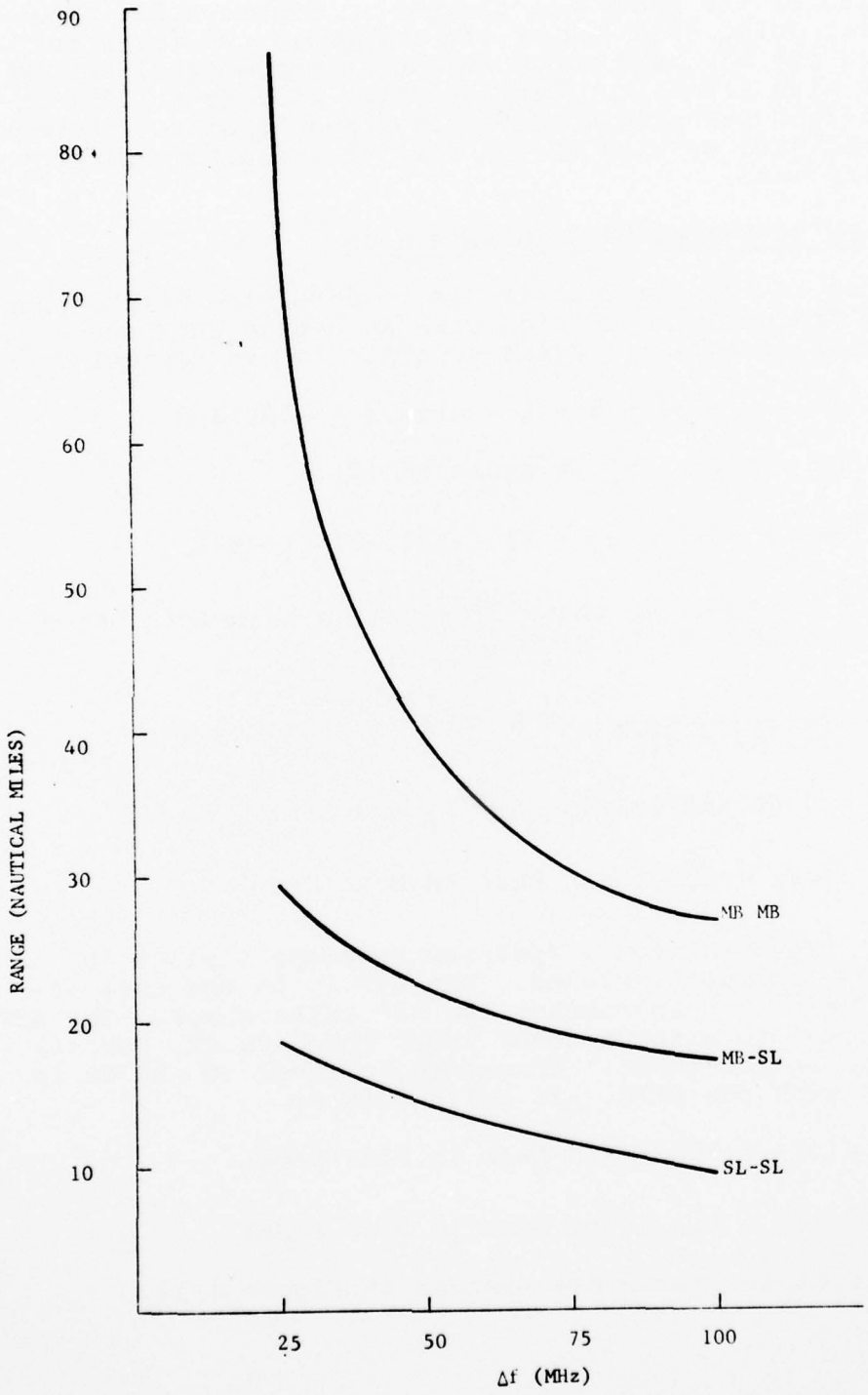

FIGURE A-11 ARSR TO L-BAND SPUR

δ = 0.1

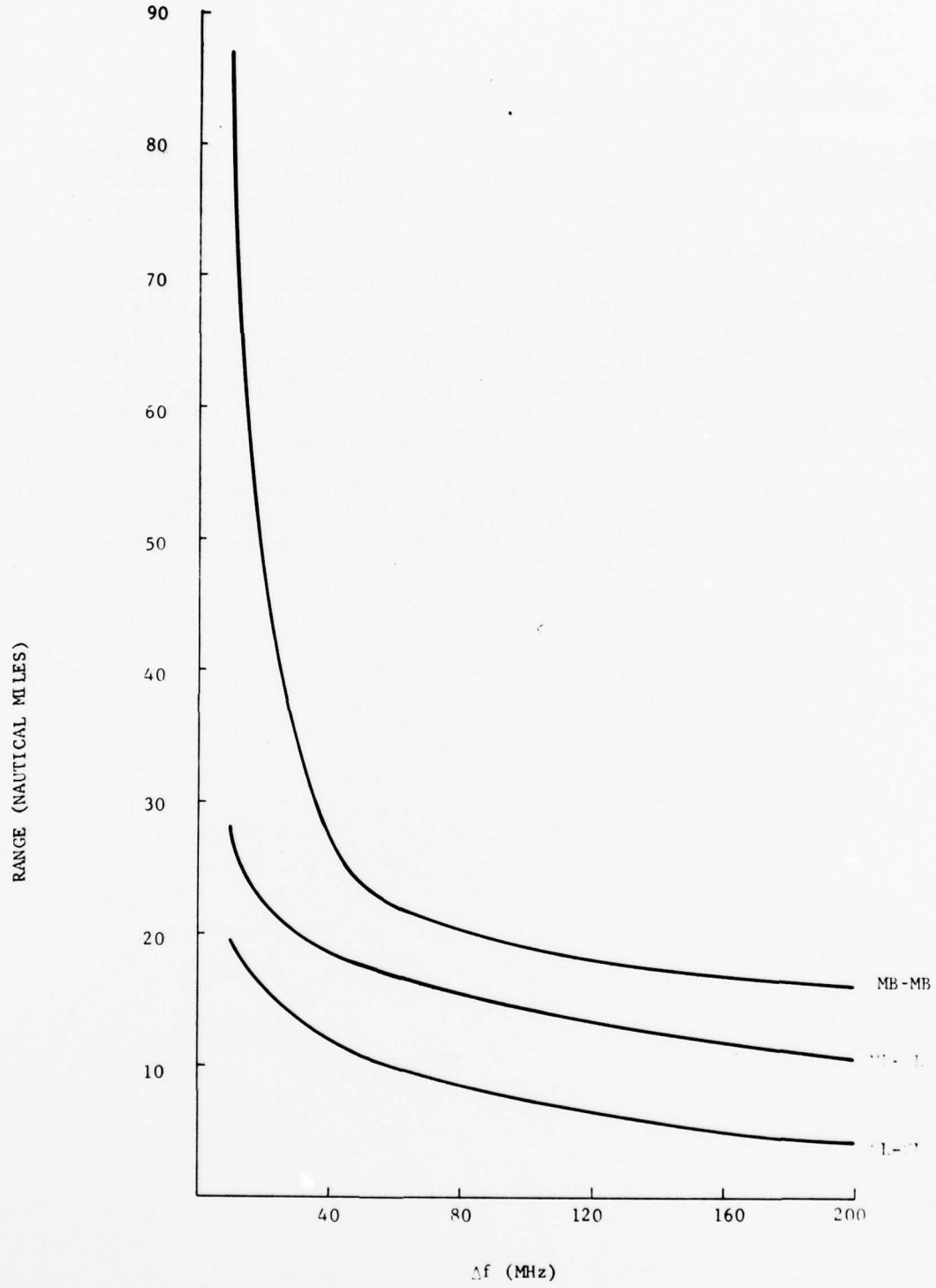

FIGURE A.12 ASR TO S-BAND SRTA

δ = 0.1τ

A.3 BANDWIDTH UTILIZATION EXAMPLE

A geometrical configuration of SRTR's operating at S' was constructed as an example of the application of bandwidth utilization. This configuration is shown in Figure A.13.

Seven SRTR's were assumed to occupy the vertices of six equilateral triangles joined together to form a hexagon. The distance between each vertex was set at 10 nautical miles. A rule was invoked requiring a frequency separation of 50 MHz for points 10 miles apart. This rule corresponds to SRTR's having no interference using a 0.2 μsec rise and fall times when mainbeam to sidelobe coupling occurs. Another rule invoked was that 10 MHz guard bands were required at band edges.

Figure A.13 shows that the desired configuration is achievable given the shown frequency selection. Note that alternate SRTR's along the perimeter are 17.3 miles apart permitting them to be 15 MHz apart in frequency.

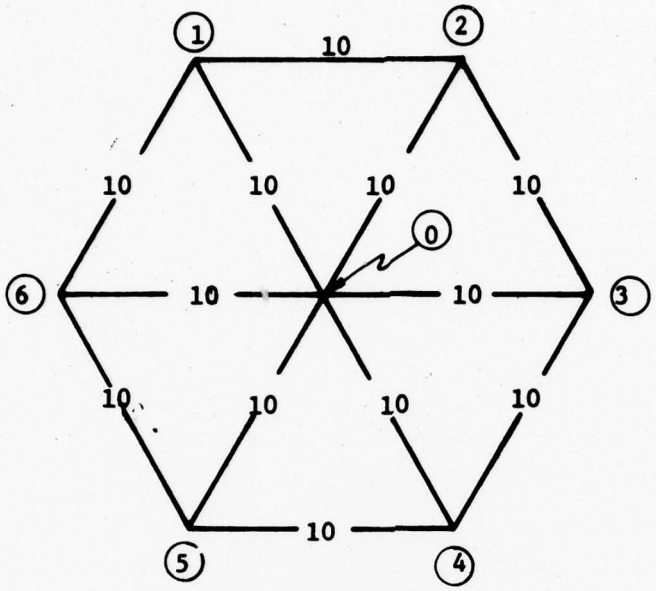

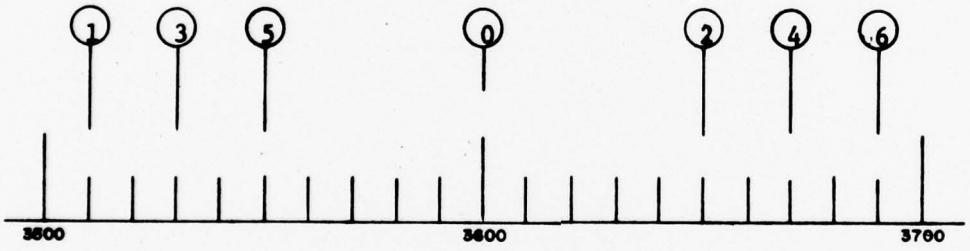

SRTR	FREQUENCY
0	3600 MHz
1	3510 MHz
2	3650 MHz
3	3530 MHz
4	3570 MHz
5	3550 MHz
6	3590 MHz

FIGURE A.13

CONCEPTUAL FREQUENCY ALLOCATION

APPENDIX B

ASR-8 (MODIFIED) CONSIDERATIONS

A potentially attractive candidate for the SRTR is a modified ASR-8 (single channel). Its attractiveness results from the fact that the engineering and design is complete and that if its cost could be reduced it might be an effective alternative to developing a new radar system. The major way that costs could be reduced is by elimination of the redundant transmitter/receiver/signal processing channel which is not dictated by the lower allowable availability of the SRTR. Such a system would have the same operational characteristics as the ASR-8 (a bit of an "overkill" for the SRTR application as far as range is concerned).

The cost of such a system has been calculated using guesstimates for the cost of various ASR-8 elements as supplied by Texas Instruments during a committee visit to Dallas on 15 October 1974. These costs are estimated as follows: (the TI estimates were given as a range of percentages of total cost and have been interpreted by the SRTR working group).

	ASR-8	ASR-8 (MOD)
Transportable bldg.	$ 40K	$ 20K
Transmitter	140K	70K
Receiver	70K	35K
Signal Processor	50K	25K
Antenna and Pedestal	70K	70K
SUBTOTAL	$370K	$220K
Tower (17')	18K	18K
TOTAL	$388K	$238K

The antenna support tower has been included in the above. The cost of these towers has been quoted at $18K for the 17' basic section plus $4.4K for each 10' section required.

Assuming that a single section is adequate, the cost of the ASR-8 (mod) would be about $238K. This is about 45 percent greater than the cost of SRTR's considered in Section 3.10 and calculated on the same basis. The cost of maintenance (primarily due to the higher transmitter power) and installation are probably also higher on the ASR-8 (mod).

These two approaches to the Short Range Terminal Radar problem can be compared in cost in several ways. The establishment costs are compared in the table below:

	SRTR	ASR-8 (1-CHANNEL)
Radar Equipment	$ 197K	$ 268K
Spares	25	34
Test Equipment	6	6
MTI Reflector	1	1
Installation	50	71*
Contractor Turnkey & Shipping	30	30
Documentation	10	10
Factory Inspection	5	5
SINGLE UNIT COST	$ 324K	$ 425K
25 UNIT COST	$8,100K	$10,625K
R and D	$1,000K	$ 0
25 UNIT TOTAL COST	$9,200K	$10,625K

*Antenna Tower Pad, Tower Erection, and Remoting Cables Needed.

The life cycle costs have been computed in the same way as in Section 3.10 and the results are shown below:

LIFE CYCLE COST COMPARISON

	SRTR	ASR-8 (MOD)
Maintenance	$ 275K	$ 399K*
R&D ($1000K/25)	40	0
Equipment Depreciation	324	425
Imputed Interest	315	413
TOTAL	$ 954K	$1,237K
Annual Cost	$ 64K/yr	$ 82K/yr
Hourly Cost	$ 7.31/hr	$ 9.36/hr

*High Power Transmitter will result in lower MTBF, higher qualified technicians, etc. - maintenance cost quoted assumed 45% greater maintenance cost for ASR-8 (mod) than for SRTR.

On a cost basis it can be seen from the above analysis that the ASR-8 approach would cost $6700K more for a 25 radar production run based on life cycle costs. The establishment cost differential alone would be $1400K.

Other considerations are also important. First, the ASR-8 (mod) would have the same signal processing as the current ASR-8. This would be deficient in the clutter environment defined for the SRTR. Secondly, the ASR-8 (mod) has potential RFI problems if more radars are assigned to S-band. Scaling to S'-band would further unbalance the cost relationship.

It is therefore concluded from these considerations that the cost effective and performance advantages both dictate the development of a new radar specifically for the SRTR application.

APPENDIX C

RADAR PARAMETER CALCULATIONS

C.1 GENERAL

At the outset of this study not many of the radar parameters were fixed. Therefore many combinations were considered. The first calculations involved computing the peak and average powers required for a range of 20 miles on a 1 square meter target (Swerling Type I fluctuations) for various combinations of azimuth beamwidth, pulse width, and pulse repetition frequency (instrumented range). Next, calculations were made of the required clutter improvement for rain rates of 16 mm/hr and a ground clutter representing the 95th percentile of ground clutter. The methods of calculation and the results are outlined in the following sections of this appendix.

C.1.1 Transmitter Power Calculations

These calculations were performed using the standard range equation relating

Range
Peak transmitter power
Antenna transmit gain
Antenna receive gain
Wavelength
Target cross section
Constant $(4\pi)^3$
Thermal noise constant (-204 dBw)
S/N required
Processing loss
RF losses - transmit
RF losses - receive

All calculations were made for a clear environment. The errors involved in neglecting atmospheric and rain attenuation are small even at S', the highest practical frequency. For example, the two-way attenuation due to the atmosphere at S' is about 0.6 dB. (see Nathanson 1969). This would reduce the range from 20 nmi to about 19.4. Rain at 16 mm/hr all the way from radar to target at maximum range (a highly unlikely occurrence) would result in attenuation of perhaps 1.6 dB, further reducing the maximum range to 17.7 nmi. These values are pessimistic but still small enough to be neglected particularly because the operational requirement to see small targets is more nearly 16 nmi and targets of interest are generally larger than 1 square meter.

A sample calculation sheet is included as Figure C.1. It shows the equation used and the form used in calculations. Generally all blanks including range but excepting transmitted power were filled in. Then working from the bottom up the peak transmitted power can be calculated. Average power was calculated by multiplying peak power times pulse length times PRF.

All values in the chart are direct entries from assumed parameters except for the required signal-to-noise ratio which was determined from curves of signal-to-noise required for various numbers of pulses integrated for various probabilities of detection and false alarm rates. The number of pulses integrated was assumed to be the number of hits per beamwidth calculated from the scan rate and the 3 dB one-way beamwidth. The curves in (NRL 1969) are for incoherent integration and may therefore give slightly pessimistic results for the signal processing schemes outlined in Section 3.4 which involve some coherent integration. The probability of detection used in all calculations was 0.75. This represents a compromise between the desire for high values for steady tracking and the lower values acceptable for initial detection. The false alarm rate was calculated using the relationship, false alarm probability equals the bandwidth divided by the allowable false alarm time. This definition is only applicable to certain kinds of detectors. The answers obtained for required transmitted power will be conservative for real detector systems. The results of the various calculations made are tabulated in Figure C.2. The antenna gains were calculated as shown in Figure C.3. The antenna gains used and the aperture sizes required are shown in Figure C.4.

C.2 CLUTTER CALCULATIONS

Another set of calculations was made to determine the amount of clutter improvement (CI) required to eliminate the two major sources of clutter, rain backscatter and ground backscatter. For the purposes of these calculations two standard conditions were assumed:

(1) heavy rain defined as 16 mm/hr, and

(2) ground clutter which would be representative of 95 percent of the returns from heavy ground clutter. Both of these numbers are derivable from data presented by Nathanson. For these calculations the following were used:

16 MM RAIN BAND	CROSS SECTION dB BELOW $1M^2/M^3$
X	- 53
S'	- 70
S	- 74
L	- 88
UHF (450 MHz)	-107

GROUND	CROSS SECTION dB BELOW 1 M^2/M^2
All Bands	- 18

AD-A061 798 FEDERAL AVIATION ADMINISTRATION WASHINGTON D C SYSTE--ETC F/G 1/2
SHORT RANGE TERMINAL RADAR (SRTR) DEFINITION STUDY.(U)
SEP 78

UNCLASSIFIED FAA/RD-78-64 NL

2 OF 2
AD
A061798

$$\beta^4 = \frac{\hat{P}_t \, G_t \, G_r \, \sigma \, \lambda^2}{(4\pi)^3 \, S/N \, L_p \, KT_o BF \, L_t \, L_r}$$

BAND S Az BW 3.4 PW 2 PRF 2000

ITEM	SYMB.	VALUE	dB VALUE	+dB	-dB
Peak TX Power	$\hat{P}_t$	59 kW	10 log $\hat{P}_t$	47.7	-
Ant. Gain - T_X	G_t	-	10 log G_t'	29.2	-
Ant Gain - R_X	G_r	-	10 log G_r'	29.2	-
Wavelength	λ	.107 M	20 log λ	-	19.4
Tgt. Cross Sect.	σ	1 M^2	10 log σ	0	-
Constant	$(4\pi)^3$	1984	30 log 4π	-	33
Thermal Noise	KT_0	$4x10^{-21}$W/Hz	10 log KT_0	204	-
Bandwidth	B	600 kHz	10 log B	-	57.8
Noise Figure	F	-	10 log F	-	5.0
S/N Required	S/N	-	10 log S/N	-	3.0
Processing Loss	L_p	-	10 log L_p	-	5.1
RF Losses - T_X	L_t	-	10 log L_t	-	2.0
RF Losses - R_X	L_r	-	10 log L_r	-	2.0
			TOTALS	310.1	127.3
			Diff.	182.8	
			÷ 4	45.7	
		10 dB/10	β-Meters	37.1K	
		$x5.396x10^{-4}$	β-NM	20	

SAMPLE RANGE EQUATION
CALCULATION SHEET

Figure C.1

SUMMARY OF POWER CALCULATIONS

NO.	RADAR	G_t	G_r	λ	σ	B	F	S/N	L_p	L_t	L_r	P_p	P_a	CI RAIN	REQ LAND
		dB	dB	M	M^2	kHz	dB	dB	dB	dB	dB	kW	W	dB	dB
Ia	L/4.5/7/3000	27.7	27.7	.231	1	175	5	1.4	5.1	1.5	1.5	4	84	12	43
Ib	L/4.5/2/3000	27.7	27.7	.231	1	600	5	1.6	5.1	1.5	1.5	15	90	7	38
Ic	L/4.5/7/1500	27.7	27.7	.231	1	175	5	3.0	5.1	1.5	1.5	6	63	14	48
Id	L/4.5/2/1500	27.7	27.7	.231	1	600	5	3.6	5.1	1.5	1.5	23	69	9	40
Ie	L/2.25/7/3000	30.7	30.7	.231	1	175	5	3.0	5.1	1.5	1.5	32	30	11	42
If	L/2.25/2/3000	30.7	30.7	.231	1	600	5	3.6	5.1	1.5	1.5	6	35	6	37
Ig	L/2.25/7/1500	30.7	30.7	.231	1	175	5	4.8	5.1	1.5	1.5	3	23	13	43
Ih	L/2.25/2/1500	30.7	30.7	.231	1	600	5	5.4	5.1	1.5	1.5	9	26	8	38
o Ii	L/3.4/2/2000	29.2	29.2	.231	1	600	5	3.0	5.1	1.5	1.5	8	32	7	38
IIa	S/4.5/7/3000	27.7	27.7	.107	1	175	5	1.4	5.1	2	2	24	504	26	43
IIb	S/4.5/2/3000	27.7	27.7	.107	1	600	5	1.6	5.1	2	2	85	510	21	38
IIc	S/4.5/7/1500	27.7	27.7	.107	1	175	5	3.0	5.1	2	2	34	357	28	48
IId	S/4.5/2/1500	27.7	27.7	.107	1	600	5	3.6	5.1	2	2	135	405	23	40
IIe	S/2.25/7/3000	30.7	30.7	.107	1	175	5	3.0	5.1	2	2	9	178	25	42
IIf	S/2.25/2/3000	30.7	30.7	.107	1	600	5	3.6	5.1	2	2	34	203	20	37
IIg	S/2.25/7/1500	30.7	30.7	.107	1	175	5	4.8	5.1	2	2	13	135	27	43
IIh	S/2.25/2/1500	30.7	30.7	.107	1	600	5	5.4	5.1	2	2	51	154	22	38
o IIi	S/3.4/2/2000	29.2	29.2	.107	1	600	5	3.0	5.1	2	2	59	236	21	38
IIIa	UHF/4.8/7/3000	24.6	24.6	.690	1	175	1.9	1.8	3.3	1	3.2	1	19	0	44
IIIb	UHF/4.8/2/3000	24.6	24.6	.690	1	600	1.9	2.4	3.3	1	3.2	4	21	0	39
IIIc	UHF/4.8/7/1500	24.6	24.6	.690	1	175	1.9	3.3	3.3	1	3.2	2	13	0	45
IIId	UHF/4.8/2/1500	24.6	24.6	.690	1	600	1.9	4.0	3.3	1	3.2	5	15	0	40
IIIe	UHF/3.4/2/2000	29.2	29.2	.632	1	600	1.9	3.0	5.1	1	3.2	1	4	0	38
IVa	X/3.4/2/2000	29.2	29.2	.030	1	600	8	3.0	5.1	3	3	2400	9600	42	38
* V	ASR-7(R=40 nmi)	34	34	.107	1	1500	4.7	6.8	3.6	2	2	400	400	22	49
VIa	S'/4.5/7/3000	27.7	27.7	.083	1	175	5	1.4	5.1	2	2	39	820	30	43
VIb	S'/4.5/2/3000	27.7	27.7	.083	1	600	5	1.6	5.1	2	2	141	846	25	38
VIc	S'/4.5/7/1500	27.7	27.7	.083	1	175	5	3.0	5.1	2	2	56	588	32	48
VId	S'/4.5/2/1500	27.7	27.7	.083	1	600	5	3.6	5.1	2	2	224	672	27	40
VIe	S'/2.25/7/3000	30.7	30.7	.083	1	175	5	3.0	5.1	2	2	14	297	29	42
VIf	S'/2.25/2/3000	30.7	30.7	.083	1	600	5	3.6	5.1	2	2	56	337	24	37
VIg	S'/2.25/7/1500	30.7	30.7	.083	1	175	5	4.8	5.1	2	2	22	224	31	43
VIh	S'/2.25/2/1500	30.7	30.7	.083	1	600	5	5.4	5.1	2	2	85	255	26	38
o VIi	S'/3.4/7/2000	29.2	29.2	.083	1	600	5	3.0	5.1	2	2	98	391	25	38

o Selected Candidates

* NOTE - ASR-7 Power was assumed; range calculated

FIGURE C.2

ANTENNA GAIN AND APERTURE CALCULATIONS

ANTENNAS CONSIDERED -

ASSUME COSINE DISTRIBUTION IN AZIMUTH

REL GAIN - 0.9 dB

HALF POWER BEAMWIDTH - $69 \frac{\lambda}{A}$

SIDELOBES - DOWN 23 dB

ASSUME COSECANT COVERAGE IN ELEVATION

GAIN LOSS $\simeq 2 - \phi_0 \cot \phi_M \simeq 1.82$ (2.6 dB)

ϕ_0 = NORMAL PATTERN - ASSUMED 6°

ϕ_M = COSECANT LIMIT - ASSUMED 30°

GAIN EQUALS $\frac{35,500}{\theta.\phi}$ X RELATIVE GAIN X COSECANT LOSS

FIGURE C.3

PERFORMANCE CALCULATIONS

ANTENNAS USED IN CALCULATIONS

Θ	ϕ_0	ϕ_N	CSC^2 LOSS	DISTRIBUTION LOSS	THEO. GAIN	NET GAIN
1.5°	6°	30°	2.6 dB	0.9 dB	36.0	32.5
2.25°	6°	30°	2.6	0.9	34.2	30.7
3.4°	6°	20°	2.3°	0.9	32.4	29.2
4.5°	6°	30°	2.6	0.9	31.2	27.7
6.0°	6°	30°	2.6	0.9	29.9	26.4

APERTURE SIZE = $69 \frac{\lambda}{\Theta}$

BAND	λ(FT)	1.5°	2.25°	3.4°	4.5°	6.0°
UHF	2.26	103'	69'	46'	35'	26'
L	0.755	35'	23'	15'	12'	9'
S	0.351	16'	11'	7'	5.4'	4.0'
S'	0.273	12.5'	8.4'	5.5'	4.2'	3.2'
X	0.106	5'	3.3'	2.2'	1.6'	1.2'

FIGURE C.4

A sample calculation sheet for rain is shown in Figure C.5 and for ground clutter in C.6. For this study all values in the calculations feet are filled in except the Clutter Improvement (CI) including Range - 20 nmi. The value of clutter improvement required is then calculated. The values calculated for the various candidates are summarized in Figure C.2.

RAIN CLUTTER

SAMPLE CALCULATION

$$R^2 = \frac{\sigma_t \, I}{\Theta \, \emptyset \, \tau \, \sigma_o \, S/C \times 6.16 \times 10^4}$$

ITEM		dB +	dB -
σ_t - dB above $1M^2$		0	
I - C.I. in dB		12.1	
Θ - Az BW - Deg.	4.5		6.5
$\emptyset$ - El BW - Deg.	6		7.8
τ - PW - μSec.	7		8.5
σ_0 - dB M^2/M^3		88	
SIG/CLUTTER REQ			3.4
K - 6.16×10^4			47.9
SUM		100.1	74.1
DIFF - 20 log R			26
R - n miles			20

BAND	σ-4mm/hr	σ 16 mm/hr
K	- 56	- 37
X	- 62	- 53
C	- 72	- 62
S	- 83	- 74 (S' = -70)
L	- 97	- 88
P (450)	-116	-107

FIGURE C.5

LAND CLUTTER

SAMPLE CALCULATION

$$R = \frac{\sigma_t \cdot C.I.}{\Theta \tau \sigma_o \; S/C \; 3.5 \times 10^3}$$

ITEM	dB +	dB -
σ_t - dB above $1M^2$	0	
C.I. in dB	48.8	
Θ - Az BW - Deg. 4.5		6.5
τ - PW - μsec. 7		8.5
σ_0 dB below 1 M^2/M^2	18	
SIG/CLUTTER REQ.		3.4
K 3.5×10^3		35.4
SUM	66.8	53.8
DIFF - 10 log R		13
R - n miles		20

σ_0 (95 percentile) = -18 dB M^2/M^2

FIGURE C.6

APPENDIX D

ENVIRONMENTAL DATA

This appendix provides supporting data for the environmental models summarized in Sections 2.4.

D.1 LAND CLUTTER MODEL

There is no typical land clutter model because there is no typical radar site; all sites have widely varying amounts of land clutter return depending upon the type of terrain, the nature and density of man-made objects, and the effect of shadowing. Nathanson (Nathanson 1969) provides a table of land clutter data (50 and 84 percentiles) at UHF, L, and S Band, for low grazing angles and radar resolution cell size of approximately 2° by 500 feet. Most land clutter reflectivity data is reasonably fitted by a log-normal distribution; the results are shown for Nathanson's data in Figure D.1. The ordinate shows the value of the unit of physical area illuminated by the radar. The radar cross section σ_c of clutter observed by a radar which has a beamwidth of θ radians and a pulsewidth τ is usually approximated by

$$\sigma_c = \sigma_o \int_{\theta,\tau} dA \simeq \sigma_o \, R\,\theta\,\frac{c\tau}{2} \qquad \text{(D-1)}$$

where R is the range and c is the speed of light.

The abcissa in Figure D.1 can be used to estimate the number of radar cells in which the clutter level exceeds a specific value. For example, a radar designed to operate in -20 dB land clutter with a 2° beamwidth and 500 feet (1 microsecond) of range resolution has about 31,000 cells at ranges between one and 15 miles. Figure D.1 shows that between 30% and 0.5% of these cells (9300-160) would exceed the σ_o value of -20 dB. This does not mean, however, that the minimum size aircraft would be undetectable in this many cells, because clutter cross section (Equation D.1) decreases as the radar range decreases.

Figure D.2 shows the conditions selected to define the ASR-( ) and SRTR clutter models. Half the land clutter region is assumed to consist of Rocky Mountain-type land clutter (curve 7 of Figure D.1) and the remainder consists of city-type clutter (curve 6 of Figure D.1).

In order to ensure that aircraft are detectable at maximum range in land clutter 90% of the time, a σ_o value of -20 dB (.1 M^2/M^2) is

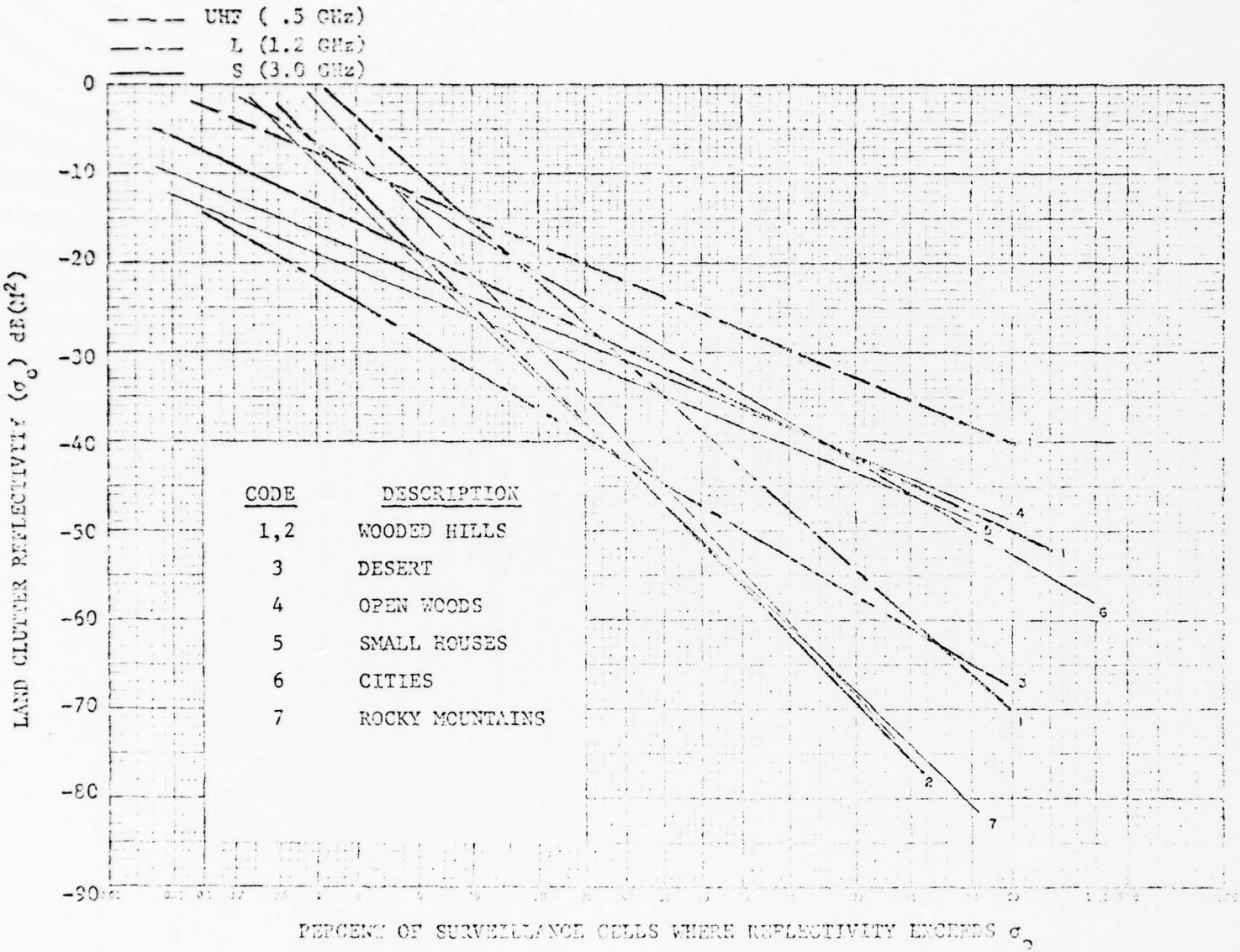

FIGURE D.1 LAND CLUTTER BACKSCATTER DATA

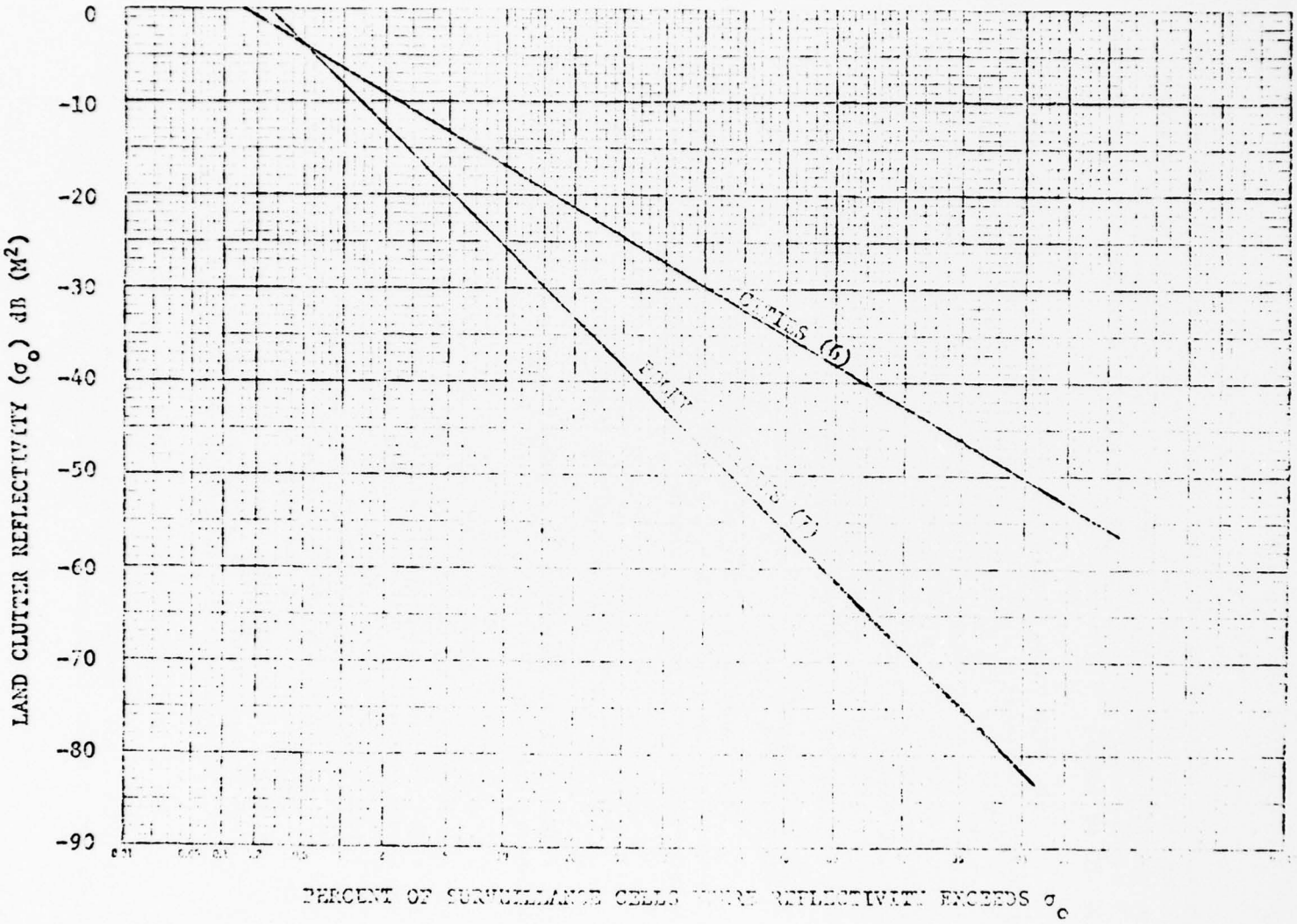

FIGURE D.2 SELECTED LAND CLUTTER MODELS

appropriate since 5% of the Rocky Mountain clutter cells and about 15% of the city clutter cells will exceed -20 dB, and half of the displays are occupied by each type of clutter. Hence a total of 10% (.5 x .05 + .5 x .15 = .1) of the resolution cells for the model exceed the -20 dB value.

The SRTR has a resolution cell which is three times as large as that of the ASR-( ) (3.4° x 2 microseconds versus 2.2° x 1 microsecond). Thus a clutter cell which exceeds the radar capability will mask out three times the area as is masked for the ASR-( ). To maintain comparable coverage in terms of area lost due to excessive clutter, the SRTR specification in terms of σ_o would have to be about -13 dB. However, cost is an important factor in the SRTR, and a value of σ_o = -18 dB ($0.016M^2/M^2$) was chosen as a reasonable specification. For the half-mountain, half-city model of Figure D.2, this value is exceeded only 8% of the time.

D.2 RAIN CLUTTER

Rain backscatter data in Nathanson (Nathanson 1969) is expressed in terms of volume reflectivity (ρ), the equivalent radar cross section of the rain backscatter per unit volume. An excellent fit to Nathanson's rain data is

$$10 \log (\rho) = -111 \text{ dB} + 40 \log F + 16.6 \log r. \qquad \text{(D-2)}$$

where F is the radar frequency in Gigahertz and r is the rainfall rate in millimeters per hour.

Figure D.3 shows the instantaneous probability of observing a given rainfall rate for three cases: New Orleans (from Nathanson) and for Florida and the East Cost/Pacific Northwest (data provided by E. C. Muehe of Lincoln Laboratory). It is seen that rain occurs above the "drizzle" level (0.25 millimeters per hour) in these regions about 3 to 6% of the time or about 250 to 500 hours per year. During periods when it is raining more than 0.25 mm/hr, the rainfall is more than the "heavy" rain condition of 16 mm/hr about 3 to 7% of the time, corresponding to 9 to 35 hours per year. In addition, single rain storms contain varying rainfall rates ranging from drizzle to very heavy; the relationship between mean storm diameter and rainfall rate (again from Nathanson) is also shown in Figure D.3.

Based upon these factors, a rain rate of 16 mm/hour was chosen as a reasonable requirement for establishing the performance of the ASR-( ) and the SRTR. The values of the reflection coefficient (Equation D-2) for the frequencies considered in the radar study are as follows:

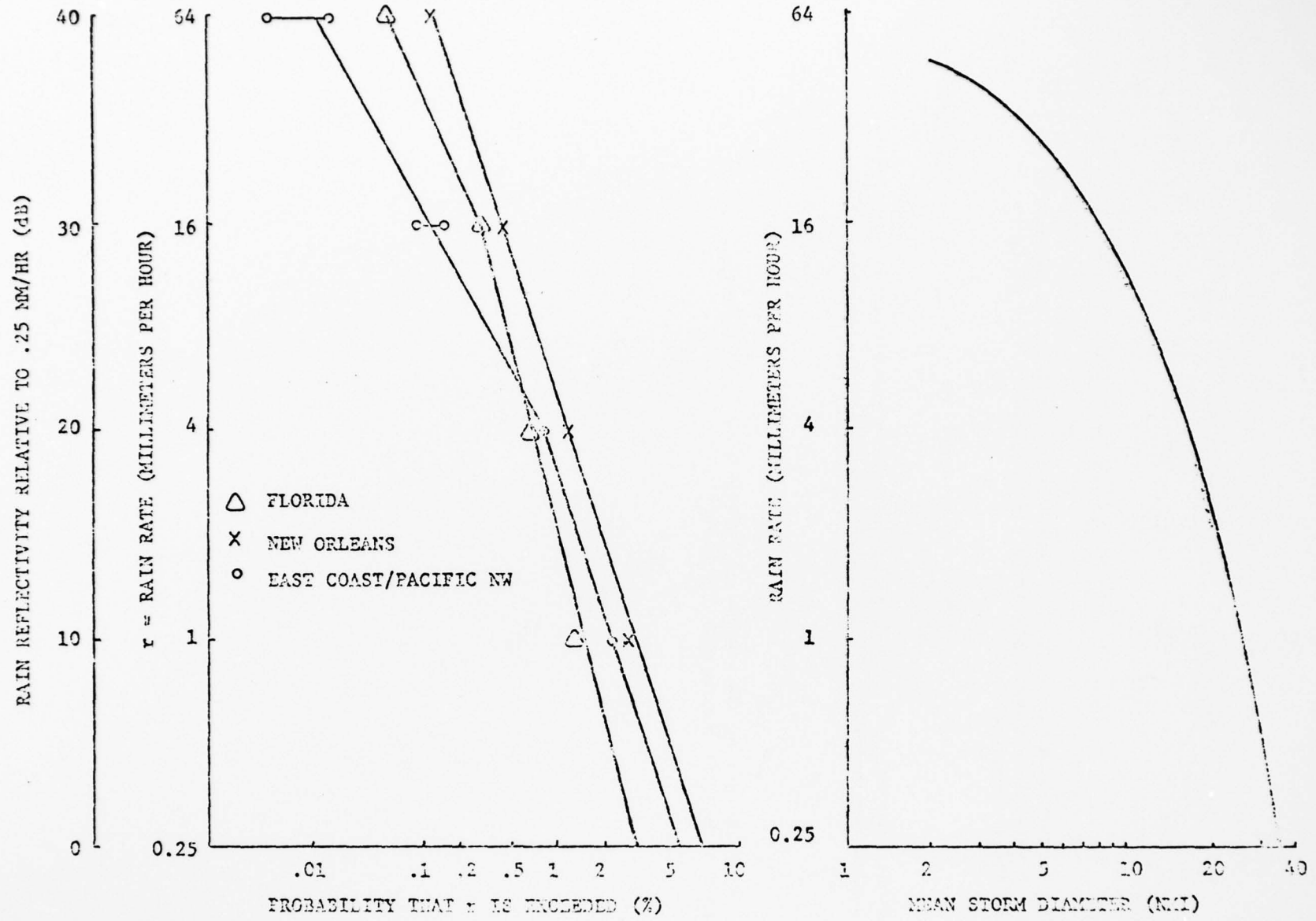

FIGURE D.3 RAIN CHARACTERISTICS

Frequency	ρ(16 mm/hr)
.43 GHz	-106 dB M^2/M^3
1.3	- 86
2.8	- 73
3.6	- 69

The cross section of rain clutter σ_c observed by a radar with azimuth beamwidth θ (radius), elevation beamwidth $\emptyset$, pulsewidth τ is given by the approximate relationship

$$\sigma_c = \rho \int_{\tau,\theta,\phi} dv \simeq \rho\, R^2\, \theta\, \phi\, \frac{c\tau}{2} \qquad \text{(D-3A)}$$

provided that the rain at range R completely fills the elevation beamwidth. When the elevation beamwidth is not completely filled by the rain, this becomes

$$\sigma_c \simeq \rho R \theta \frac{c\tau}{2} h \qquad \text{(D-3B)}$$

where h is the height of the rain. A reasonable value for maximum rain height h is 3,000 meters (10,000 feet).

D.4 ANGEL CLUTTER

Angel clutter (often referred to as AP in air traffic controller jargon) appears on Airport Surveillance Radar PPI displays as large masses of point targets which occur at locations where there are no known aircraft or normally-expected sources of radar clutter (land and weather returns). Birds and flocks of birds are the predominant sources of angel clutter on the ASR displays.

The radar cross section of a single bird is frequency-dependent if the wavelength is comparable to or longer than the size of the bird. The radar cross section of individual birds are generally quite small, even for large birds such as swans and vultures, and most detectable angels consist of flocks of birds within a single resolution cell of the radar which can have substantial radar cross sections.

Pollin (Pollin 1972) provides a model for the average radar cross section of single birds as a function of bird weight and radar wavelength. The short dotted lines in Figure D.4 show his data for the four frequencies of interest to the Radar Study. Also shown near the abscissa is the percentile by weight of several different species of birds.

In order to translate these data to average radar cross section of bird flocks, it was assumed that flock size was inversely proportional to bird size; that is, the cube root of bird weight. (Flocks of sparrows are considerably larger than flocks of ducks.) It was further assumed that a reasonable flock size for ducks was about 12; the resulting estimated flock size $\overline{N}$ is also plotted in Figure D.4. Combining the individual bird cross section data with the assumed flock size $\overline{N}$ results in the solid curves in Figure D.4, which represent the estimated average radar cross section of bird flocks for the four frequencies as a function of bird weight.

These data show that, at UHF, smaller birds contribute little angel clutter, while large birds produce larger cross sections at UHF than at the higher radar frequencies. The two S-band frequencies are uniformly affected by flocks of birds of all sizes, and L-band is worse than S-band except for birds smaller than starlings.

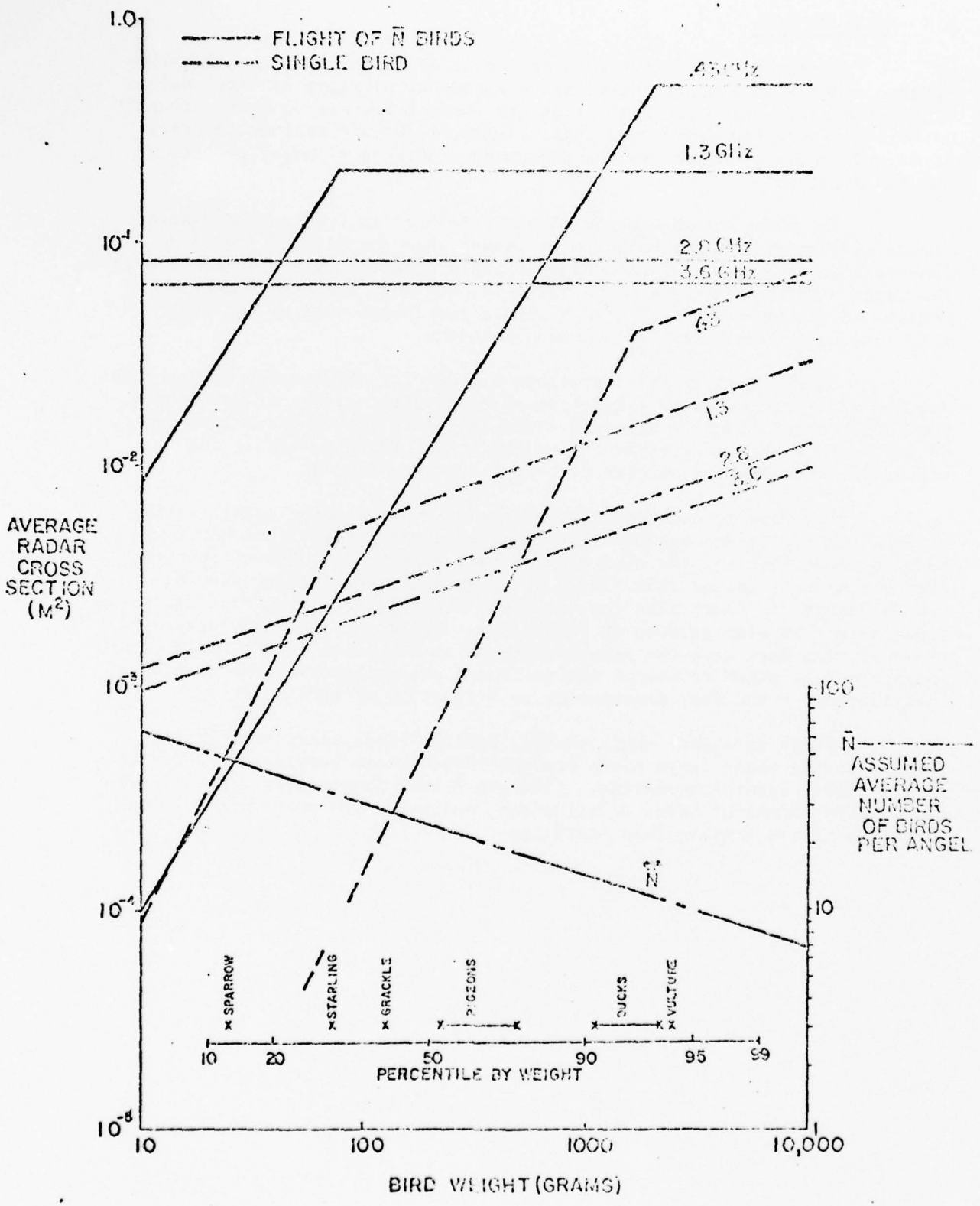

FIGURE D.4 BIRD ANGEL RADAR CROSS SECTION MODEL

APPENDIX E

TARGET CHARACTERISTICS

E.1 INTRODUCTION AND SUMMARY

Since an air traffic control radar must provide surveillance against all aircraft within its required coverage volume, a small general aviation aircraft was chosen for defining the performance of the ASR-( ) and the Short Range Terminal Radar. In FAA 1973E, three representative general aviation aircraft were measured on a test range at the Holloman Air Force Base Radar Target Scatter (RATSCAT) facility. All three were small single engine aircraft: a Cessna 150L (all metal, high wing), a Piper Cherokee 140 (all metal, low wing) and a Piper Super Cub (high wing, fabric covered, metal frame). The purpose of this Appendix is to summarize the results of these measurements and to define an appropriate target model for ASR-( ) and SRTR range performance calculations.

It is concluded that a one square meter, Rayleigh fluctuating (Swerling Case I or II) target is an appropriate model for small general aviation aircraft in terminal airspace for linear polarization. For circular polarization a loss of 2 dB is appropriate.

E.2 DATA

The reference provides data for L, S, and C Bands at horizontal, vertical, and circular polarization. Frequencies closest to those considered for the ASR-( ) and the SRTR are 1.25 GHz (L Band) and 2.8 GHz (S Band). The L Band data was taken only for 0° roll and 0° pitch. However, roll and pitch variations at S Band were greatest for the broadside aspect angles (90° and 270°) where the radar cross section tends to be large, hence consideration of only the 0° roll 0° pitch case should provide properly conservative results.

Figure E.1 shows the probability distribution function of the Piper Cherokee 140 for vertical (VV) and horizontal (HH) polarization at L and S Bands and for right-circular (RR) polarization at S Band. These curves were obtained (quite tediously) by expanding dividers along raw data plots of radar cross section versus azimuth in the reference. Figure E.1 shows:

a) negligible difference between L and S Band radar cross section distributions for horizontal polarization, with a median value of about $1M^2$.

b) A loss for circular polarization (at S Band) of about 3 dB, resulting in a median value of about $0.5M^2$.

Figures E.2 and E.3 are polar plots of median radar cross section as a function of aircraft aspect angle (azimuth) for the same Piper Cherokee 140 aircraft for L and S Band. The median values were calculated by RATSCAT over 10° intervals, and are for the 0° pitch, 0° roll condition. Several interesting

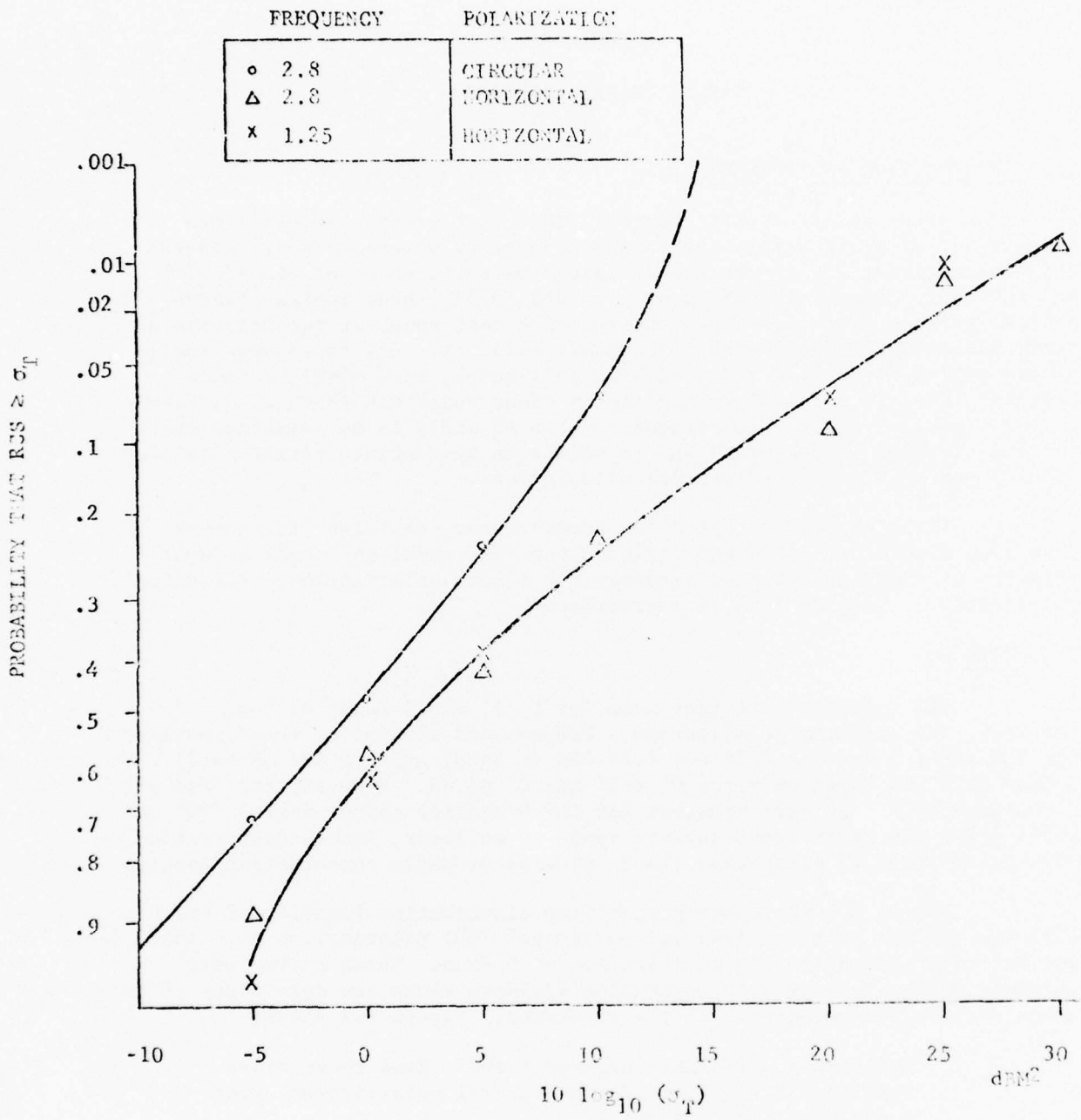

FIGURE E.1 RADAR CROSS SECTION DISTRIBUTION FOR PIPER CHEROKEE 140 OVER ALL ASPECT ANGLES (0° PITCH, 0° ROLL)

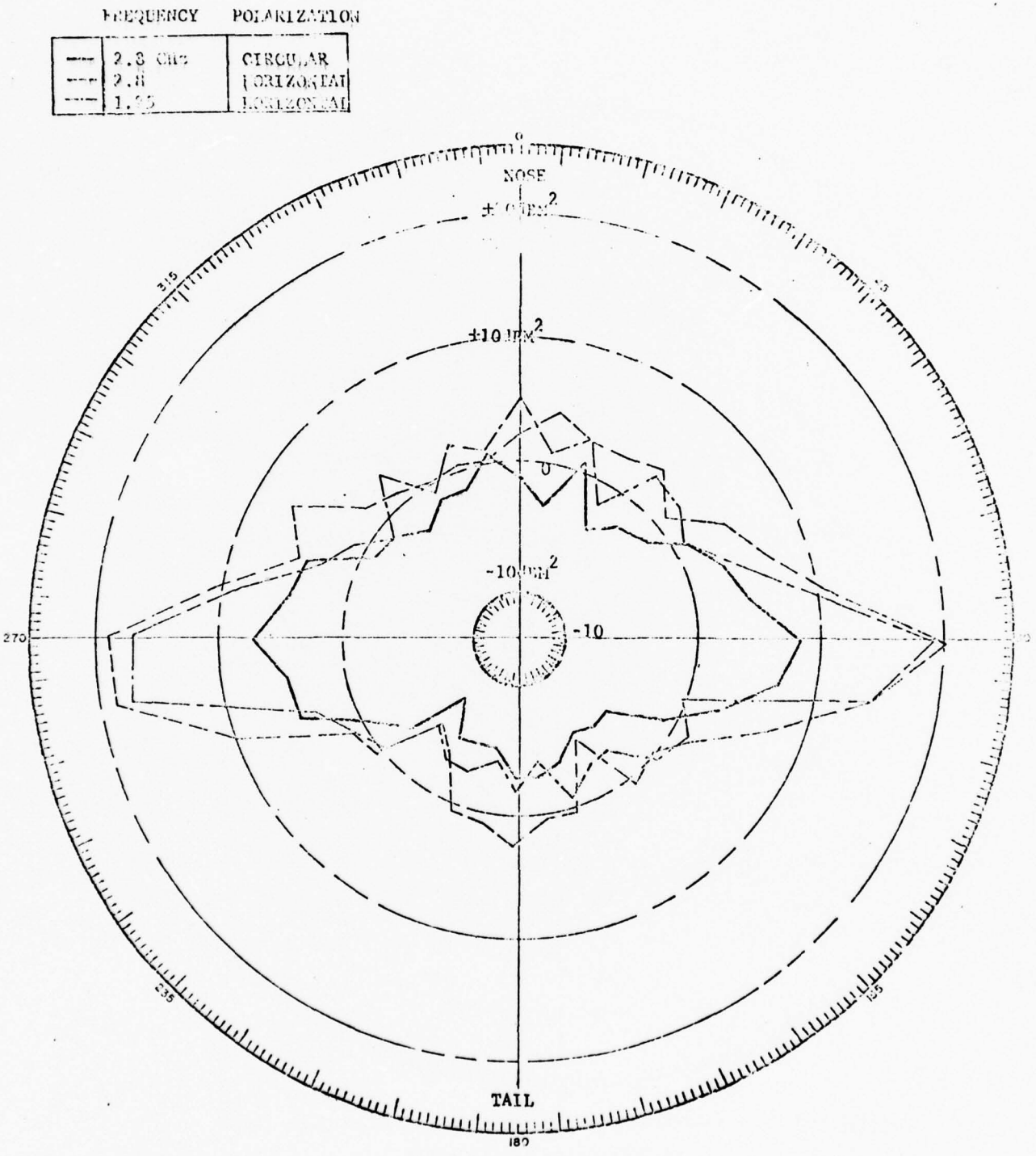

FIGURE E.2 PIPER CHEROKEE 140 MEDIAN RADAR CROSS SECTION (dBM^2) VERSUS AIRCRAFT ASPECT ANGLE

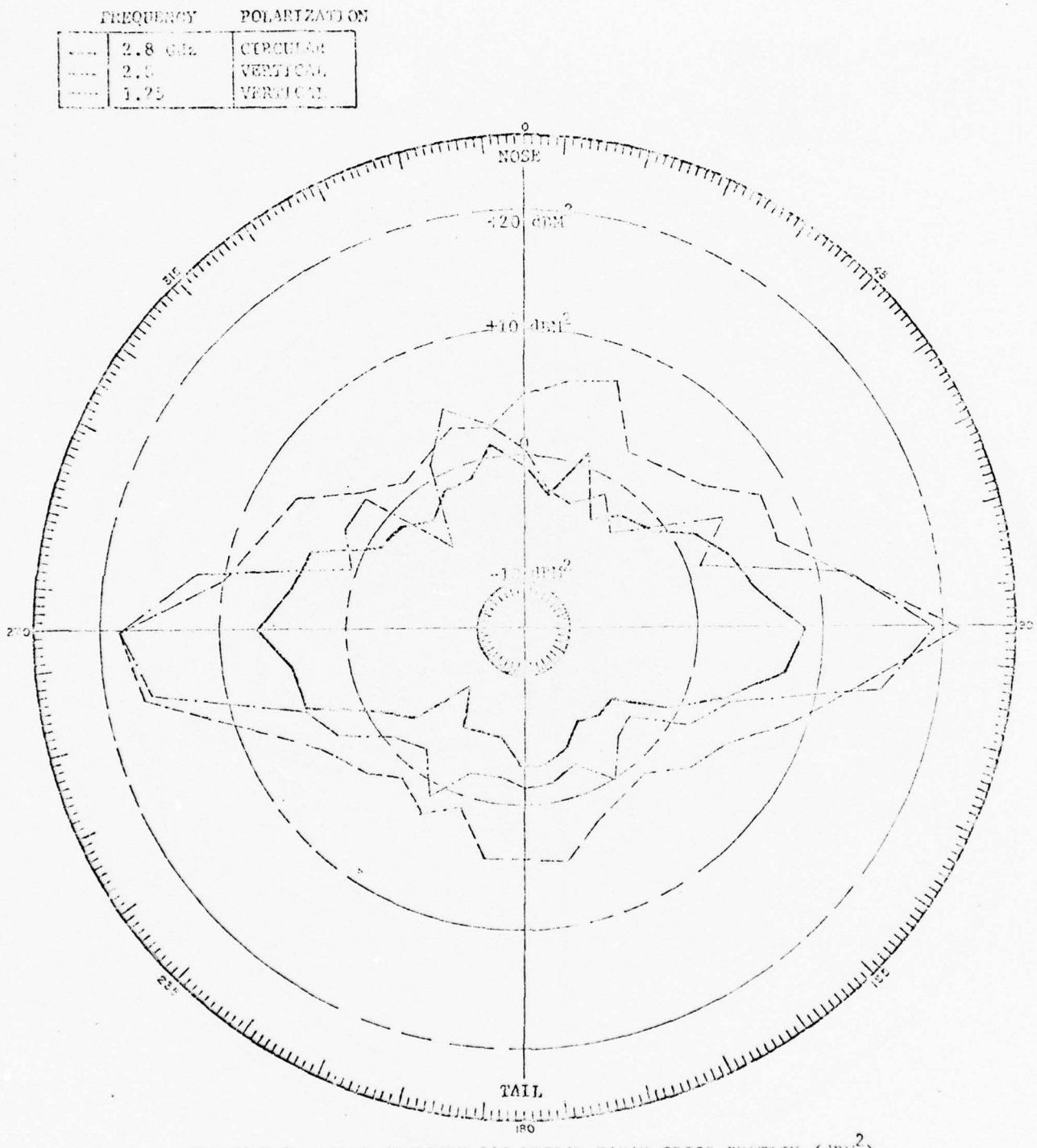

FIGURE E.3 PIPER CHEROKEE 140 MEDIAN RADAR CROSS SECTION (dBM^2) VERSUS AIRCRAFT ASPECT ANGLE

points can be made from these plots:

a) Within ±50° of the nose or tail aspects, vertical polarization at S Band produces a slightly larger median cross section than horizontal polarization, while at L-Band both polarizations produce about the same results as S-Band horizontal polarization (Figure A-1).

b) Within ±20° of broadside both linear polarizations (S and L Band) produce about the same results. However, circular polarization reduces the S-Band radar cross section by about 12 dB.

c) At S-Band, circular polarization produces losses at all aircraft aspect angles, the loss being greater for vertical than for horizontal polarization.

The 12 dB broadside loss for circular polarization is particularly unfortunate because aircraft flying tangential courses do not have the benefit of MTI cancellation in rain. One would therefore expect better performance from an L-Band radar (which does not require circular polarization for rain rejection) than from an S Band radar with circular polarization for tangential targets.

Table E.1 provides numerical values for the median radar cross section data plotted in Figures E.2 and E.3 for the Piper Cherokee 140. Values for L-Band circular polarization were included for completeness, although circular polarization was considered unnecessary for rain rejection at L-Band. Median values are shown for the full 360° and for the nose-on ±5° and ±50° aspects. Results can be summarized as follows:

a) For horizontal polarization, there is little difference between L and S Band. Radar range differences are less than 7% over 360° and 1% for within ±50° of the nose-on aspect.

b) For vertical polarization, S-Band produces a higher median radar cross section than L-Band. Radar range improvement is 20-26%.

c) Circular polarization reduces the S-Band medians by 4-6 dB over 360° and 4-5 dB for the nose ±50° aspects.

d) There is no significant difference between the 360° medians and the ±50° medians for linear polarization.

e) Nose-on ±5° medians are larger than the medians for larger ranges of aspect angles for most cases.

Table E.2 provides similar data for all three aircraft for the nose-on ±50° range of aspect angles. Interesting differences are:

TABLE E.1

MEDIAN RADAR CROSS SECTION (SQUARE METERS) FOR PIPER CHEROKEE 140

0° PITCH, 0° ROLL

RANGE OF ASPECT ANGLES	360°		NOSE ±50°		NOSE ±5°	
FREQUENCY	1.25 GHz	2.8 GHz	1.25 GHz	2.8 GHz	1.25 GHz	2.8 GHz
HORIZONTAL POL.	1.3 M^2	1.7 M^2	1.5 M^2	1.6 M^2	3.5	1.8 M^2
VERTICAL POL.	1.25	2.8	.85	2.2	1.1	3.3
CIRCULAR POL.	1.1	0.69	1.3	0.68	0.91	0.78

TABLE E.2

MEDIAN RADAR CROSS SECTION (SQUARE METERS) FOR THREE AIRCRAFT

0° PITCH, 0° ROLL, NOSE ±50° ASPECT

AIRCRAFT	PIPER CHEROKEE 140		CESSNA 150		PIPER SUPER CUB	
TYPE	LOW WING, METAL SKIN		HIGH WING, METAL SKIN		HIGH WING, FABRIC COVERED METAL FRAME	
FREQUENCY	1.25 GHz	2.8 GHz	1.25 GHz	2.8 GHz	1.25 GHz	2.8 GHz
HORIZONTAL POL	1.5 M^2	1.6 M^2	1.1 M^2	1.3 M^2	1.6 M^2	.91 M^2
VERTICAL POL.	.85	2.2	1.3	1.3	3.2	3.2
CIRCULAR POL.	1.3	0.68	0.66	1.7	1.1	1.7

a) The high wing aircraft tend to favor vertical polarization and have the same medians at L and S Bands.

b) The metal frame of the fabric-covered Super Cub enhances its reflectivity relative to the metal-skinned aircraft except at S Band with horizontal polarization.

c) Circular polarization at S Band provides a gain in median radar cross section for the Cessna 150. For the Super Cub, circular polarization produces a gain of 2.7 dB over horizontal and a loss of 2.8 dB relative to vertical polarization.

d) Vertical polarization provides better performance for all cases except for the Cherokee 140 at L Band.

Comparison of the median cross section computed for ±5° from the nose-on aspect with the data from Table E.2 (nose-on ±50°) shows that the ±5° median is larger than the ±50° median for all cases except L Band circular polarization for the Super Cub and the Cherokee 140. The average decibel increase is 2.9 dB at S Band and 3.6 dB for L Band. The nose-on ±50° case produces comparable results to the tail-on ±50° aspects.

E.3 RESULTS

E.3.1 Median Radar Cross Section

For the three aircraft, there is no clear trend in median cross section data as a function of frequency or polarization. Although it is reasonable to assume that all aircraft aspects are equally likely for surveillance at long range, it is appropriate to exclude the large returns at broadside ±40° from the model used in radar performance calculations in order to ensure a reasonably conservative design. The nose-on ±50° range of aspect angles is therefore appropriate for defining the target model used in ASR-( ) and SRTR performance computations.

Assuming that the three aircraft considered here are a reasonable sample of small general aviation aircraft, and that the smallest should be detectable at maximum range, an appropriate radar cross section for linear polarization at L and S bands is one square meter. Comparing this value with the smallest medians, the errors are +0.7 and -0.4 dB at L Band and +0.4 and -1.1 dB at S Band. The corresponding radar range variations are 2 to 6%. For circular polarization at S Band, a loss of 2 dB relative to one square meter ($0.63M^2$) is appropriate.

E.3.2 Extensions to UHF and High-S Bands

The available RATSCAT data does not consider the high S Band (3.5 - 3.7 GHz) and UHF (.43 GHz) frequencies considered in the ASR-( ) and SRTR studies. Consequently, the same one square meter radar cross section was used for high-S and UHF bands. In the case of UHF, this is a

poor assumption and the resulting radar calculations have a higher degree of uncertainty. Until comparable measurements are made on the same aircraft at UHF, it is difficult to state whether a one square meter cross section at UHF is conservative or not since the radar wavelength (2.3 ft.) is comparable in size to a number of the individual scatters in the aircraft structure.

E.3.3 Fluctuation Statistics

A fluctuation model is necessary to relate measured radar cross section data to the probability of detection on a given scan, since the probability of observing a given cross section on each scan must be computed. The most widely used fluctuation model for aircraft targets is the Rayleigh model, which assumes that the aircraft behaves as a random assembly of scatters, no one of which is dominant. The resulting probability density function for the input signal-to-noise power ratio is exponential:

$$W(X,\overline{X}) = \frac{1}{\overline{X}} \exp - \frac{-X}{\overline{X}} \quad X \geq 0 \qquad \text{(E-1)}$$

where X = input signal-to-noise (power) ratio
$\overline{X}$ = average value of X over all target fluctuations.

Using this expression, Swerling (Swerling 1954) has computed detection probability curves which relate false alarm rate, detection probability, and signal-to-noise ratio for two cases. Swerling Case 1 assumes that the radar cross section remains constant on any given scan of the radar but fluctuates independently from scan to scan, while the Swerling Case 2 model assumes that the radar cross section varies independently from pulse to pulse as well as from scan to scan. The Case 1 model is applicable to fixed frequency radars since the target aspect angle changes little during the few milliseconds that the radar beam illuminates the target. The Case 2 model is appropriate if the radar frequency is changed from pulse-to-pulse by an amount Δf sufficient to decorrelate the target:

$$\Delta f = 150/L \text{ in MHz} \qquad \text{(E-2)}$$

where L is the target radial extent in meters. Assuming a 10 meter length for small aircraft, 15 MHz of pulse to pulse frequency agility should be sufficient to change the target from Case 1 to Case 2. Pulse-to-pulse polarization agility may also have a similar effect in some cases.

In order to check the assumption of Rayleigh fluctuations with the measured radar cross section data, cumulative distributions of radar cross section for the Piper Cherokee 140 were extracted from the raw data for the nose-on ±50° range of aspects. Figures E.4 and F.5 compare the S-Band and L-Band data points (respectively) with the Rayleigh fluctuation model (Equation A-1) for a one-square meter mean cross section. Straight-line fits to the data points produce a slope that is essentially the same as the dotted line for the Rayleigh model, indicating that use of this model is

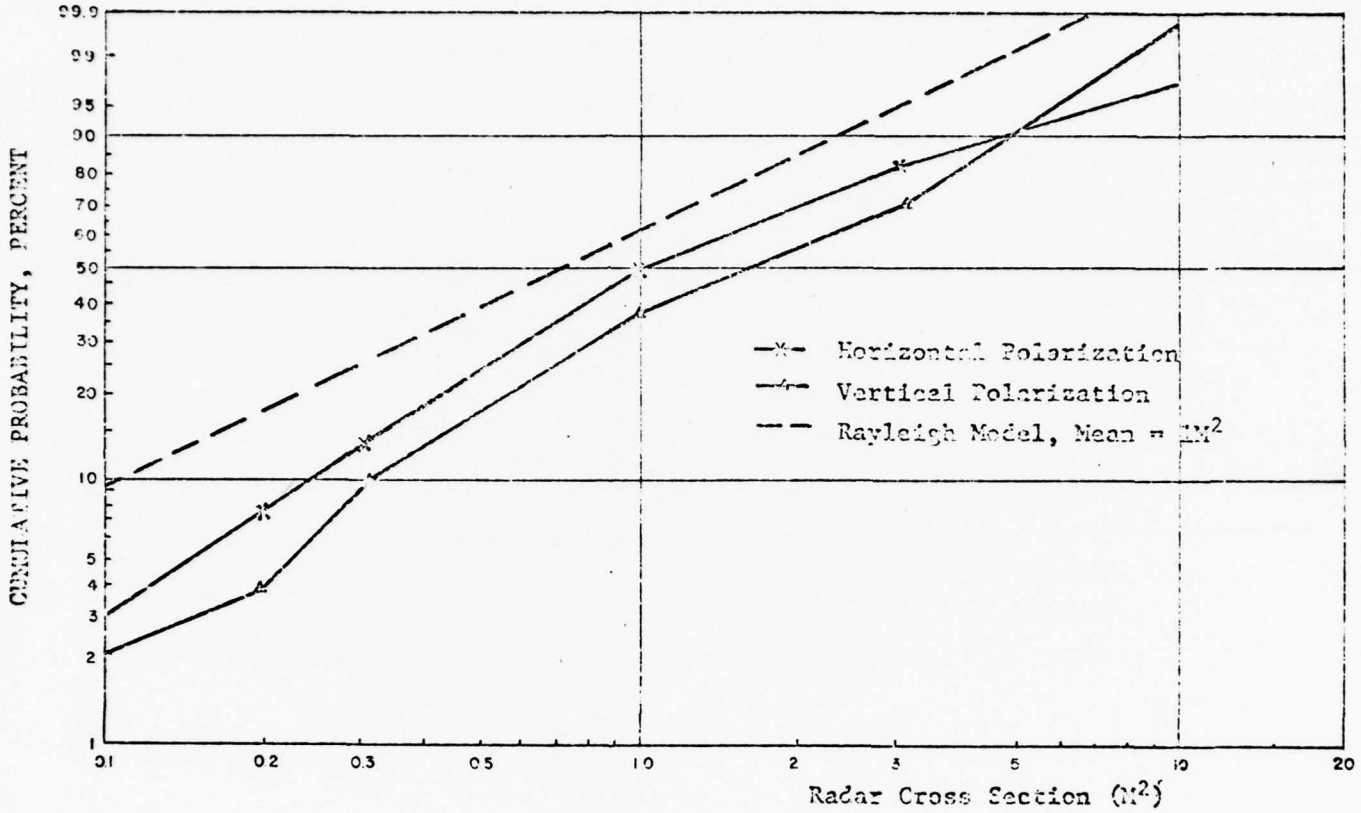

FIGURE E.4

COMPARISON OF PIPER CHEROKEE 140 S-BAND CROSS SECTION DISTRIBUTIONS WITH RAYLEIGH MODEL FOR NOSE-ON ± 50° ASPECTS

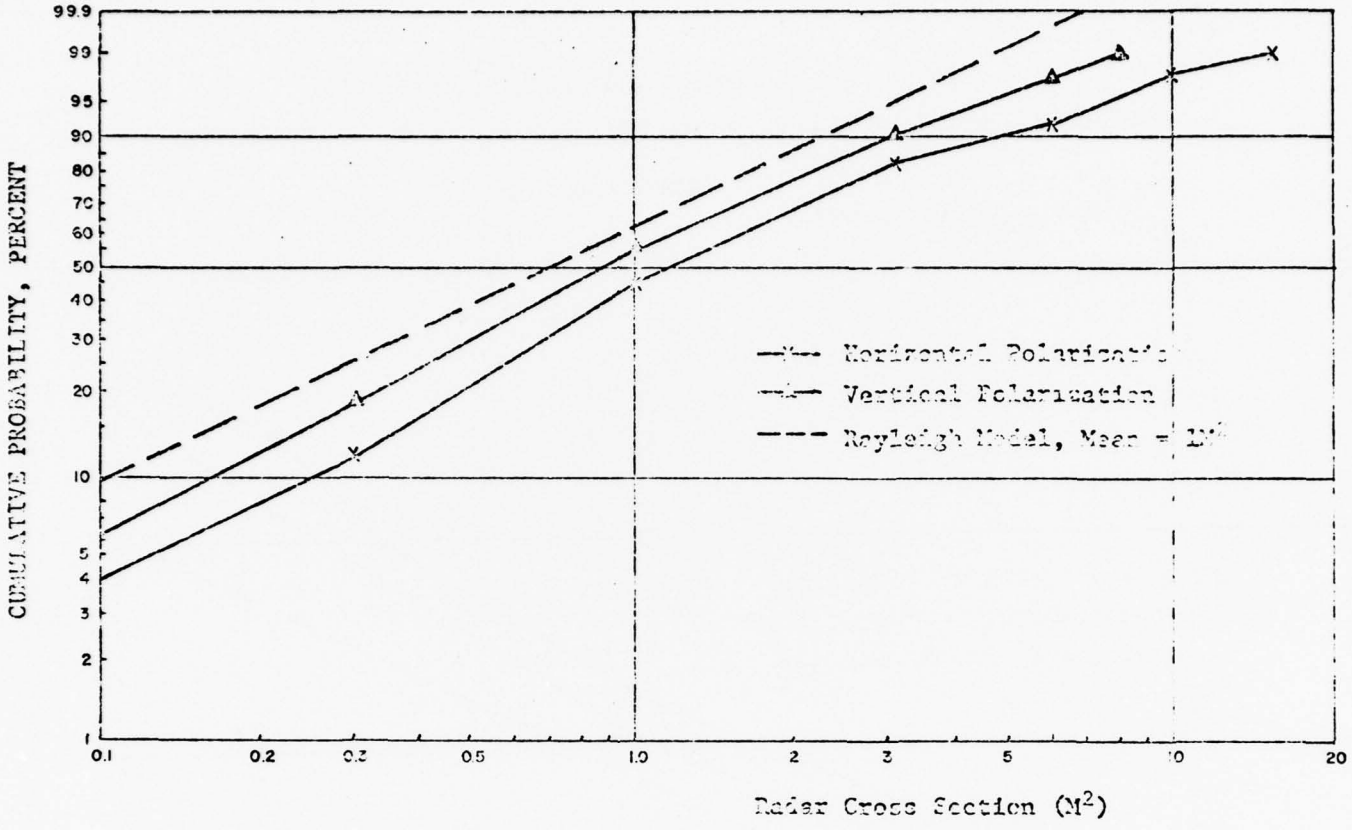

FIGURE E.5

COMPARISON OF PIPER CHEROKEE 140 L-BAND CROSS SECTION DISTRIBUTIONS WITH RAYLEIGH MODEL FOR NOSE-ON ± 30° ASPECTS

valid for the Piper Cherokee 140 within ±50° of the nose-on aspects. The data points are below the Rayleigh line because the mean radar cross sections of the Cherokee are larger than the one square meter value used for the Rayleigh line. It should also be noted that the S-Band median (50%) cross sections in Figure F.4 are slightly different from the PATSCAT printout medians tabulated in Table F.1; this inaccuracy is not unexpected since the data in the figure was obtained by expanding dividers across the raw data plots, which contain very many close-spaced peaks and nulls.

The Rayleigh fluctuating target model (Swerling Case 1 and Case 2 detection probability statistics) is therefore appropriate for aspects of interest (those excluding large cross sections near broadside) to the ASR-( ) and Short Range Terminal Radar studies. Since Swerling's work used the average signal-to-noise power ratio (Equation E.1), the mean radar cross section is the appropriate value to use in the radar equation. For the Rayleigh target, the mean corresponds to the 63rd percentile value and is 1.44 times (1.6 dB) larger than the median. Because of the inherent uncertainties in radar cross section measurements, this correction factor is often justifiably ignored. In a free space environment, radar detection range predictions are about 10% conservative if the median, rather than the mean, cross section is used.

APPENDIX F

TWO-HORN FEED SYSTEM

Two of the simpler ways to obtain the csc^2 coverage required to see targets below some fixed altitude are:

(1) to distort or "spoil" the pattern by changing the shape of the reflector, and

(2) to change the aperture distribution by shaping the primary feed pattern by using multiple feeds. It is the purpose of this appendix to evaluate the possibility of using a simple two-horn feed to produce the desired pattern or an approximation thereof. If possible, this approach might lead to a smaller size than that required for the shaped reflector case.

In Figure F.1 the patterns produced by two horns (dotted) in a common reflector are shown. One feed is at the focal point of the paraboloidal reflector and the other is moved vertically (down) so as to deflect the beam upward. Note that the second horn is displaced from the first in angle by 6 degrees or one beamwidth. Note also that the second beam is broadened. The broadening is a function of both displacement from the focus and also the size of the feedhorns. It is assumed here that the broadening factor is about 1.6. It is further assumed that the peak power of the second beam is down 6 dB from the first pattern. The composite pattern (neglecting sidelobes) is shown as the solid line in Figure F.1.

This pattern has been plotted on a range-height diagram in Figure F.2. Note that the resulting pattern meets the requirement for coverage to 16 nmi and altitudes up to 10K feet up to elevation angles of 20 degrees with the small exception of the 20°/10K foot corner.

Such a feed could take the form shown in Figure F.3. An approximation to the coupler size shown can be calculated by assuming that the 6 dB difference between patterns is made up of that part due to the coupler and that part due to the gain reduction of the pattern from the second feed. The gain reduction should be roughly proportional to the beam broadening, a factor of 1.6, or 2 dB. The other 4 dB would be obtained in the coupler.

Such a coupler is shown in Figure F.3. Neglecting ohmic loss, the coupler provides power out of port A which is down 1.5 dB from the input and port B which is down 5.4 dB from the input. This means that the gain on the peak of the beam will be down 1.5 dB from the normal gain of the feed/reflector combination. This is well within the -2.3 dB used when calculating the gain in Appendix C. If a more pronounced "thumb" pattern is desired, it is only necessary to obtain more power from B and take the reduction in power at A.

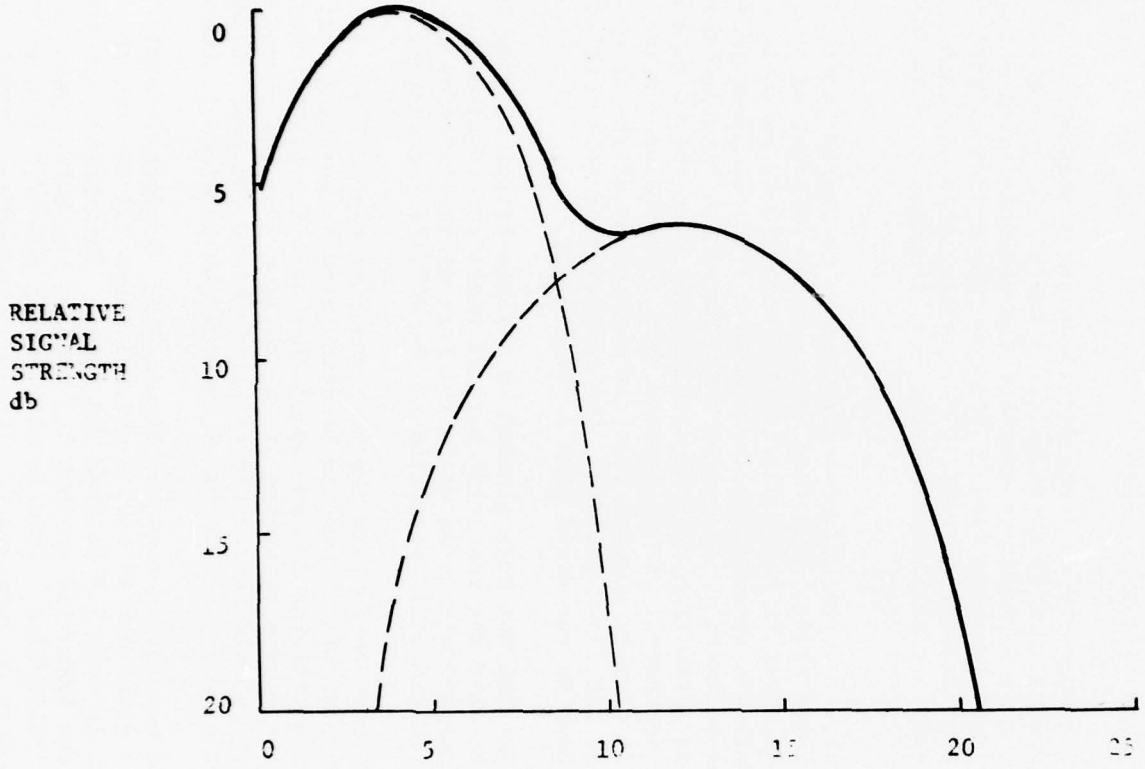

FIGURE F.1

TWO-HORN FEED PATTERNS

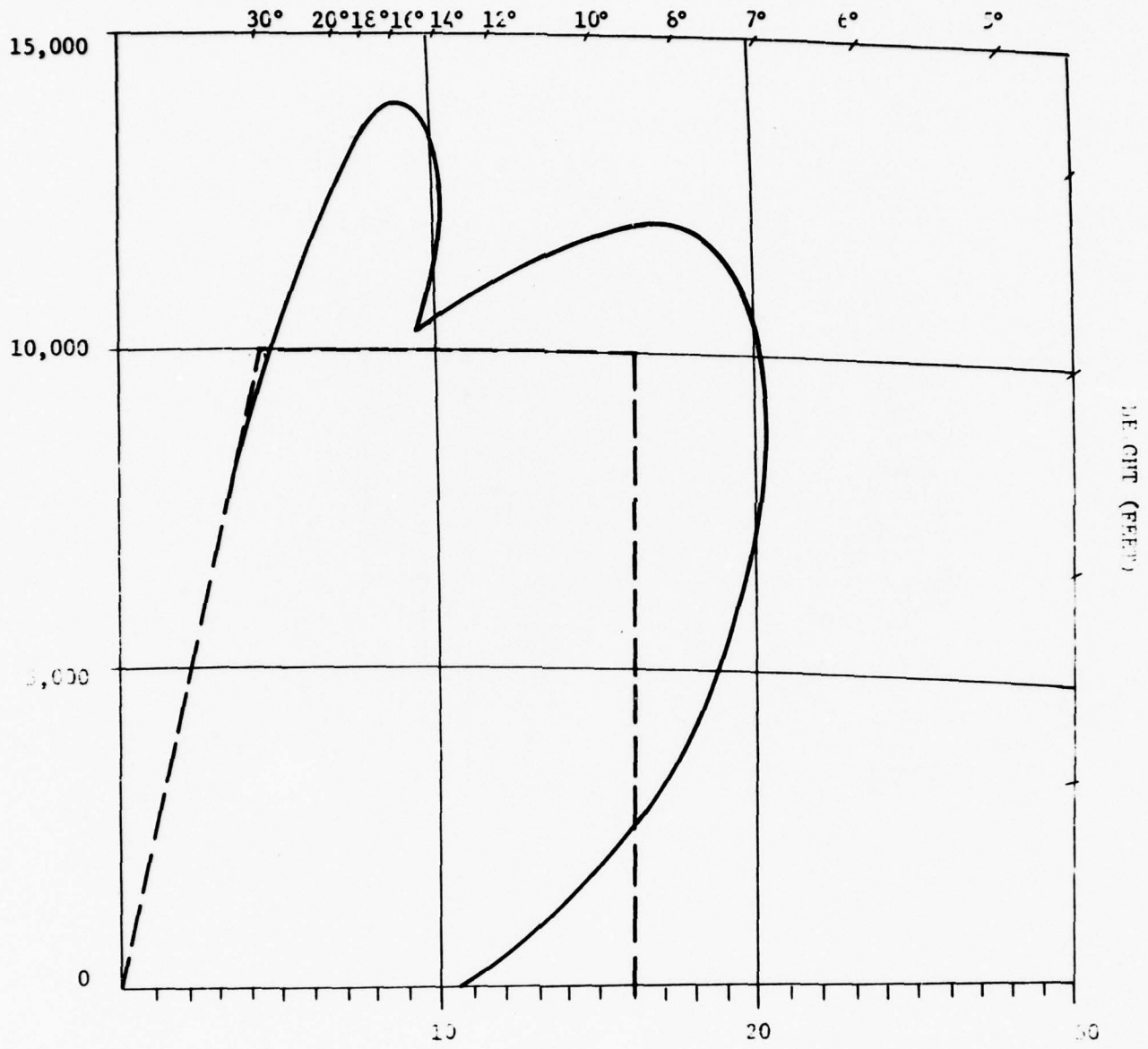

FIGURE F.2 TWO-HORN FEED - COVERAGE

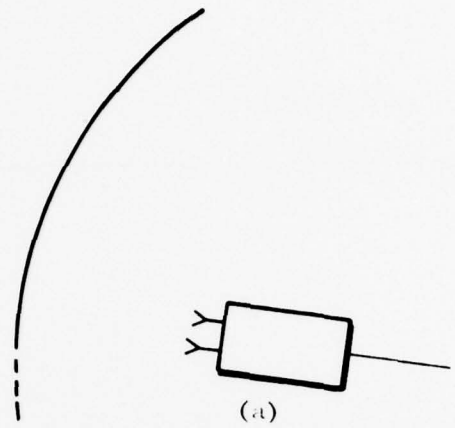

(a)

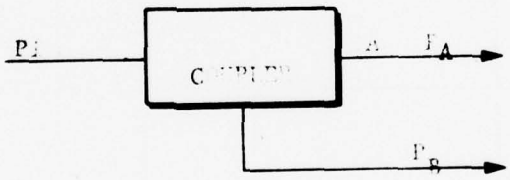

$$Pi = P_A + P_B$$

$$\frac{P_A}{P_B} = 2.5 \ (4db)$$

THEREFORE:

$$P_A = .286 \ Pi \ (-5.56db)$$

$$P_B = .714 \ Pi \ (-1.46db)$$

(b)

FIGURE F.3

BEAM SHAPING

APPENDIX G

MTD (MOVING TARGET DETECTOR)

G.1 MTD-I

The first generation MTD-I processor is a special purpose, hard-wired, signal processor which is capable of processing the full 360° coverage of the FPS-18 radar out to a nominal range of 48 nmi. A block diagram of the processor is presented in Figure G.1. The I and Q (In-phase and Quadrature) signals are sampled at a 2.6 MHz rate by 10-bit A/D converters. The I and Q are then added coherently, two at a time. Then consecutive samples of both the I and Q channels for each of 760 range gates are stored in an 8192-word memory. These 7600 words of the 8192-word memory are then processed sequentially (ten time samples for each range cell) by a 3-pulse MTI canceller. The I and Q channels are processed by separate hardware in the 3-pulse canceller section of the processor. Note that the 10 pulses of 11-bit I and Q channel samples exist after the 3-pulse canceller as eight pulses of 13-bit words. The output of the 3-pulse canceller for both the I and Q channels (real and imaginary parts of the signal) is fed into an 8-point Discrete Fourier Transform (DFT) which produces eight doppler cells.

Weighting of the I and Q channel signals to reduce the sidelobe level is done after the DFT. Subtracting from the cell of interest one-fourth of the signal from the two adjacent doppler cells is equivalent to a Hamming weighting performed in the time domain.

Since the 3-pulse canceller has poor low doppler velocity response, a zero velocity filter (ZVF) is employed to see low radial velocity targets. This low pass filter is implemented by coherently adding the first five samples of each of the I and Q channels, respectively, taking their magnitude and adding to this the magnitude of the sum of the last five samples. This gives a somewhat broader frequency response than simply adding coherently all 10 samples and then taking the magnitude. The magnitudes of the output signals of the 3-pulse canceller, DFT and weighting chain are then taken.

After magnitudes are taken, adaptive background levels and thresholds are set and threshold crossings (detections) are noted and output. The adaptive background levels and thresholds are set depending on the clutter phenomenon which is present. The doppler domain is divided into three domains; doppler cell 0, doppler cells 2 through 6 and doppler cells 1 and 7.

In doppler cell 0 the clutter is generally due to ground backscatter. The average ground backscatter cross section varies from range azimuth cell to range azimuth cell. The average backscatter signal level for each cell is measured and stored on the disc. A recursive filter is used to update on a

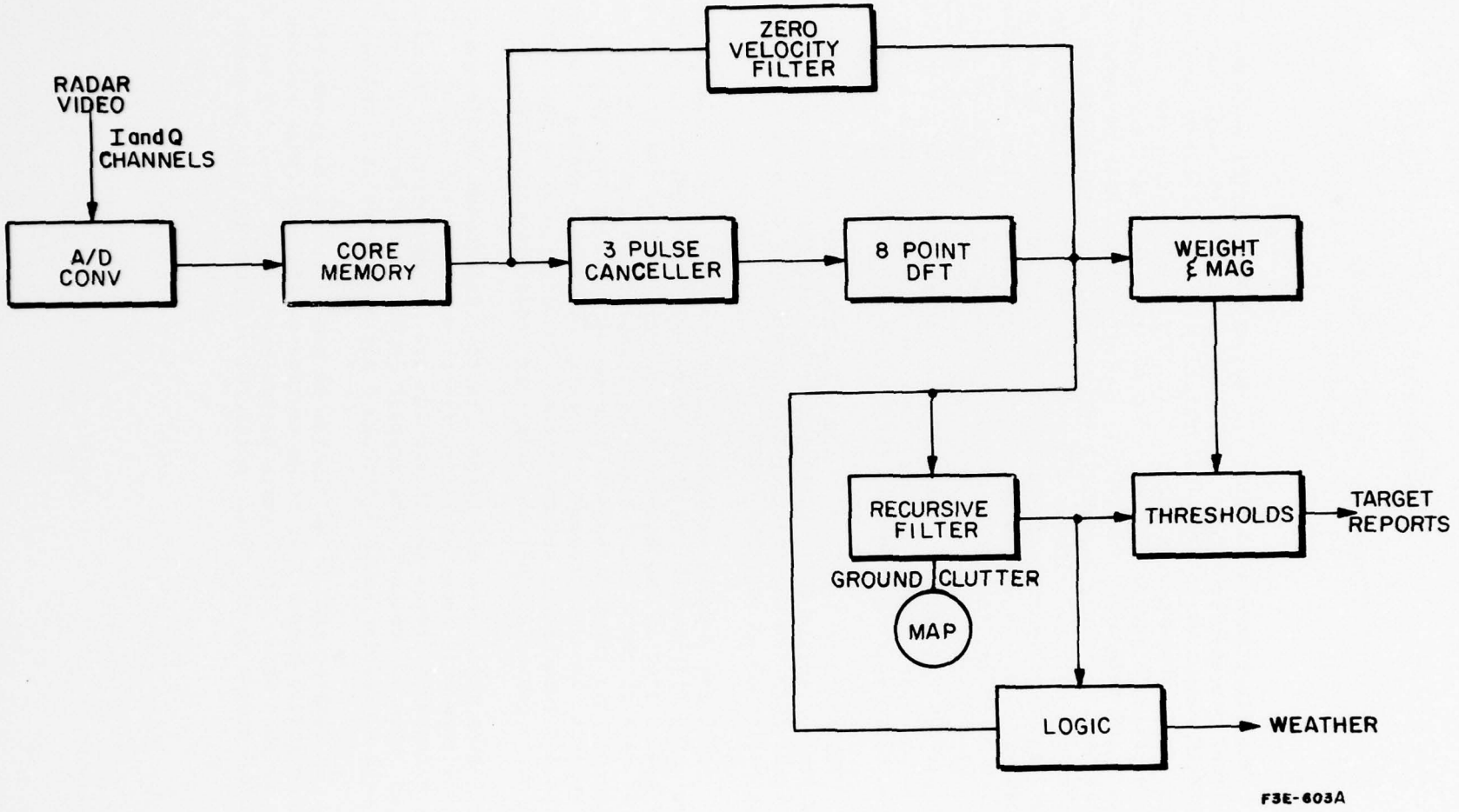

FIGURE G.1

MTD-I SIGNAL PROCESSING BLOCK DIAGRAM

scan-to-scan basis the average signal level stored on the disc. On each scan, 1/nth of the stored clutter level is subtracted from the stored level. One nth of the signal level output from the VF is added to the value remaining after subtraction. This new level is then stored on the disc for thresholding in the next scan. The threshold for the 0 doppler cell is a fixed value between four and eight times the level stored on the disc. This fixed value may be altered by the use of a wire jump on the hardware.

In doppler cells 2 through 6 the clutter is due chiefly to rain. For each doppler and angle cell the average signal level is measured by averaging the received signal over 16 range cells (one mile) centered on the range cell of interest. The threshold for these cells is a fixed value set at 4 to 8 times the measured average signal level.

Doppler cells 1 and 7 can contain clutter due to rain and spillover from the ground backscatter in cell 0. The threshold in these cells is set as the greater of two thresholds; (a) the threshold set as in doppler cells 2 through 6, or (b) a fixed binary fraction of the threshold set in doppler cell 0.

Finally, it must be noted that if any I or Q channel sample is noted to have all the bits on (i.e., be in saturation), then any target detections for that range cell are deleted.

G.2 MTD-II

Analysis and design studies have been made which result in the detailed design of a second generation Moving Target Detector (MTD-II) radar signal processor with even better MTI performance, lower doppler filter sidelobe level and with increased dynamic range, reliability and maintainability. The present MTD processor, which is undergoing detailed system tests at NAFEC, approximates the "optimum" processor by cascading a 3-pulse canceller, an 8-point FFT and weighting in the frequency domain to reduce sidelobes. The "optimum" processor was not implemented in the hard-wired processor because it required too many multiplies to be cost effective and because its sidelobes were so high (8 to 13 dB) that rain clutter would leak into adjacent doppler velocity filters, thus unnecessarily reducing the detection sensitivity of these doppler filters.

The recent development of integrated circuit component and architecture technology allows the multiplications inherent in the "optimum" processor implementation to be accomplished easily. Also, there are other significant advantages to using a microprogrammable approach. First, microprogrammable processors are programmable devices so that even complex changes of the processing algorithms may be coded and debugged in software rather than making extensive hardware changes as would be the case if the integrated circuits were hard-wired together. Secondly, in the case of the SRTR, the

signal processor will consist of two or three identical processing elements all run by the same control device (see Figure G.2). Each of these processing elements has identical hardware and consists of about 230 MSI integrated circuits. Each element can process a fraction of the range cells.

The original MTD processor was designed and built in such a way as to minimize the number of integrated circuits. Most multiplications and divisions were by powers of two and thus could be implemented by simple shifting of bits in the data word. The use of a microprogrammable processor version of the MTD allows one to use any filter weights desired since the processor has been designed to do multiplies quickly and efficiently. With this opportunity in mind, the clutter spectrum input to the optimum processor calculation was modified to include an interference term whose effect is to reduce significantly the doppler filter sidelobes with only minor degradation from the optimum capability (approximately 1 dB) of the processor to detect moving targets in the presence of ground clutter.

The advanced MTD-II processor will have an MTI improvement factor of 49 dB with most doppler filter sidelobes almost 40 dB down from the doppler filter peak. Also, the modularity of the microprocessor approach to the processor design will greatly facilitate both repair and/or replacement of any defective section of the processor when employed in the field.

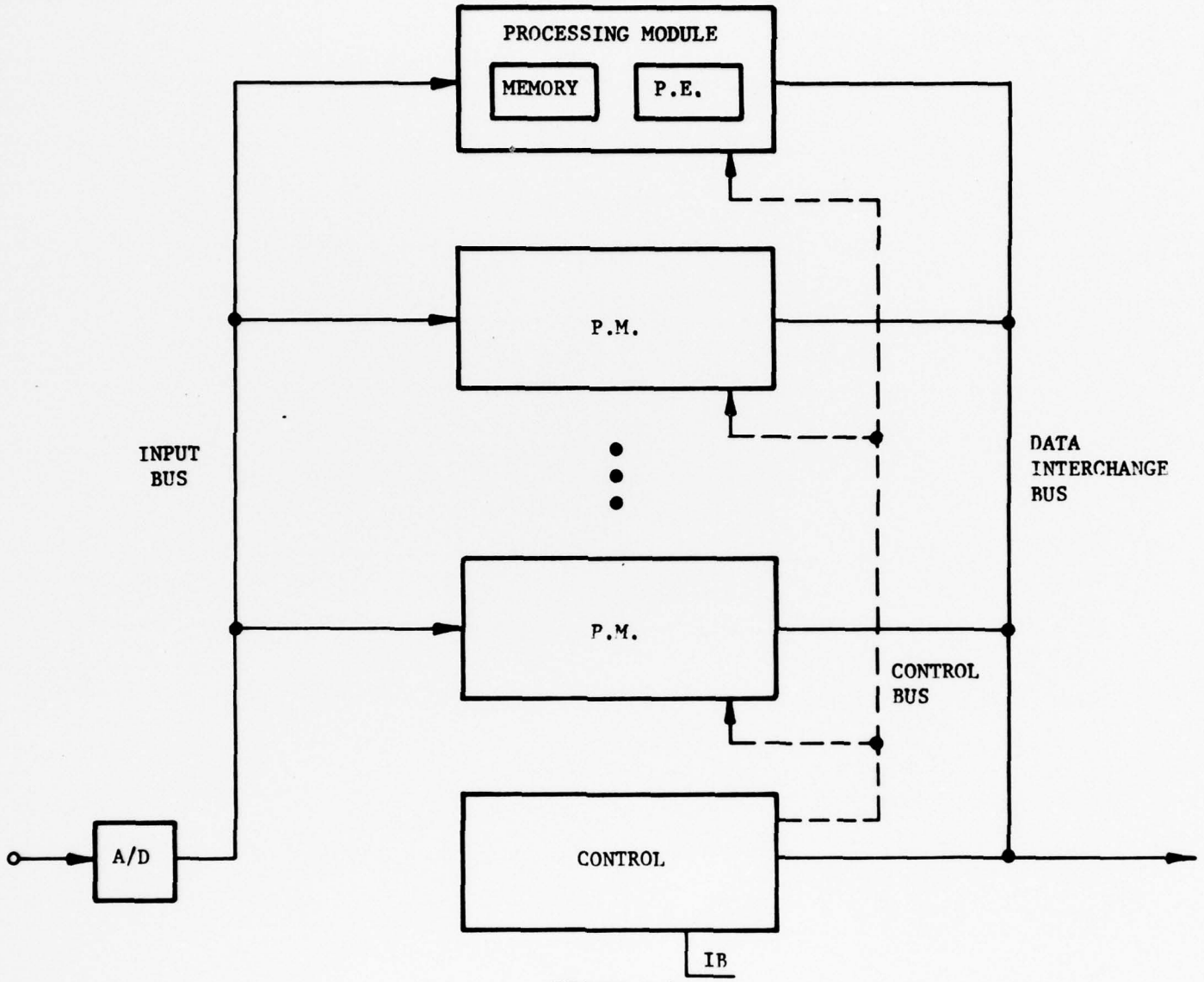

FIGURE G.2

PARALLEL MICROPROGRAMMED PROCESSOR (PMP)

APPENDIX H

DUCTING AND ITS EFFECT ON FREQUENCY SELECTION OF AN AIRCRAFT SURVEILLANCE RADAR

H.1 INTRODUCTION

This appendix describes the effect of tropospheric ducting on the frequency selection and siting of an aircraft surveillance radar system. As expected from waveguide theory, ducting is less probable at lower frequencies. Areas with extensive ducting are noted.

A radar beam that is propagated through the earth's normal atmosphere is refracted or bent. This refraction of the radar beam is caused by the variation of the index of refraction of the atmosphere with altitude. The effect of this normal refraction is to introduce errors in the measurement of elevation angle in the normal atmosphere. For elevation angles between 1 and 10 degrees, the error in elevation angle is less than 0.5 degrees.

However, certain meteorological conditions, such as temperature inversion, can cause the index of refraction to change with altitude sufficiently fast so that the radar beam follows the curvature of the earth. This abnormal propagation of electromagnetic waves is called super-refraction, ducting, trapping or anomalous propagation. The effect of this anomalous propagation is to increase greatly the backscattered ground return seen by an aircraft surveillance radar.

Extensive data collection and ducting predictions have been made by ESSA Institute of Telecommunications Services at Boulder, Colorado. Their analysis shows that there is significantly less ducting at UHF than at L-band, and less ducting at L-band than at S-band. Finally, the ESSA data is in good agreement with ducting measured at the FPS-85 at Eglin AFB.

H.2 ANOMALOUS PROPAGATION

H.2.1 General

Radio waves are bent in the normal atmosphere of the earth. This bending or refraction is dependent upon the gradient of the index of refraction along the path. Usually the horizontal gradient is negligibly small. If the vertical gradient of the index of refraction is sufficiently strong, initially horizontal radio waves can be bent around the surface of the earth. A refractivity gradient of only -157 N units/km will cause initially horizontal rays to follow the curvature of the earth. This effect is called anomalous propagation* of radio waves.

*Other terms used to describe this effect are ducting, trapping or super-refraction

A rigorous treatment of ducting requires solution of the wave equation. In their classic paper, Booker and Walkinshaw (see Booker 1947) show that the propagation through a tropospheric duct is similar to that of a waveguide. Taking a more mathematically simplistic approach, Kerr (see Freehafer 1951) has shown that simple ray tracing based upon geometrical optics can be used to predict the frequency dependence of ducting.

The index of refraction depends on the temperature, pressure and relative humidity. Normally, temperature and humidity decrease with height in the atmosphere since turbulence prevents any great changes in structure. However, when the air becomes calm, temperature inversions alone must be very pronounced to cause tropospheric ducting, but they are important because they can be widespread in area, persist over a long period of time and can be a stabilizing influence over air motion; so much so that turbulence is suppressed and humidity gradients of sufficient strength can develop and cause super-refraction. The three main processes (see Bean 1968) that can cause temperature inversion are listed below.

H.2.1.1 Advection

Advection is the horizontal flow of air having different temperature properties (e.g., dry air above a warm land surface flowing out over a cold sea).

H.2.1.2 Radiation

The surface heat loss produced by radiation at night time is a key factor in the formation of temperature inversions. Radiation induced temperature inversions are seldom strong enough to cause ducting in the middle and low latitudes but are of prime importance in the formation of ducts in the northern latitudes.

H.2.1.3 Subsidence

Subsidence is the slow settling of air from a high pressure system. Adiabatic compression of the air as it descends produces not only temperature inversions and stable layers, but a decrease in relative humidity.

Any meteorological conditions which produce small scale turbulence and tend to break up stratification will prohibit formation of tropospheric ducts. These effects (e.g., surface roughness or differential surface heating) cause a uniform vertical distribution of moisture and very small temperature lapse rates. Thus, as one would expect, the ducts are not seen over areas of moderate or great surface roughness when the winds at the surface are more than a few meters per second, independent of cloud conditions.

It is reasonable to expect that the characteristics of super-refraction will be different over sea than over land because land masses change temperature much more quickly than does the sea.

Ground-based ducts may also be caused by the diverging down draft under a thunderstorm (Skolnik 1962). The relatively cool air which spreads out from the base of a thunderstorm results in a temperature inversion in the lowest few thousand feet. The humidity gradient of the storm also contributes to the duct formation. Although thunderstorms are not a major cause of anomalous propagation, the presence of the thunderstorm may be detected by a radar operator by noticing a sudden increase in the number and range of ground targets.

H.2.2 Wavelength Dependence

Kerr (Freehafer 1951) has shown that propagation in a tropospheric duct is similar to that in a waveguide with a leaky top wall. In both cases propagation may be resolved into a sum of elementary modes or waves which penetrate the top of the duct. Also, in both cases propagation is inhibited at wavelengths longer than a critical wavelength. Using this model the maximum wavelength that can be propagated is related to the thickness of the duct and the rate of change of index of refraction with height (see Freehafer 1951).

$$\lambda_{max} = 2.5 \left(\frac{\Delta n}{\Delta h}\right)^{1/2} d^{3/2}$$

where $\frac{\Delta n}{\Delta h}$ is the rate of change of index of refraction with height and is the thickness of the duct. A typical value for $\frac{\Delta n}{\Delta h}$ within a duct is 1.3×10^{-7}/meter. Since tropospheric ducts are rarely more than 200 meters thick, ducting can be an important propagation phenomena for wavelengths shorter than 250 cm. However, it must be noted as Kerr points out that "(These) values of λ_{max}... do not represent cut off conditions. Although radiation at these and shorter wavelengths is strongly guided, radiation at several times these wavelengths may also be affected strongly by the duct."

H.2.3 Elevation Angle Dependence

Tropospheric ducting is primarily limited to low elevation angles. Bean and Dutton (Bean et al 1968) have calculated, using Snell's Law, the refractivity gradients needed to support ducting as a function of θ_0, the initial elevation angle of the radio wave, for typical values of sea level refractivity and duct height. Their results are presented in Figures H.1 and H.2. Since the approximate upper limit of radio-sonde observed gradients is about -500 N units/km, ducting will affect radar detection only if part of the main lobe has an elevation angle less than about 10 milliradians (about $\simeq 1/2°$).

H.3 GROUND-BASED DUCTS AND RADAR FREQUENCY SELECTION AND SITING

H.3.1 Data Base

The most extensive data base of ground-based atmospheric duct properties has been compiled by Bean, Cahoon and co-workers (Bean et al 1968) at the Institute for Telecommunication Sciences and Aeronomy at Boulder, Colorado. They have collected over a period of at least five years radio-sonde data, consisting of pressure, temperature and relative humidity as a function of height and month of the year at 268 locations geographically distributed throughout the world. Using the pressure, temperature and relative humidity data, they have calculated the refractivity and refractivity gradient as a function of height. These results and the methods discussed in the previous section were used to generate world maps of the contours of the percentage of the time the trapping frequency is less than a certain value for different months of the year. Some of these curves are presented in Figures H.3, H.4 and H.5.

H.3.2 Results and Conclusions

From these curves it is apparent that there is significantly less ducting at UHF (435 MHz) than at L-band (1300 MHz) or S-band (3000 MHz). Typically, ducting is about twice as probable at L-band than at UHF frequencies. These curves which predict the frequency of occurrence of ducting may be compared with the observed ducting on the FPS-85 at Eglin AFB, Florida. The FPS-85 has a detection mode with the surveillance beam at a low elevation angle. The effect of ducting on the FPS-85 while in this mode was to bend part of the main lobe into the sea and thus increase both the average sea clutter return and the number of large clutter discretes (such as ships and airplanes) to a level which swamps the capacity of FPS-85 track banks. Bendix personnel have stated that based on about one month's observation in June, due to tropospheric ducting, the minimum detection range of the radar would be increased by a factor of 3 about 5 days a year. This measurement is in reasonable agreement with the 1 to 2 percent ducting predicted at UHF in the area of Eglin AFB, Florida by the Bean data. The problem of ducting can be partially alleviated by raising the elevation angle of the surveillance fan so that no part of the main lobe can be ducted. Typically, this means placing the first null of the beam at about 8 milliradians (0.5°). Unfortunately, this method of obtaining low flying aircraft coverage while ducting conditions are present must be traded off with loss of low altitude coverage caused by raising the radar surveillance beam. Another solution is to develop radars with increased ability to see moving targets in the presence of heavy ground clutter due to ducting. This approach has been taken in the radar development work at Lincoln Laboratory and has resulted in 100 times the radar sensitivity in heavy ground clutter.

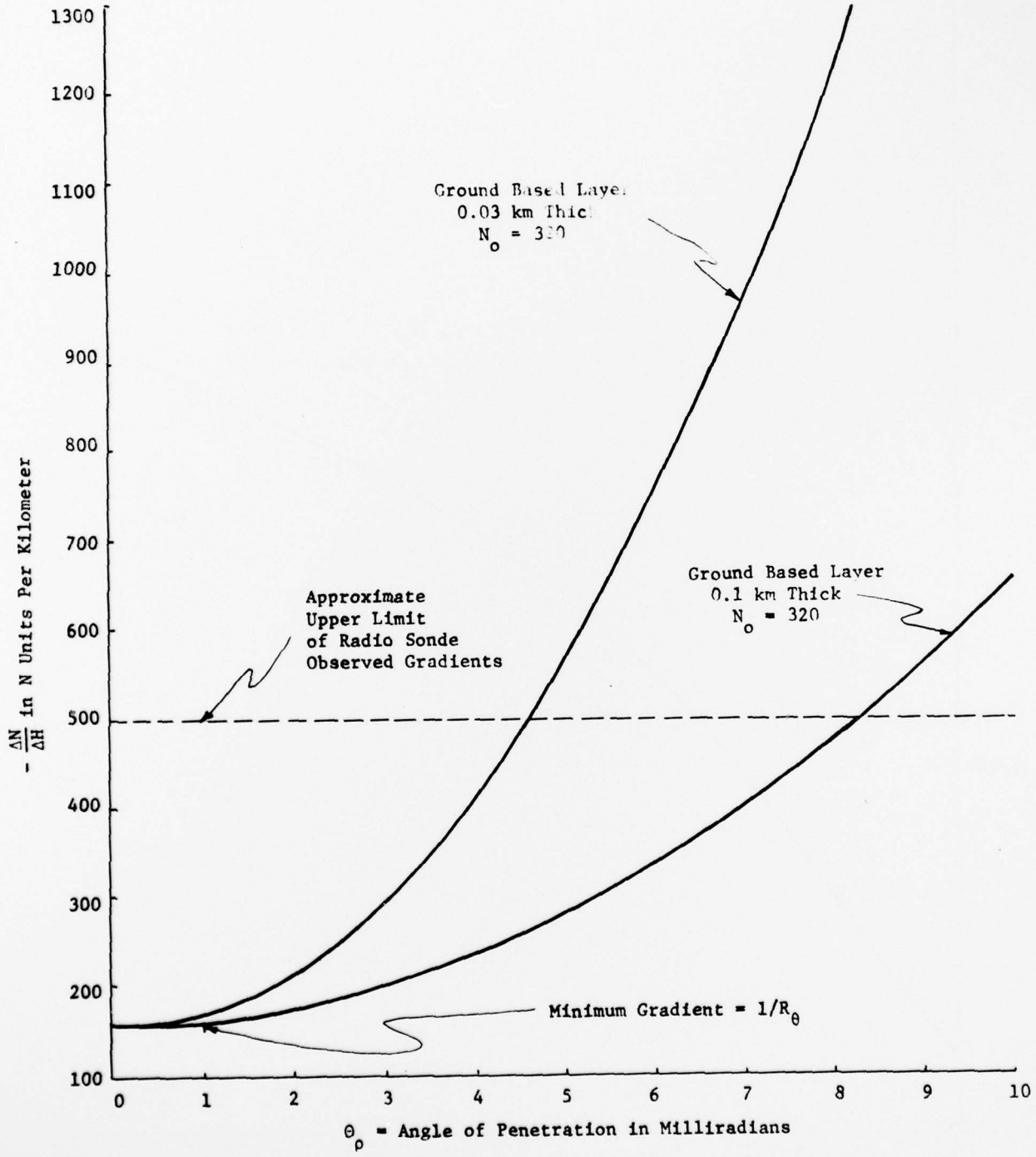

FIGURE H.1 REFRACTIVITY GRADIENTS NEEDED TO SUPPORT DUCTING

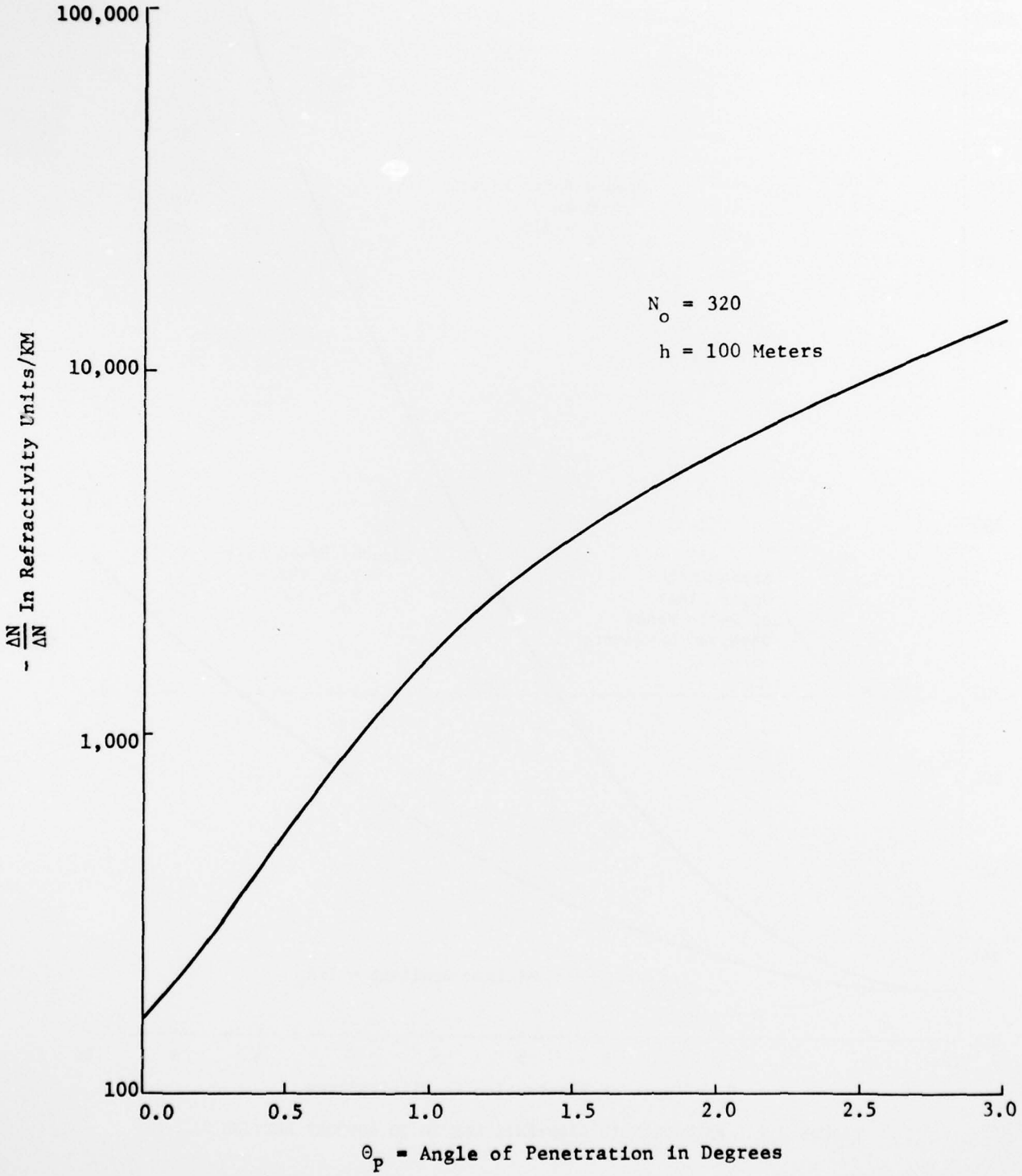

FIGURE H.2 REFRACTIVITY GRADIENTS NEEDED TO SUPPORT DUCTING

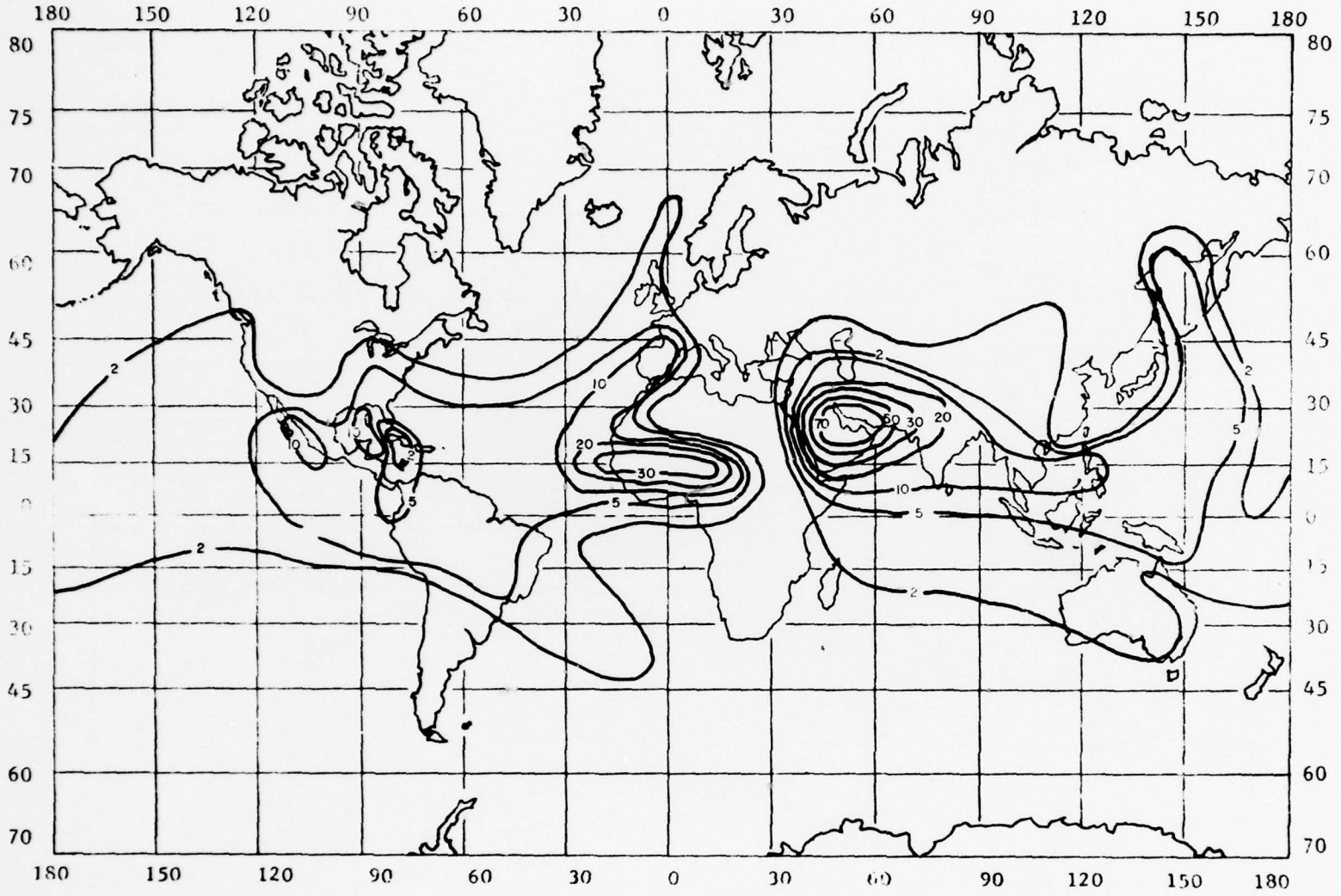

FIGURE H.3 PERCENT OF TIME TRAPPING FREQUENCY LESS THAN 3000 MHz - MAY (REF. 18)

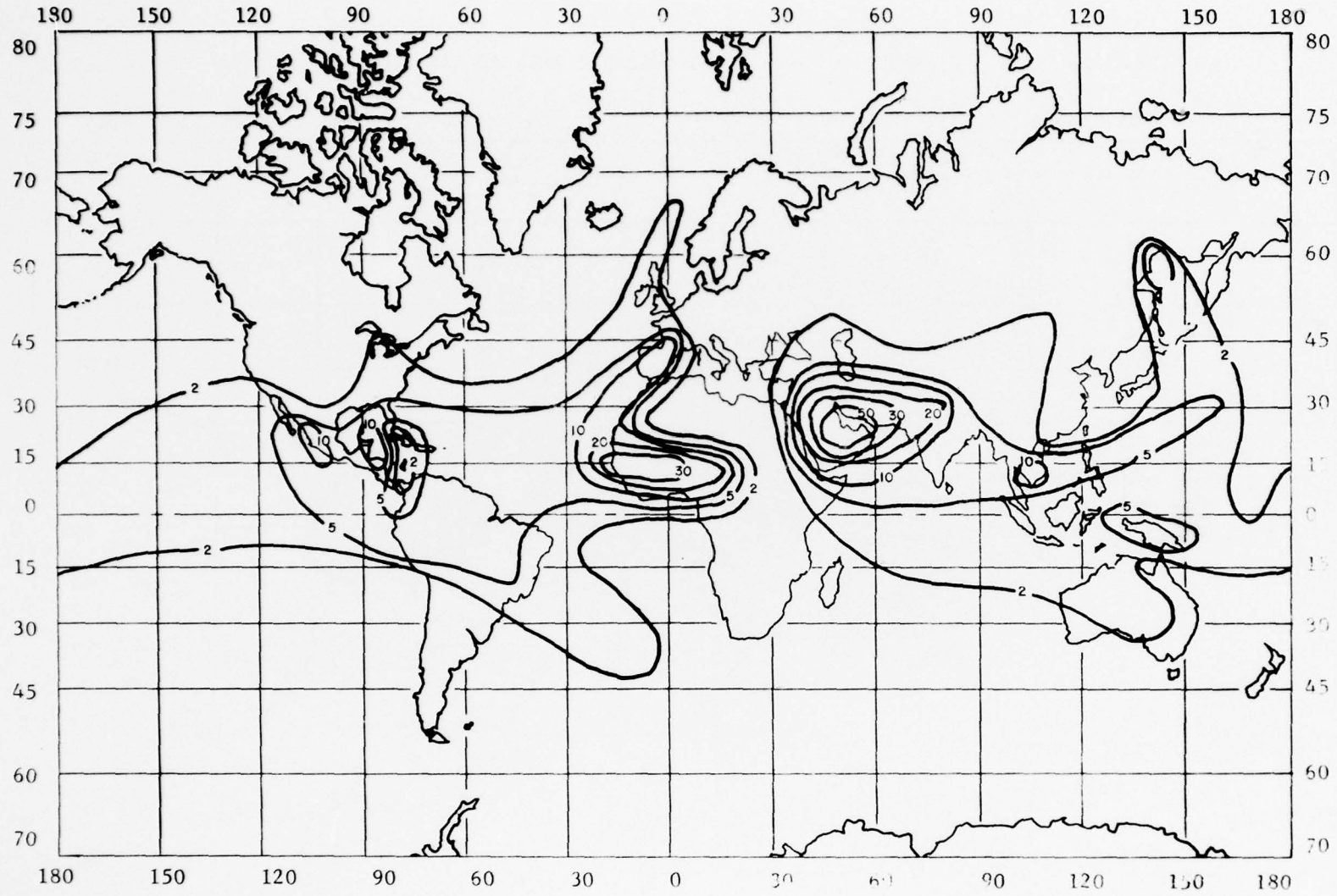

FIGURE H.4 PERCENT OF TIME TRAPPING FREQUENCY LESS THAN 1000 MHz - MAY (REF. 18)

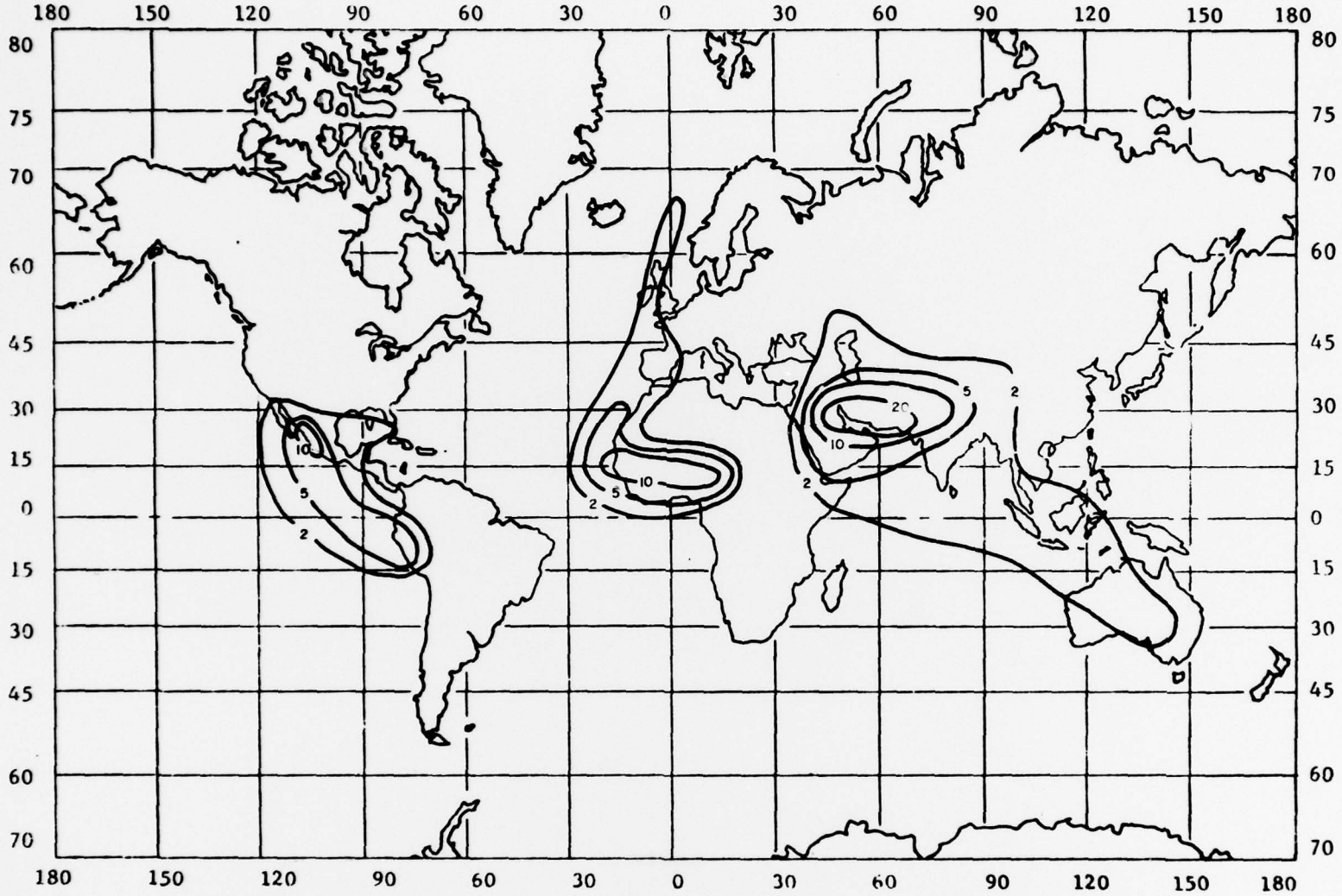

FIGURE H.5 PERCENT OF TIME TRAPPING FREQUENCY LESS THAN 300 MHz - MAY (REF. 18)